AN INVESTIGATION OF THE EFFECT OF AUTO-THROTTLE DEVICES ON AIRCRAFT CONTROL IN THE CARRIER LANDING APPROACH

GERALD R. BELL

AN INVESTIGATION OF THE EFFECT OF AUTO-THROTTLE DEVICES ON AIRCRAFT CONTROL IN THE CARRIER LANDING APPROACH

* * * * *

Gerald R. Bell

AN INVESTIGATION OF THE EFFECT OF AUTO-THROTTLE DEVICES ON AIRCRAFT CONTROL IN THE CARRIER LANDING APPROACH

by

Gerald R. Bell

Lieutenant Commander, United States Navy

Submitted in partial fulfillment of
the requirements for the degree of

MASTER OF SCIENCE
IN
AERONAUTICAL ENGINEERING

United States Naval Postgraduate School
Monterey, California

1963

AN INVESTIGATION OF THE EFFECT OF AUTO-THROTTLE DEVICES ON AIRCRAFT CONTROL IN THE CARRIER LANDING APPROACH

by

Gerald R. Bell

This work is accepted as fulfilling

the thesis requirements for the degree of

MASTER OF SCIENCE

IN

AERONAUTICAL ENGINEERING

from the

United States Naval Postgraduate School

ABSTRACT

An automatic-throttle compensation system has the capability of removing the problem of aircraft speed instability in the carrier landing approach. Various systems have been proposed and tested, each differing in input sensed variables. Two representative systems are investigated analytically and by the use of digital programmed Nyquist plots and analog simulations. An attempt is made to determine optimum gain constants by using various forcing functions in the analog simulation. Comparisons of the responses of the two systems are made using time history analog records. A digital computer stability program, applicable to any aircraft, is included.

The writer wishes to express his appreciation for the assistance and encouragement given him by Professor E. J. Andrews of the U. S. Naval Postgraduate School. Gratitude is also due Ling-Temco-Vought Incorporated, Specialties Incorporated and Bell Aerosystems for providing the necessary data used in the investigation. In particular, the author wishes to thank the Stability and Control Section, Airframe Design Division, of the Bureau of Naval Weapons for the valuable assistance supplied in the form of pertinent technical reports.

TABLE OF CONTENTS

LIST OF ILLUSTRATIONS

TABLE OF SYMBOLS

For those symbols not defined in the text.

C_D	=	Drag coefficient, Drag/qS
C_{Do}	=	Drag coefficient in trimmed condition
C_L	=	Lift coefficient, Lift/qS
a	=	$dC_L/d\alpha$, Lift curve slope
dC_D/dC_L	=	Rate of change of drag with lift
T	=	Thrust, lbs.
S	=	Wing area, sq. ft.
q	=	Dynamic pressure, $1/2\rho V^2$, lbs./sq.ft.
V, U_o	=	Forward velocity, reference steady state, ft./sec.
V_{SL}	=	Stall velocity, ft./sec.
u	=	Perturbation forward velocity, ft./sec.
w	=	Perturbation vertical velocity, ft./sec.
γ	=	Flight path angle, measured from the horizontal, radians
θ	=	Pitch angle, measured from horizontal to FRL, radians
Δ ( )	=	Error quantity, increment, perturbation
n_z	=	Normal load factor, g units
$\Delta T_{\delta C}$	=	Thrust command increment, lbs.
C_{AS}	=	Equivalent propulsion system drag $= -\frac{1}{S}\frac{\partial T}{\partial q}$
τ	=	Time constant, time in seconds to reach 63% steady state
K_α	=	Gain constant for α input
Kn_z	=	Gain constant for n_z input

K_θ	=	Gain constant for pitch error input
K_{V1}, Ku	=	Gain constant for airspeed error input
K_{V2}, $K_{\int} u$	=	Gain constant for integral of airspeed error input
ω_n	=	Undamped natural frequency, radians/sec.
ζ	=	Damping ratio

AN INVESTIGATION OF THE EFFECT OF AUTO-THROTTLE DEVICES ON AIRCRAFT CONTROL IN THE CARRIER LANDING APPROACH

1. Introduction

The carrier landing approach speed of current swept wing aircraft is influenced by many factors. One of the most important of these factors is often referred to as speed instability. Speed instability can be explained with the help of Fig. 1. It will be noted that for Aircraft "A", a slight deviation in airspeed from the normal approach speed makes very little difference in thrust required. This curve is typical of the AF-1E type aircraft. On the other hand, a deviation towards slower speed for Aircraft "B" causes a large increase in thrust required. This increase, if uncorrected, causes a loss of altitude. Thus, in effect, the normal approach of Aircraft "B" is made on the "backside" of the thrust versus airspeed curve. This curve is typical of the F-8 aircraft. Essentially this steep backside of the curve is caused by a high value of $C_{D\alpha}$, drag increase due to angle of attack (or lift).

Still another factor contributing to airspeed instability is slow engine response. With a comparatively long time lag in engine response, any hesitation on the part of the pilot in correcting an incipient airspeed loss leads to wide variations in altitude or airspeed before effective thrust can be realized.

With an aircraft that displays speed instability tendencies, either a faster approach speed or an automatic compensating device is required to prevent undesired altitude loss due to airspeed deviations. Faster

approach speeds are not desirable for carrier approaches. It will be the purpose of this paper to investigate some methods of applying automatic power compensation to counteract airspeed instability. A swept wing fighter, patterned after the F-8 airplane is used as the vehicle of the investigation. Both digital and analog computers are exploited in simulating auto-throttle and anti-drag system response to various inputs. Real-time, pilot controlled, analog simulated mirror approaches are also used in qualitatively evaluating each system.

This investigation is the first of a continuing series to be conducted at the U. S. Naval Postgraduate School to evaluate systems of automatic airplane control.

2. Discussion

The aircraft-carrier mirror-landing approach is made at a constant speed and a constant angle of glide slope. This type of approach allows precision control of the landing, a factor of the utmost importance in carrier operations. However, the approach is usually made at a minimum airspeed that is dictated by performance and/or aircraft flying qualities. Thus, the airspeed must be monitored closely while making flight path angle adjustments. A simplified equation (given in Ref. 1) shows that flight path angle, γ, is approximated by the formula:

Eq. (1) $$\gamma \cong \frac{D}{L} - \frac{T}{W} + \frac{dV}{dt}\frac{1}{g} \quad .$$

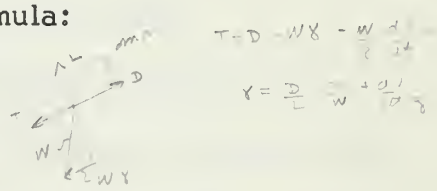

Flight path angle, then, is dependent on lift/drag (L/D) ratio, thrust/weight ratio, and rate of speed change. In the mirror approach the pilot can adjust γ and airspeed by manipulating the throttle and elevator. The manner in which each of these controls can be used, however, is dependent upon the L/D ratio. For aircraft with a high L/D ratio, the elevator is used to control γ, while thrust is used to maintain constant airspeed. With a L/D ratio in the vicinity of 4 - 5 the rate of speed change is large during maneuvers. If, in addition, the L/D ratio decreases with increasing C_L in the approach speed range then speed instability is accentuated.

A variation of lift/drag ratio versus lift coefficient for the F-8 airplane is shown as Fig. 2. It can be seen that at the approach speeds used, ($1.1 - 1.2\, V_{SL}$), L/D decreases rapidly with increase in C_L. As reported in Ref. 1, pilots stated that in order to change γ for an

airplane of this class, increased reliance on thrust rather than elevator was necessary. In the case of the F-8 airplane, however, height response to throttle input is slow due to small thrust line angle of attack and negligible trim changes due to power. The F-8 pilot, therefore, is forced into using the stick as the primary flight path control. Then, since the airspeed mode of oscillation (the phugoid) is lightly damped, the aircraft will hunt about a new equilibrium airspeed and glide slope angle in response to an elevator deflection. These speed changes in the 5 to 10 seconds following elevator input are disturbing to the pilot.

Another way of interpreting airspeed instability is referred to in Ref. 2. A curve similar to Fig. 1 can be drawn for thrust required versus dynamic pressure, q. A definition of a stable speed regime can then be postulated as that portion of the curve where

Ineq. (2) $$\frac{d\, T_{required}}{dq} > 0$$

To express this inequality in terms of the lift and drag coefficients, we use the fundamental equilibrium equations for level flight:

$$C_D' S q = Drag = T_{req}$$
$$C_L S q = Lift = W$$

therefore $$T_{req} = W \frac{C_D'}{C_L}$$

and $$q = \frac{W}{S C_L}$$

and $$\frac{dT_{req}}{dq} = \frac{d\left(W \frac{C_D'}{C_L}\right)}{d\left(\frac{W}{S C_L}\right)} = \frac{W\, d\left(\frac{C_D'}{C_L}\right)}{\frac{W}{S}\, d\left(\frac{1}{C_L}\right)}$$

since W and S are constant.

Therefore $$\frac{d\,T_{req}}{d\,q} = \frac{S\,d\left(\frac{C_D'}{C_L}\right)}{d\left(\frac{1}{C_L}\right)}$$

which result is substituted into Ineq. (2). $$\frac{S\,d\left(\frac{C_D'}{C_L}\right)}{d\left(\frac{1}{C_L}\right)} > 0$$

Since S is greater than O, this implies that

$$d\left(\frac{C_D'}{C_L}\right) \Big/ d\left(\frac{1}{C_L}\right) > 0$$

Taking the differentials of numerator and denominator:

$$\frac{\frac{(-1)}{C_L^2}\,C_D'\,dC_L + \frac{1}{C_L}\,dC_D}{-\frac{1}{C_L^2}\,dC_L} = \frac{C_L\,dC_D' - C_D'\,dC_L}{-dC_L} > 0$$

or

Ineq. (3): $$\frac{C_D'}{C_L} - \frac{dC_D'}{dC_L} > 0$$

Thus, satisfaction of Ineq. (3) implies speed stability.

The C_D' term used above is composed of $C_D + C_{AS}$, where C_{AS} is equivalent propulsion system drag. C_{AS} is defined as

$$C_{AS} \triangleq -\frac{1}{S}\frac{\partial T}{\partial q}\,;$$

or for constant altitude and slow speeds,

$$C_{AS} = -\frac{K}{S}\frac{\partial T}{\partial V^2}$$

C_{AS} is seen to be proportional to the negative of the thrust change with respect to the velocity change. Inequality (3) may then be written as

Ineq. (4) $$I = \frac{C_D + C_{AS}}{C_L} - \frac{dC_D}{dC_L} > 0$$

A more sophisticated approach, based on the suppression of altitude disturbances by the pilot's use of the elevator, and originating with the basic equations of motion, would produce essentially the same inequality, with a small modification factor included. (See Ref. 2) The resulting inequality is

$$\frac{C_D + C_{AS}}{C_L} - \frac{\frac{dC_D}{dC_L}}{1 + \frac{C_D}{a}} > 0$$

However, the correction term, $C_{D/a}$, is of relatively small magnitude and may be ignored. From this same analysis the time constant, τ, of the subsidence of an airspeed error is shown to be proportional to:

Eq. (5) $$\tau = K C_L \left(\frac{C_D + C_{AS}}{C_L} - \frac{dC_D}{dC_L} \right)$$

Typical values of the parameter I for the F-8 are given below. At 1.1 V_{SL}, I = .22 - .548 = - .328, showing distinct speed instability. At 1.2 V_{SL}, I = .200 - .222 = - .022, a less unstable value.

From an examination of the speed instability parameter, Ineq. (4), it will be seen that positive stability can be produced if either drag in trimmed conditions (C_{DO}) or C_{AS} is artificially increased.

C_{DO} could be increased, for example, by extending the speed brakes during an approach. This would accomplish two objectives; one, increase C_{DO} in the stability formula, and two, cause the engine to operate in a higher RPM range to produce the added thrust necessary, thus effectively causing a slight decrease in the inherent engine time constant.

Remembering the definition for C_{AS}, the drag coefficient corresponding to the thrust/speed variation, it will be seen that an artificial means of increasing thrust with decreasing airspeed accomplishes the desired objective. This is exactly what automatic throttle or approach

power compensator devices are intended to do. Still another method of increasing C_{AS} is by the use of an anti-drag technique. This may be accomplished by having a drag producing device (such as side extending speed brakes) extended during the approach. Then, by using an airspeed controller type device to regulate the amount of drag produced (by opening or closing the speed brakes) in response to thrust (or anti-drag) required, airspeed deviations can be closely controlled. This particular method, within its limitations of having enough anti-drag available, theoretically has the advantage of a much shorter time lag than an engine response scheme.

3. Artificial Speed Stability through Automatic-Throttle Techniques

There is a choice of inputs to an automatic-throttle type controller, including various combinations of derivatives and integrals of airspeed error, pitch attitude error, angle of attack error, and normal acceleration. There are also many different philosophies by manufacturers concerning the ideal combination for best performance under all conditions. Two representative systems, one utilizing angle of attack and normal acceleration, and the other using airspeed error and pitch angle, were chosen for investigation.

A) Angle of Attack, Normal Acceleration Inputs

The Specialties, Inc. Automatic Power Compensator, (APC), an auto-throttle in use in the F-8 and F-4 aircraft, is an example of a control using these inputs. A block diagram, typical of this type of system is shown in Fig. 3. In this system, constant angle of attack is maintained in the landing approach using the two sensed inputs of instantaneous angle of attack and acceleration normal to the glide slope in g units. The normal g input supplies anticipation whenever the aircraft is not in a one g flight condition. A thrust command is calculated in the system computer dependent upon error signals and chosen gain and temperature factors. This thrust command then becomes an input to the engine which in turn adds an appropriate thrust to the airframe. This thrust, acting as the forcing function to the airframe modes of motion, changes the velocity of the aircraft. Thus the APC computer indirectly controls airframe velocity through the equations

$$\Delta T = K_\alpha \Delta\alpha + K_n \Delta n_z \quad ; \quad \Delta V = K_T \Delta T$$

Eq. (6) $$\therefore \quad \Delta V = K_\alpha' \Delta\alpha + K_n' \Delta n_z$$

where the K values are appropriate shaping, filtering and simulation networks.

Or, looking at it differently, the C_{AS} of Ineq. (4) has now been given a greater value $\left(C_{AS} \cong -\frac{\partial T}{\partial V} \right)$

artifically, thus making the speed stability parameter more positive or stable.

The transfer function equations for this auto-throttle as supplied by Specialties, Inc., are also shown in Fig. 3. It will be noted that the throttle servo is simulated by a .1 second time constant first order lag. Angle of attack input is treated by both an integrator and lag network. Normal g input is also integrated.

The results of the analog simulation runs using this type of control are reported in Section IV of this paper, Experimental Methods and Results.

B) Pitch Angle, Airspeed Change Input

Flight path angle, γ, is given by the equation

Eq. (7) $$\gamma = \theta - \alpha$$

During constant airspeed flight, pitch attitude change ($\Delta\theta$) and flight path angle change ($\Delta\gamma$) are proportional; but dynamically, $\Delta\theta$ occurs before $\Delta\gamma$. Thus the means of anticipating flight path angle changes is available through pitch attitude changes recorded by a

vertical gyro mounted in the aircraft. This is the theory underlying the pitch angle, airspeed change type of automatic-throttle controller. Through the use of a properly designed network, these inputs make it possible to minimize transient airspeed changes and to eliminate steady state airspeed changes resulting from variations in flight path.

The governing equation for this controller may be of the form:

Eq. (8) $$\Delta T_{\delta c} = \left[K_\theta \Delta\theta - \frac{K_{V1}\Delta V}{(1+\tau_a s)} - \frac{K_{V2}\Delta V}{s(1+\tau_a s)} \right]$$

Here the K_{V2} term is inserted as a steady state error washout term. The lag term $(1+\tau_a s)$ simulates the airspeed sensor and filter. The filter attenuates the short period wind gust signals entering the system and acts as a smoothing influence.

This equation was reduced to a linear open loop transfer function of the auto-throttle controller. The block diagram for this system, combined with the analytically derived block diagram and transfer functions of the airframe and engine, are shown in Fig. 4. The stability derivatives for the F-8 in landing configuration were used for the airframe transfer functions. The derivation is shown in Appendix I.

The system open loop transfer function was calculated as:

Eq. (9) $$-\frac{u}{u_\varepsilon} = \frac{\left(\frac{\Delta T}{u_\varepsilon}\right)_{AT}\left(\frac{u}{\Delta T}\right)_{AF}}{1+\left(\frac{\theta}{\delta e}\right)_{AF}\left(\frac{\delta e}{u}\right)_{AF}\left(\frac{\Delta T}{\theta}\right)_{AT}\left(\frac{u}{\Delta T}\right)_{AF}}$$

where; $\left(\frac{\Delta T}{u_\varepsilon}\right)_{AT} = \frac{\Delta K_u + K_{\dot{u}}}{\Delta(1+1.16\Delta)(1+.1\Delta)}$

$$\left(\frac{u}{\Delta T}\right)_{AF} = \frac{.624\times10^{-5}\,(1+272\Delta+18.9\Delta^2+23.25\Delta^3)}{.416\,(1+1.67\Delta+27.7\Delta^2+2.08\Delta^3+2.402\Delta^4)}$$

$$\left(\frac{\theta}{\delta e}\right)\left(\frac{\delta e}{u}\right)_{AF} = \frac{-.0142}{16.8}\,\frac{(1+37.9\Delta+176\Delta^2)}{(1+5.29\Delta+.01173\Delta^2)}$$

$$\left(\frac{\Delta T}{\theta}\right)_{AT} = \frac{K_\theta}{(1+1.16\Delta)}$$

This equation was programmed on the digital computer to produce a series of Nyquist plots, each utilizing different gain constants. Fig. 5 shows the Nyquist plot for the equation using the same gain constants as were used in the analog simulation. From this figure the open loop gain margin is seen to be 19.2.

The system closed loop transfer function, $-\left(\frac{u}{u_{ref}}\right)$ was then derived. This is shown symbolically as follows:

Eq. (10) $$-\frac{u}{u_{ref}} = \frac{\left(\frac{\Delta T}{\Delta u}\right)_{AT}\left(\frac{u}{\Delta T}\right)_{AF}}{1+\left(\frac{\Delta T}{\Delta\theta}\right)_{AT}\left(\frac{\theta}{\delta e}\right)\left(\frac{\delta e}{u}\right)\left(\frac{u}{\Delta T}\right)_{AF}+\left(\frac{\Delta T}{u_\varepsilon}\right)_{AT}\left(\frac{u}{\Delta T}\right)_{AF}}$$

A digital program was devised to calculate the values of the poles of the closed loop transfer function for various values of auto-throttle K's. This procedure would have produced families of Root Loci Plots. However, because of lack of time and computer malfunctions, this particular investigation was not completed. Equation (10) would be used in an optimizing analysis for gain constants.

In addition the equations of the auto-throttle were set up on the

the analog computer. This was incorporated into the complete system using approximately optimum values of K_θ , Ku, and $K\int u$. All simulation was done in real time. These results are also reported in Section IV. Analog mechanization is shown in Appendix III. A composite block diagram showing the relative positions of the two automatic throttle systems in the airspeed loop is presented as Fig. 6.

C) Auto-Throttle Controller Linked to Anti-Thrust Device

Another possible approach to the airspeed instability problem is the use of an auto-throttle controlling an anti-thrust or drag device. This could be accomplished by flying the approach with speed brakes extended. The output of the auto-throttle would then reduce or increase the drag by closing or opening the speed brakes as required. Thus, instead of supplying additional thrust when the airspeed drops, the speed brakes would be closed a proportionate amount, reducing the drag and in effect accomplishing the same purpose as an increase in thrust. Note that the time lag of the hydraulically actuated speed brake system is much less than that of the engine, thus allowing a faster response. The time constant of the hydraulic system is of the order of .1 second, while that of the F-8 engine is about 1.16 seconds. This approach was also investigated on the analog computer by replacing the engine with a first order time lag of .1 seconds (simulating the hydraulic system) and using the thrust command output of the auto-throttle computer to control the speed brakes.

Obviously the limiting feature to such a system is the amount of drag the speed brakes are capable of supplying. Of course it goes without saying that such a device can not be installed on an aircraft incapable of completing an approach while varying the positioning of the speed brakes. An airplane in this category is the F-8 which has a lower fuselage speed brake. Insufficient deck clearance is available when this brake is extended, thereby prohibiting its use during an approach.

4. Experimental Methods and Results

A) Equations and Analysis

The basic 3-degrees of freedom aircraft longitudinal equations of motion (in British notation) used in the analysis are shown below. The equations are based on the small perturbation linear theory. Lower case letters represent perturbation quantities. Upper case, subscripted o, letters represent initial steady state conditions. Body axes are used throughout. The assumptions made are as follows:

1. The airplane has a longitudinal plane of symmetry.

2. The direction of the relative wind, in steady flight, lies in the plane of symmetry, and in steady state, all angular velocities are zero.

3. Initial flight condition is wings level.

4. Products and squares of perturbation velocities are small and are ignored, and sines of all perturbation angles are approximated by the angle itself in radians.

5. The longitudinal modes of motion are independent of the lateral modes.

6. Structural deformations are not considered.

Three degree of freedom non-dimensional equations of motion, British notation: (See Ref. 3) Figure 7 displays angular definitions and signs.

X Force Equation:

$$\left[\frac{d}{d\tau} - X_u\right]\frac{u}{U_o} \quad -X_w\frac{w}{U_o} - \left[X_\theta - \frac{X_{\dot{w}}}{\mu_1}\frac{d}{d\tau}\right]\theta = X_T\Delta T$$

Z Force Equation:

$$-z_u \frac{u}{U_0} + \left[\frac{d}{d\tau} - z_w\right]\frac{w}{U_0} - \left[(1 + \frac{z_{\dot{\alpha}}}{\mu_1})\frac{d}{d\tau}\right]\theta = \left[z_\eta + z_{\dot{\eta}}\right]\eta$$

Moment Equation:

$$\left[-\frac{\mu_1 m_u}{i_b}\right]\frac{u}{U_0} + \left[-\frac{\bar{m}_{\dot{w}}}{i_b}\frac{d}{d\tau} - \frac{\mu_1 m_w}{i_b}\right]\frac{w}{U_0} + \left[\left(\frac{d}{d\tau} - \frac{m_q}{i_b}\right)\frac{d}{d\tau}\right]\theta = \left[\frac{\mu_1 m_\eta}{i_b}\right]\eta + \left[\frac{\mu_1 m_T}{i_b}\right]\Delta T$$

where symbols are defined as follows:

$\hat{t} = \frac{m}{\rho U S}$, air secs.

$\frac{d(\ )}{d\tau} = \frac{\hat{t}\, d(\ )}{dt}$

$\tau = \frac{t}{\hat{t}}$ $\frac{\text{real time}}{\text{air secs}}$

u = perturbation horizontal velocity, ft./sec.

w = perturbation vertical velocity, ft./sec.

η = elevator deflection, positive down, radians

ΔT = change in thrust required, lbs.

$\frac{w}{U_0}$ = α, angle of attack, radians

θ = pitch angle, radians

i_b = $\frac{I_{yy}}{m l_t^2}$, Inertia Coefficient

I_{yy} = Moment of inertia, slug - ft^2

m = mass, slugs

l_t = tail length, ft.

μ_1 = $\frac{m}{\rho S l_t}$ = relative density

c = mean wing chord, ft.

S = reference Wing area, square ft.

X = Force parallel to x - axis, lbs.

Z = Force parallel to z - axis, lbs.

M = Moment about lateral axis, lbs. - ft.

h = distance from thrust line to CG, ft.

$x_u = 1/2 \dfrac{\partial\left(\frac{X}{\frac{1}{2}\rho U^2 S}\right)}{\partial\left(\frac{u}{U}\right)}$ non-dimensional Force Stability derivative and similar identities obtained by permuting x, z and u, w independently.

$x_q = 1/2 \dfrac{\partial\left(\frac{X}{\frac{1}{2}\rho U^2 S}\right)}{\partial\left(\frac{q l_t}{U}\right)}$ non-dimensional stability derivative and similar identities obtained by permuting x, z

$x_T = 1/2 \dfrac{\partial\left(\frac{X}{\frac{1}{2}\rho U^2 S}\right)}{\partial T}$ non-dimensional stability derivative and similar identify obtained by permuting x and z, η and T

$m_u = 1/2 \dfrac{c}{l_t} \dfrac{\partial\left(\frac{M}{\frac{1}{2}\rho U^2 S c}\right)}{\partial\left(\frac{u}{U}\right)}$ non-dimensional moment stability derivative and similar identities obtained by permuting u and w

$x_\theta = 1/2 \dfrac{\partial\left(\frac{X}{\frac{1}{2}\rho U^2 S}\right)}{\partial \theta}$ non-dimensional stability derivative and similar identities obtained by permuting x, and z

$\overline{m}_{\dot{w}} = 1/2 \dfrac{c}{l_t} \dfrac{\partial\left(\frac{M}{\frac{1}{2}\rho U^2 S c}\right)}{\partial\left(\frac{\dot{w} l_t}{U^2}\right)}$ non-dimensional stability derivative

$m_T = X_T \dfrac{h}{l_t}$ non-dimensional stability derivative; h = distance from thrust line to C.G. position

The necessary stability derivatives were evaluated by making use of a longitudinal dynamic stability Fortran program, designated LONGSTAB. The program was compiled while undertaking the course in dynamic aircraft stability given at the Postgraduate School. This program computed the necessary British stability derivatives and then used these derivatives in the aerodynamic equations of motion. The resulting stability quartic was then solved, by the program, for the phugoid and short period complex roots. Finally, the periods and times to damp to 1/2 amplitude

were computed for both modes. Necessary aircraft parameters used by the program were taken from F-8 data supplied by Ling-Temco-Vought, Inc. or calculated. The program-computed stability-derivatives used in the investigation are shown in Table I, as are the other aircraft parameters. All program-computed derivatives, after necessary conversions were found to be in close agreement with those listed in Ref. 6[1]. The computer program is explained in Appendix II. A sample printout is shown in Table II.

From the program printout, the phugoid period is 33.5 seconds and that of the short period mode is 6.06 seconds. Times to damp to 1/2 amplitude are 29.9 and 1.73 seconds respectively. Undamped natural frequency, $\omega_{n\ \text{phugoid}}$, is calculated as .189 radians/sec., ζ as .123. Short period ω_n is calculated as 1.19 rad./sec., ζ as .360.

Ref. 6 lists a phugoid ω_n of 0.188 rad./sec., and a ζ of .12. Short period results found were listed as ω_n = 1.19 rad./sec., ζ = 0.35. The results given by LONGSTAB and those given by Ref. 6 are in excellent agreement.

Thus, as previously remarked, it is seen that the phugoid is very lightly damped.

[1]Ref. 6 reports on the results of an investigation conducted along similar lines as the subject of this paper. The two investigations were performed concurrently and independently of each other. After completion, the results of the author's analysis were verified insofar as possible with those given in Ref. 6.

These non-dimensional equations of motion were dimensionalized for the analog simulation. The engine time lag and auto-throttle blocks were next added. Real time stick and throttle simulators were then introduced into the system, together with the F-8 linearized longitudinal control system dynamics supplied by Ling-Temco-Vought. All analog runs were conducted in real time. The analog computers used were Donner 3100 and 3400 machines. An eight channel Brush recorder was used to record the time histories.

The following types of computer runs were then conducted:

(a) Transient analysis runs using step inputs of elevator deflection, horizontal velocity gusts, and pitch attitude; first with basic airframe alone and then with the two basic types of auto-throttle controllers incorporated. Finally sample runs were made with the speed brake device replacing the engine.

(b) Optimizing runs using triangular inputs of elevator deflection, to determine the optimum gain for this type of forcing function.

(c) Sinusoidal gust inputs.

(d) Real time pilot controlled runs using a simulated glide slope, with and without the aid of the auto-throttle. Horizontal turbulence was also added to determine the controller effectiveness.

Analog mechanization diagrams are shown in Appendix III. Potentiometer settings are shown in Table 1 to Appendix III. Time histories for these runs are displayed in Figs. 10 to 35.

B) Evaluations of Experimental Analog Runs

The systems referred to are as follows:

System 1, Inputs of angle of attack, and normal acceleration in g units.

System Equation: $\Delta T = \frac{1}{1+.1s}\left[\frac{K_\alpha \Delta\alpha}{1+.5s} - \frac{K_{\Delta V}\Delta V}{1+s} + \frac{K_\gamma \Delta\alpha}{s}\right]$

System 1-a gain constants;

K_α = 1970 lbs./degree
$K_{\Delta V}$ = 280 lbs./knot
K_γ = 183 lbs./degree - sec.

System 1-b gain constants;

K_α = 3420 lbs./degree
$K_{\Delta V}$ = 72 lbs./knot
K_γ = 190 lbs./degree - sec.

System 2, Inputs of pitch angle, airspeed error

System Equation: $\Delta T = K_\theta \Delta\theta - \frac{u}{1+.1s}\left[Ku + \frac{K_{\int u}}{s}\right]$

Gain constants;

K_θ = 318 lbs./degree
K_u = 360 lbs./knot
$K_{\int u}$ = 22.3 lbs./knot - sec.

1) Step input of 1.32° up elevator deflection

Fig. 10 is the analog time history response to a 1.3° step of up elevator deflection, using the System 1-a auto-throttle. Airspeed displays a slight oscillatory tendency, reaching an equilibrium speed of +.6% of V_o (.8 kts. above V_o). Thrust is applied smoothly in response to demand.

Fig. 11 shows the response of System 1-b. This system had the gain factors optimized for a step input of horizontal gust velocity. Note the high airspeed overshoot due to step elevator input.

Fig. 12 is the same situation using System 2. Airspeed is much more highly damped as compared to Fig. 11. Equilibrium airspeed is -1% of V_o (1.39 kts. below V_o). Thrust is also applied smoothly.

2) 5 knots of horizontal gust input

Fig. 13 displays the record of System 1-a in response to this input. The system is oscillatory with an approximate damping ratio of $\zeta = .15, \omega_n = .677$ rad/sec. The initial velocity overshoot is 61% of initial error. These values of gain constants are less than optimum for this type of input disturbance.

Fig. 14 displays the response of System 1-b, which has been optimized to this input disturbance. Equivalent ζ is now .58, ω_n is .73 rad/sec. Thrust response is somewhat oscillatory. Final value of airspeed is +.2% of V_o.

Fig. 15 is the record of System 2. This shows a damped response with final airspeed of about -2.2% V_o. Thrust changes are less than that required by System 1.

3) 4^o step input of pitch angle.

Fig. 16 shows the response of System 1-a to this input. Initial velocity transient is +.8% V_o or 1.12 kts. Steady state error is +.4% V_o. Thrust application is slightly oscillatory.

Fig. 17 shows System 1-b response. Initial velocity transient is .6% V_o. Steady state error is also .6% V_o.

Fig. 18 displays the response of System 2. Initial velocity transient amounts to +1.6% V_o. Airspeed damps to +.4% V_o steady state error in 19

seconds, reaching less than 1% error in 9 seconds.

Fig. 19 shows the response of the basic airframe to this same input disturbance, without the aid of the auto-throttle. Airspeed oscillation is +1% V_o, with a steady state value of about .5% V_o.

4) Optimizing runs using triangular elevator input

Fig. 20 shows System 1-a under the influence of a .02 cps triangular elevator deflection (maximum amplitude 1.32^o) forcing function. Airspeed error is kept within a range of +2% to -1% of V_o. Thrust varies within the range of +1600 to -2400 lbs. about the trim setting. Thrust application follows elevator movement closely.

Fig. 21 shows the reaction of System 1-b. Note how airspeed fluctuates $\pm$ 4% V_o ($\pm$ 5.56 kts.). Thrust has very noticeable oscillatory tendencies and gyrates within rather wide limits.

Fig. 22 shows System 2 under the influence of this same forcing function. Airspeed is seen to vary $\pm$ 1.7 kts. or $\pm$ 1.2% of V_o. Thrust varies approximately 2400 lbs. about trim thrust. Application of thrust, however, is smoother and displays less hunting characteristics than shown by System 1-a.

Figs. 23, 24 and 25 show the response of these same systems to a triangular elevator forcing function of the same magnitude as previously, but of .06 cps frequency.

Fig. 26 shows the reaction of the airplane to this same forcing function without the benefit of the auto-throttle. Note airspeed deviation is less than that obtained with System 1-b engaged.

5) Human pilot controlled flight on simulated glide slope

For this series of runs a pilot flew the simulated airplane on the glide slope, using the auto-throttle. Glide slope reference was obtained from a zero centered panel meter. The zero voltage level was considered the correct glide slope. This is shown on Channel 1 of Figs. 27, 28 and 29. The pilot was then told to manipulate the stick to fly the aircraft to a new 4° higher glide slope. This corresponded to a + 14 volt reading on channel 1, or 14 volts on his reference meter. This simulated a low "meatball" on a mirror approach and the flight path correction necessary. This new flight path angle was held momentarily. The pilot was then told to fly the airplane down to a - 4° glide slope, after which he was to return to the normal flight path (0 volts).

The response of the aircraft, and speed control is shown in Figs. 27, 28 and 29 for Systems 1-a, 1-b and 2 respectively.

It will be noted that Systems 1-a and 2 maintain airspeed close to within 1% of V_o, whereas System 1-b has much greater airspeed fluctuations. Thrust application is again much more oscillatory in System 1-b.

6) Human pilot controlled flight on glide slope with sinusoidal input of 5 knots horizontal velocity gust

Figs. 30 and 31 are records of System 1 runs utilizing a pilot controlled stick with a forcing function sinusoidal input of 5 knots of horizontal velocity, frequency .05 cps. The pilot was again attempting to fly the glide slope 4° up and down.

Fig. 32 is the record of the response to this same forcing function under the influence of the pilot and the System 2 auto-throttle.

Fig. 33 displays the record of the pilot attempting to maintain original glide slope while the aircraft was being influenced by a sinusoidal u turbulence forcing function, without the benefit of the auto-throttle.

7) Speed brake anti-thrust system

Fig. 34 shows the history of the speed brake anti-thrust system in response to a 5 knot horizontal velocity step input. Mechanically, the System 2 auto-throttle was used to supply a thrust command, but this thrust command was used to drive a .1 second time constant anti-drag device, simulating the movement of the speed brakes. It will be noted that in comparison with Fig. 15, (standard System 2 setup) response and damping is faster. It required 9 seconds for the transient to steady within 1% of V_o in the case of Fig. 34, while it required 11 seconds for System 2.

Fig. 35 shows the response of the anti-thrust system to the same forcing function, but utilizing different gain factors. Response is more oscillatory.

C) Summary of Analog Results

From the foregoing evaluations it can be seen that the response of the different systems investigated is dependent upon the sensed variables and the applied forcing functions. System 1-a, optimized to an elevator deflection input, is marginal to unsatisfactory in performance when subjected to a horizontal gust input. On the other hand, system 1-b, using the same sensed variables, but with gains optimized to horizontal

velocity input, does not perform well when subjected to elevator deflection inputs. System 2, utilizing different sensed inputs, also displays varying reactions to each of the forcing functions.

In general, it can be seen that System 2 has the capability of a smoother application of thrust in response to an airspeed error. System 1 has the capability of a more highly damped response, but causes a more erratic application of thrust. Further investigation as to the optimum values of gain constants is required to accomplish the desired task more efficiently.

It is further recommended that additional sensed variables or integrals of such terms be added to the analog set-up to help optimize system response. A fruitful area might be to incorporate a normal g input to System 2 to help the damping characteristics. It is anticipated that further investigations along this line will be conducted at the U. S. Naval Postgraduate School. These investigations will attempt to utilize the simplified equations obtained by the elimination of the short period mode, to develop a more tractable analysis.

5. Conclusions

The two major approach power compensator systems investigated appear to have the capability of performing the desired task. The major difference are degree of anticipation and erraticism of thrust application. With proper choice of gains and input variables, it seems feasible that a composite system can be designed to provide the advantages of both individual systems.

The speed brake or anti-thrust system has the capability of providing faster response, but is limited by drag area available and the physical feasibility of approaching with speed brakes extended.

The preceding investigation has firmly convinced the author that an auto-throttle mechanism is an important contribution to carrier aviation safety. An aircraft that is difficult to fly in the approach because of inherent speed instability problems, can have its whole character changed by an auto-throttle. By removing the undesired instability an auto-throttle relieves the pilot of concentrating on airspeed control, thus allowing more precision in glide slope and line-up control. This advantage by itself, should tend to reduce the frequency of ramp accidents.

In addition, when an automatic landing system is considered, the pilot-controlled airspeed loop must be replaced by an automatic system to provide consistency and predictability of response.

Still another advantage of the automatic airspeed control system is the reduction of minimum approach speed below that recommended by the pilots when airspeed is controlled by manual throttle manipulation. In

addition the automatic device can be designed to provide the anticipation and instant response that can only be obtained from much actual pilot experience. Thus it is seen that the auto-throttle can act as the great equalizer in carrier approach training.

TABLE I

Computed F8 Stability Derivatives and Associated Aircraft Parameters
British Non-Dimensional Notation

X_u = -.2630

X_w = .16996

X_q = 0.0

X_θ = -.450

Z_u = -.90

Z_w = -1.5915

Z_q = -.5878

Z_θ = -.0640

M_u = .006052

M_w = -.15896

$\bar{M}_{\dot{w}}$ = -.1422

M_q = -.5119

μ_1 = 54.466

i_B = .7081

$\hat{t}$ = 3.2772

C_L = .90

C_D = .263

C_T = .195

S_w = 375 ft^2

C_{m_α} = -.380

θ_o = 8.1°

$\frac{\partial \varepsilon}{\partial \alpha}$ = .4772

C_g position = 24%

Weight = 22,000 lbs

U_o = 139 kts = 234 ft/sec

Z_η = -.1949

M_η = -.349

X_T = $.2046X10^{-4}$

M_T = $-.635X10^{-6}$

INPUT PARAMETERS

TAIL AREA= 93.4000 WING AREA= 375.0000 CL ALFA TAIL= 2.393000 ETA TAIL= 1.000000 BODY AREA= 688.50
BODY LENGTH=52.80000 RHO= .0023780 GCE=32.17000 WEIGHT= 28000.0000 LBS D EPSILON/D ALFA= .477200
INITIAL PITCH ANGLE= 8.100000 DEGREES THRUST LINE DISTANCE= -.437000 FEET THRUST COEF CT= .195000
CMALFA= -.380000 I SUB YY= 96000.000 SLUG FT SQUARED

STABILITY DERIVATIVES

FORWARD VELOCITY= 234.000 T CARAT= 3.277273 C= 65.1049

C SUBL= .900000 C SUBD= .263000

XU= -.2630 XW= .16996 XQ= .0000 XTHETA= -.45000 ZU= -.90000 ZW= -1.5915 TOTAL ZQ= -.5878

ZTHETA= -.0640 MU= .006052 MW= -.15896 MBAR W DOT= -.1422 MQ= -.5119 MUCNE= 54.466 I SUB BETA= .7081

A= 1.00000 B= 2.7764 C= 14.04677 D= 3.020209 E= 5.08454

THE VALUE OF ROUTHS DESCRIMINANT = 69.47
THE AIRCRAFT IS STABLE

RUN 3 C.G. 24, V=139 KTS,234 FPS 3/3/63 LEVEL FLITE

THE COEFFICIENTS OF THE GIVEN POLYNOMIAL ARE

REAL PART	1.0000000	2.7764450	14.0467662	3.0202908	5.0845393
IMAGINARY PART	.0000000	.0000000	.0000000	.0000000	.0000000

TABLE OF ROOTS

ROOT NUMBER	REAL PART OF ROOT	IMAG PART OF ROOT	PERIOD	TIME TO DAMP TO HALF AMPL
1	-.075930	-.614444	10.2128 SECS	29.9173 SECS
2	-.075930	.614444	10.2128 SECS	29.9173 SECS
3	-1.312092	-3.397553	1.8487 SECS	1.7313 SECS
4	-1.312092	3.397553	1.8487 SECS	1.7313 SECS

Table II

Sample Printout, Fortran Stability Program, LONGSTAB

Fig. 1

Thrust Required Versus Airspeed

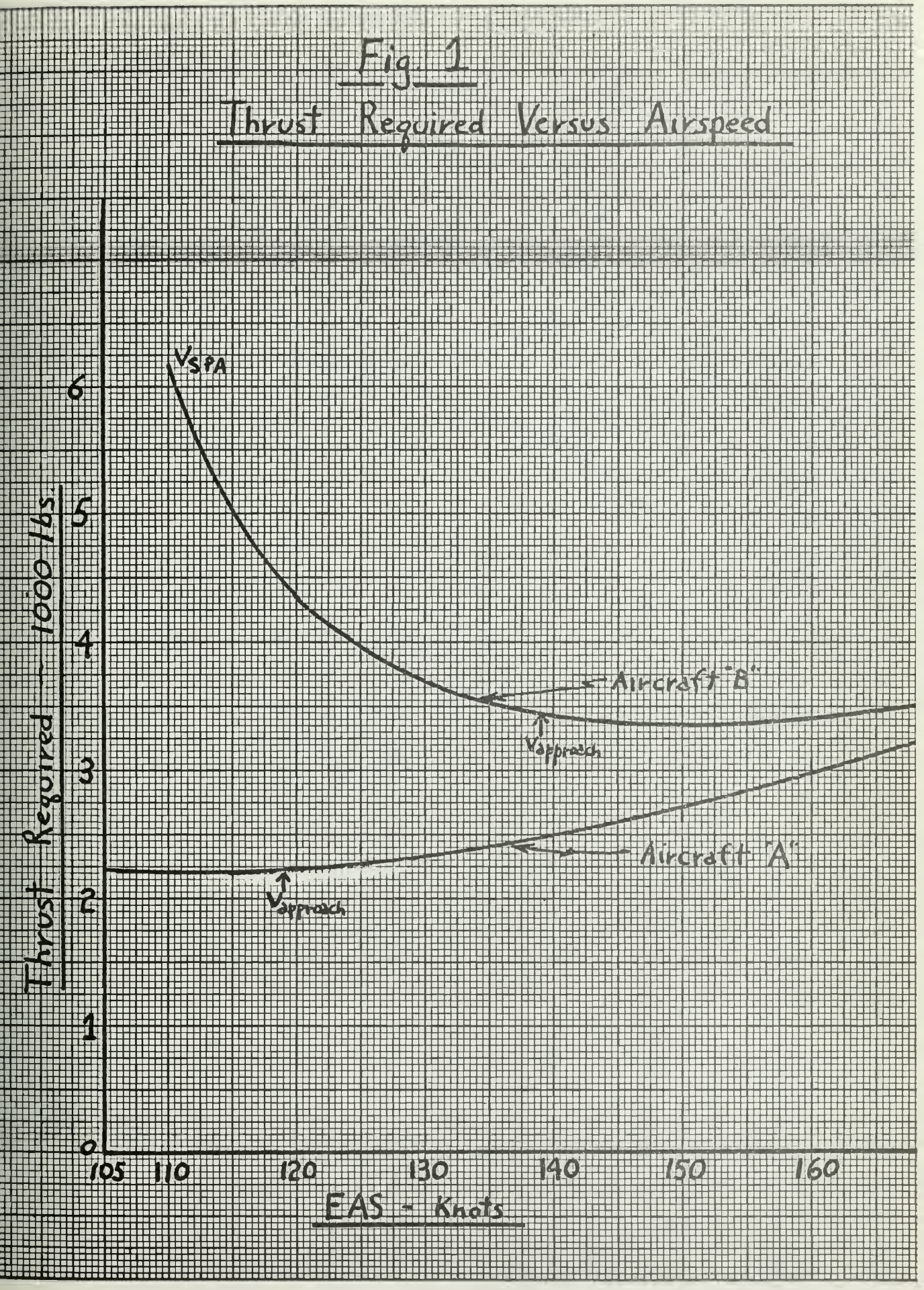

Fig. 2
C_L versus L/D, F-8 Airplane

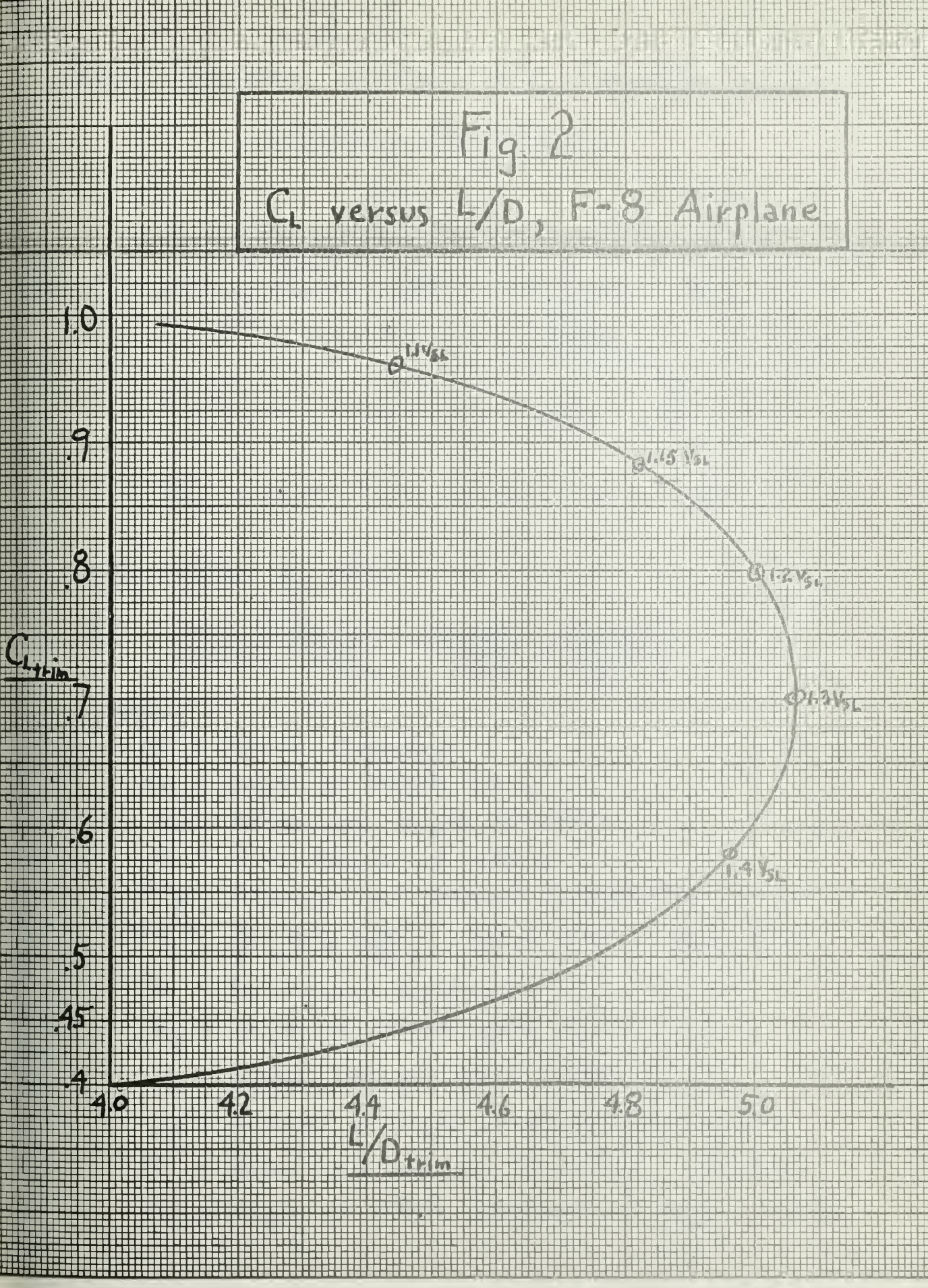

Fig. 3

Block Diagram, System 1 Auto-Throttle with Transfer Functions

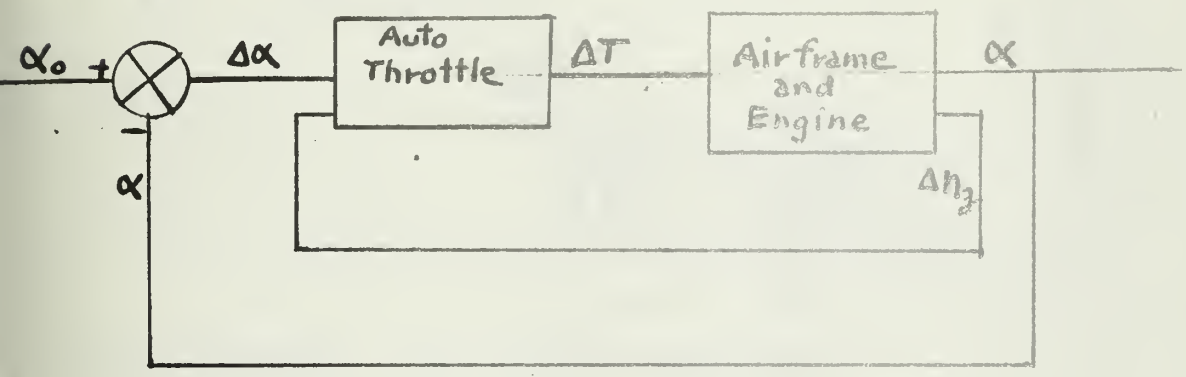

Auto throttle Equation:

$$\Delta T = \frac{1}{1+\tau_1 s}\left[\frac{K_\alpha \Delta\alpha}{1+\tau_2 s} - \frac{K_V \Delta V}{1+s} + \frac{K_\gamma \Delta\alpha}{s}\right]$$

Where:

ΔT = Thrust Command

$\Delta\alpha$ = Angle of attack error

α_o = Reference Angle of attack

α = True Angle of attack

Δn_z = change of normal acceleration

$\Delta V = \frac{V_o}{2}\left(\Delta n_z - \frac{\Delta\alpha}{\alpha_o}\right)$, speed change parameter

V_o = Reference Airspeed

K_α = Angle of attack gain factor

K_V = Speed Change gain factor

K_γ = Integral of angle of attack gain factor

τ_1 = Servo and actuator time lag (.1 sec)

τ_2 = Angle of attack shaping time lag. (.5 sec)

Fig 4

Block Diagram, System 2 Auto Throttle and Engine with Transfer Functions

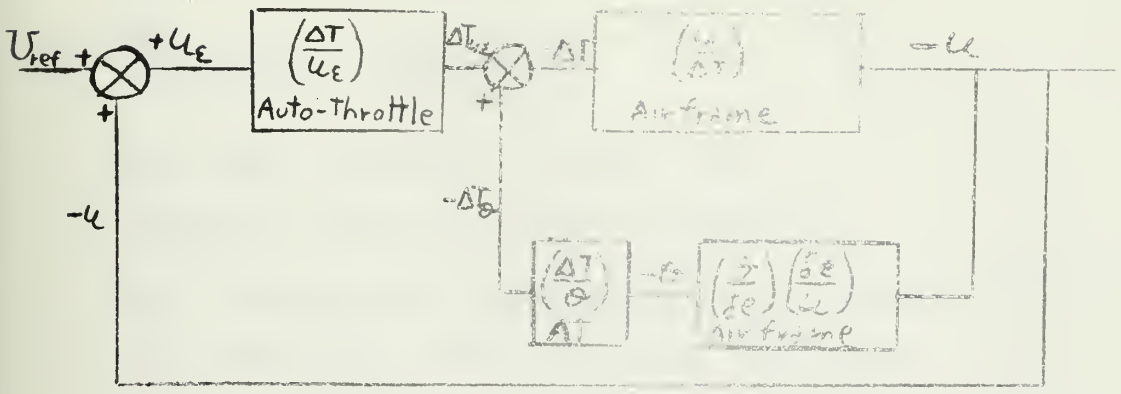

Auto Throttle and Engine Equation:

$$\Delta T = \frac{1}{1+\tau_e s} K_\theta \theta - \frac{u_\varepsilon}{(1+\tau_e s)(1+\tau_f s)}\left[K_u + \frac{K_{fu}}{s}\right]$$

τ_e = Engine Time Constant

τ_f = Airspeed Sensor Time Constant

θ = Pitch Angle Change

U_{ref} = Reference Airspeed

u_ε = Airspeed Error

K_u = Airspeed Gain Constant

K_{fu} = Integral of Airspeed Gain Constant

K_θ = Pitch Angle Gain Constant

$\left(\frac{\Delta T}{u_\varepsilon}\right)_{AT}$ = Auto Throttle Transfer Function = $\frac{K_u + \frac{K_{fu}}{s}}{(1+\tau_e s)(1+\tau_f s)}$

$\left(\frac{\Delta T}{\theta}\right)_{AT}$ = Auto Throttle Transfer Function = $\frac{K_\theta}{(1+\tau_e s)}$

$\left(\frac{u}{\Delta T}\right)_{Airframe}$ = Airframe Transfer Function $\frac{K_{D1} N_1(s)}{K_{D1} D_1(s)}$

Fig. 4 (continued)

$$\left(\frac{\delta e}{u}\right)_{\text{Airframe}} = \frac{K_{D1}\, D_1(s)}{K_{N2}\, N_2(s)}$$

$$\left(\frac{\theta}{\delta e}\right)_{\text{Airframe}} = \frac{K_{n3}\, N_3(s)}{K_{D1}\, D_1(s)}$$

K_{n_1} = Gain Constant = $.624 \times 10^{-5}$

$N_1(s) = [1 + 272s + 18.9s^2 - 23.25s^3]$

K_{D1} = Characteristic Equation Gain Constant = .416

$D_1(s)$ = Stability Characteristic Quartic

$= [1 + 1.67s + 27.7s^2 + 2.08s^3 + 2.462s^4]$

K_{n2} = Gain Constant = 18.8

$N_2(s) = [1 + 5.29s + .01173s^2]$

K_{n3} = Gain Constant = - 0192

$N_3(s) = [1 + 37.9s + 176s^2]$

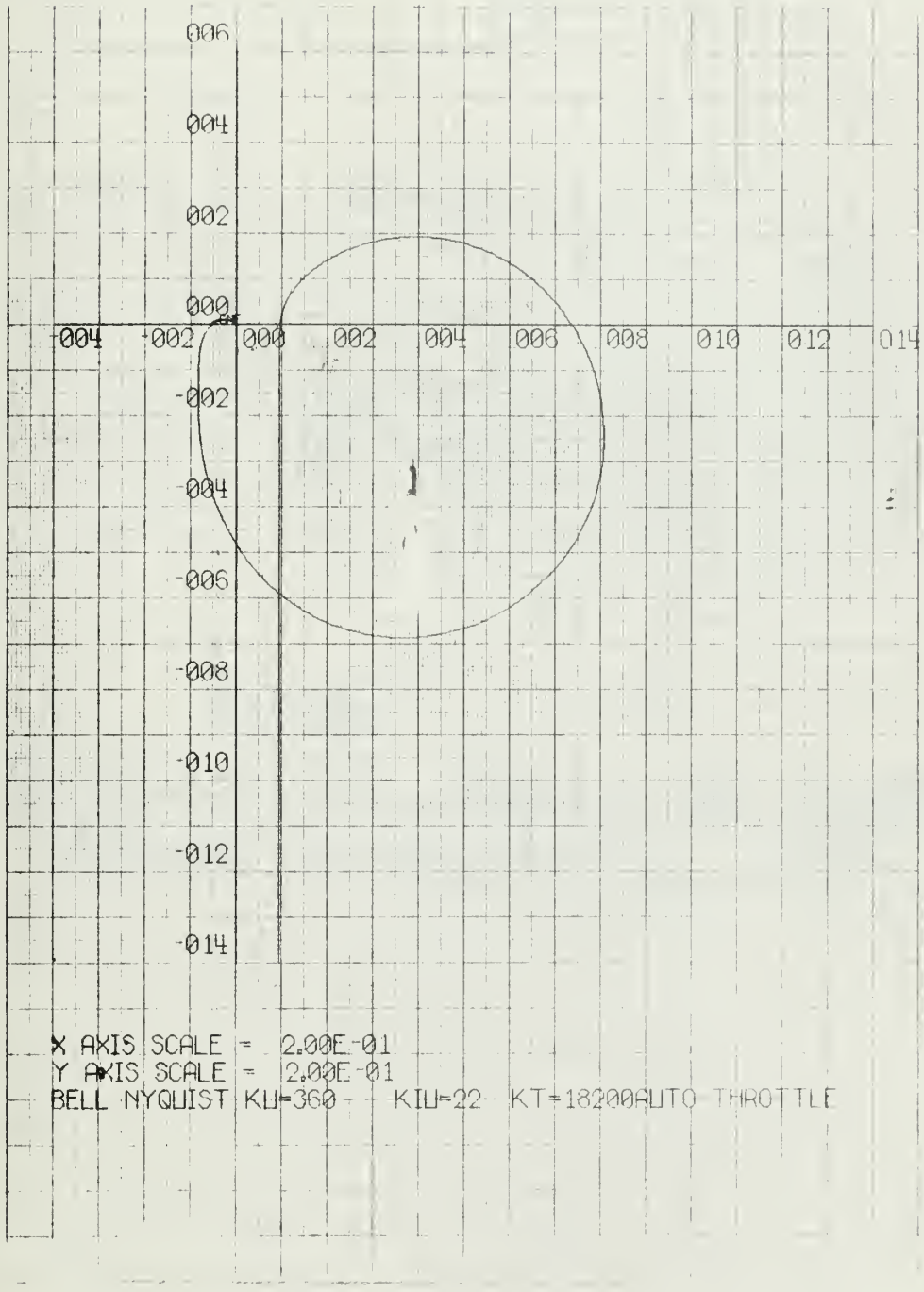

Fig. 5

Nyquist Diagram of System 2 Auto-Throttle Open Loop Transfer Function

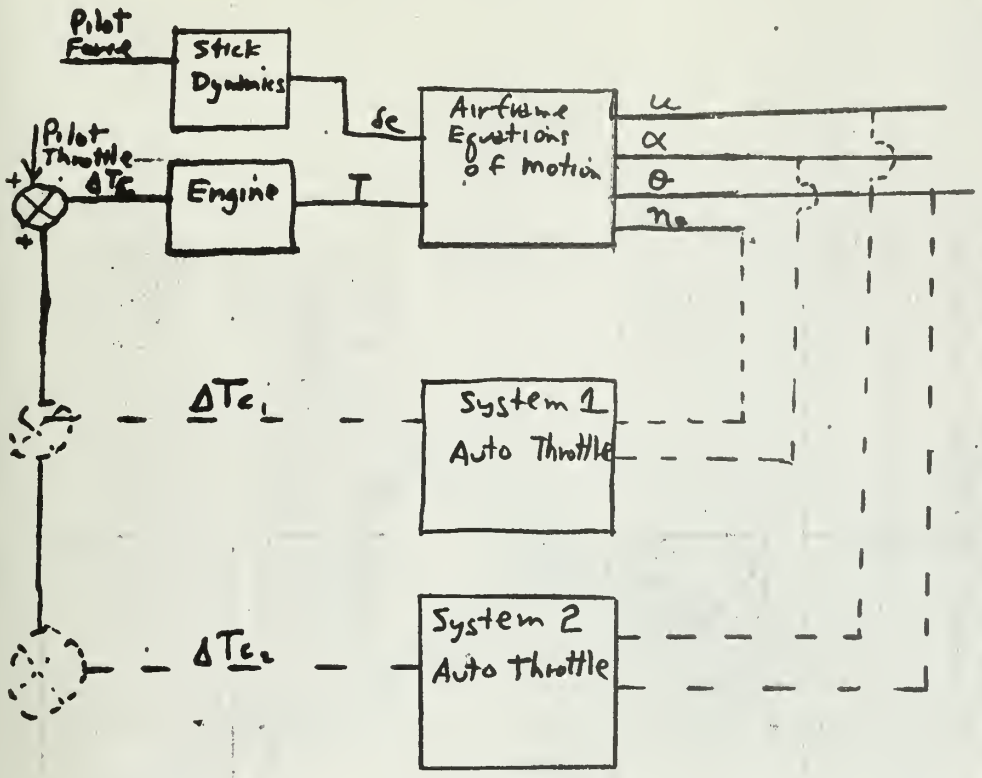

Fig. 6

Composite Block Diagram of Complete Automatic Throttle - Airframe System

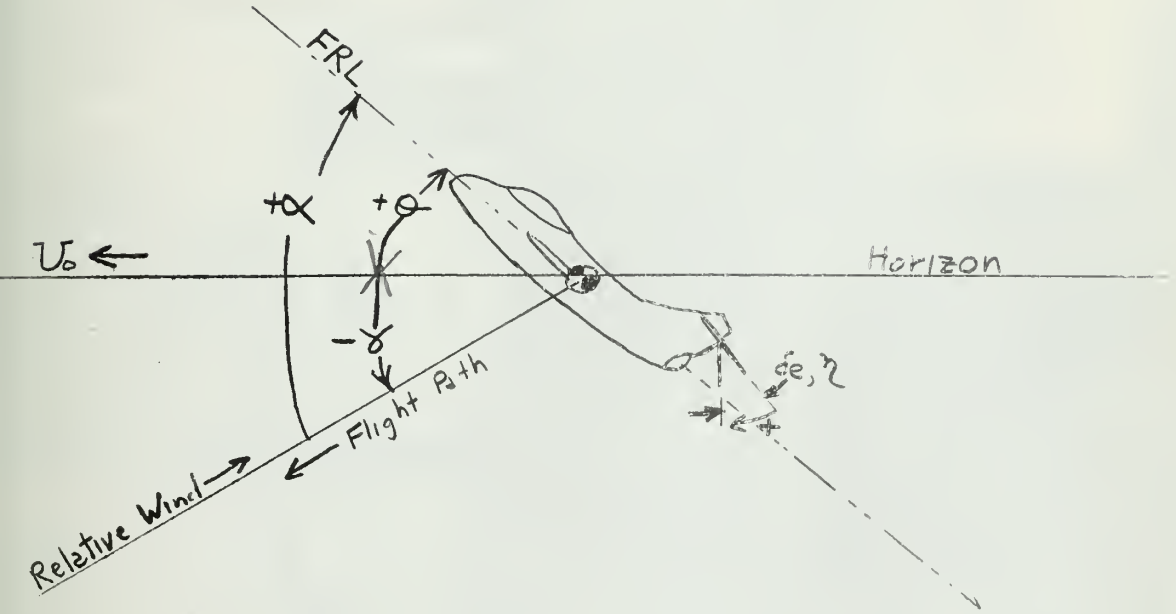

Fig. 7

Angular Definitions and Signs

Fig. 8
Analog Computer Setup

Fig. 9
Analog Computer Setup
39

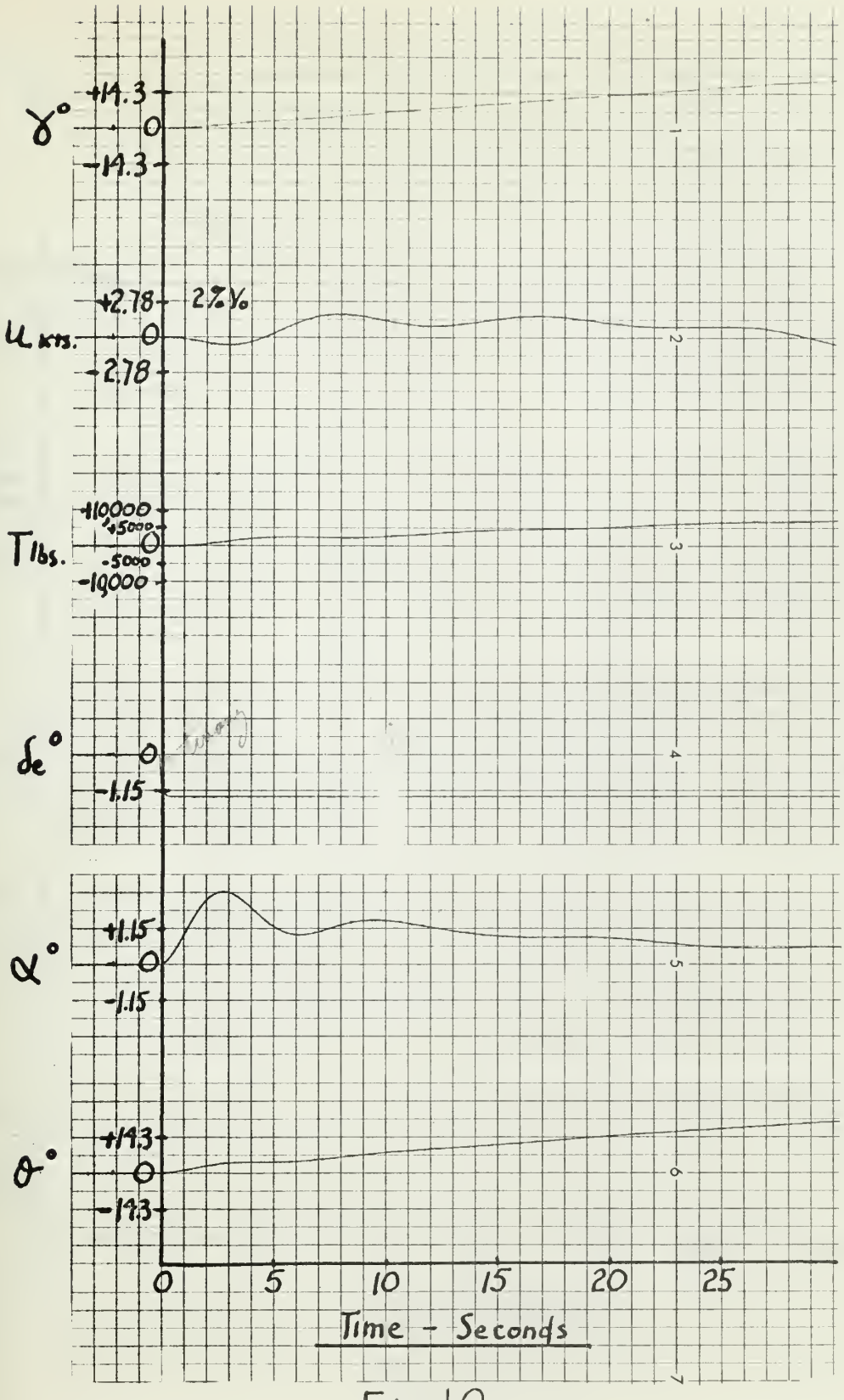

Fig. 10

Time History, 1.3° Up Elevator Deflection Input, System 1-a

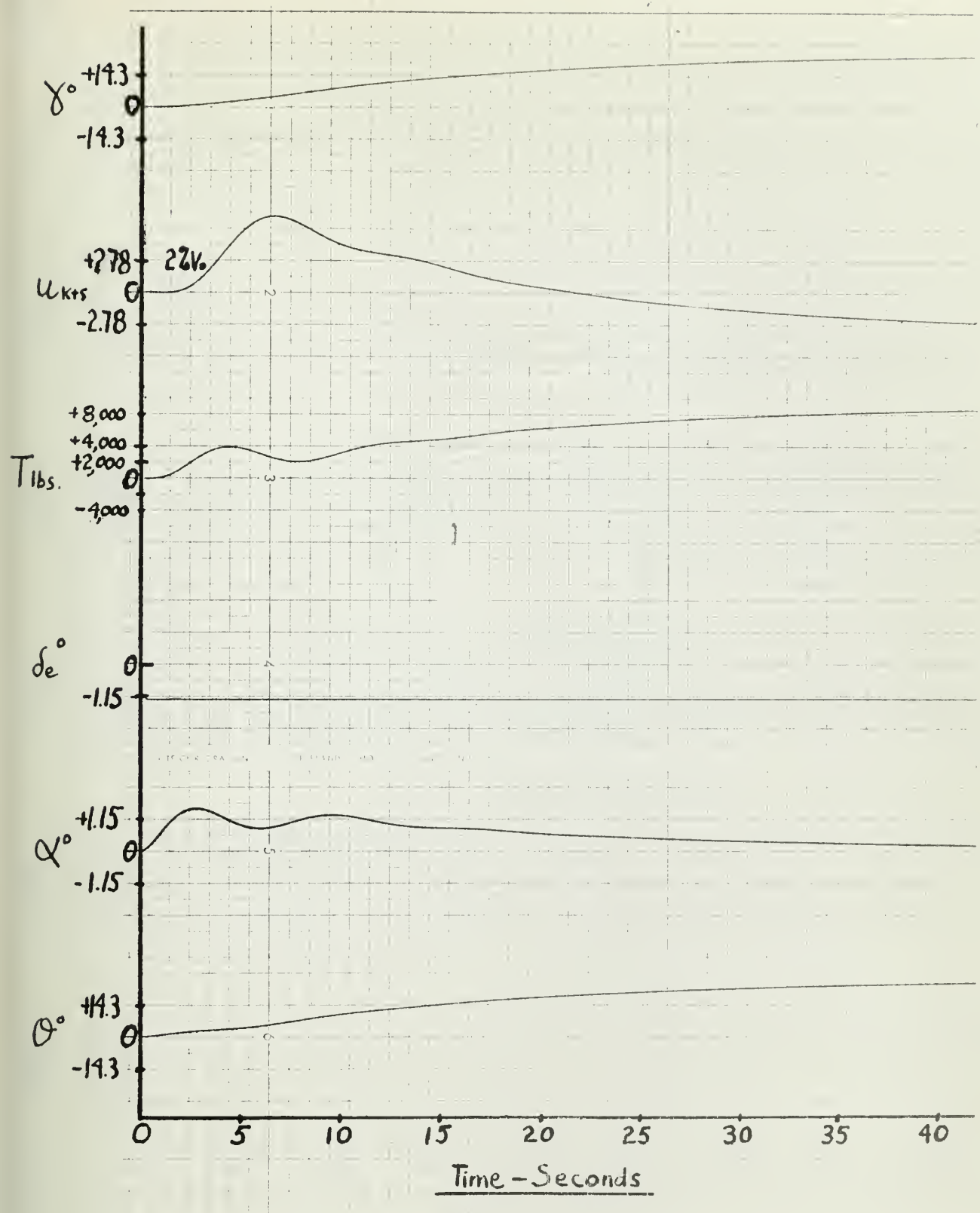

Fig. 11

Time History, 1.3° Up Elevator Deflection Input, System 1-b

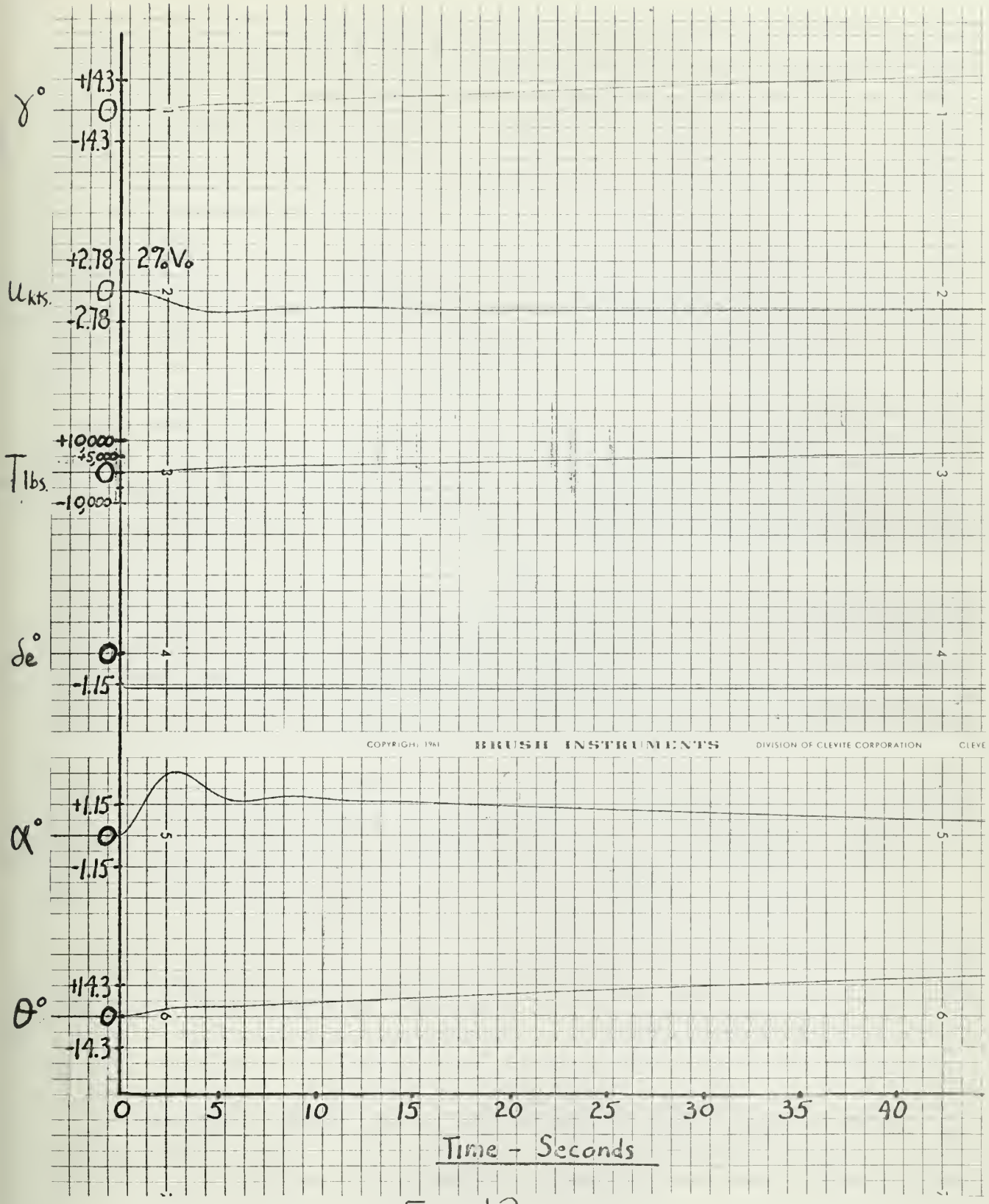

Fig. 12

Time History, 1.3° Up Elevator Deflection Input,
System 2 i.e θ, Δu

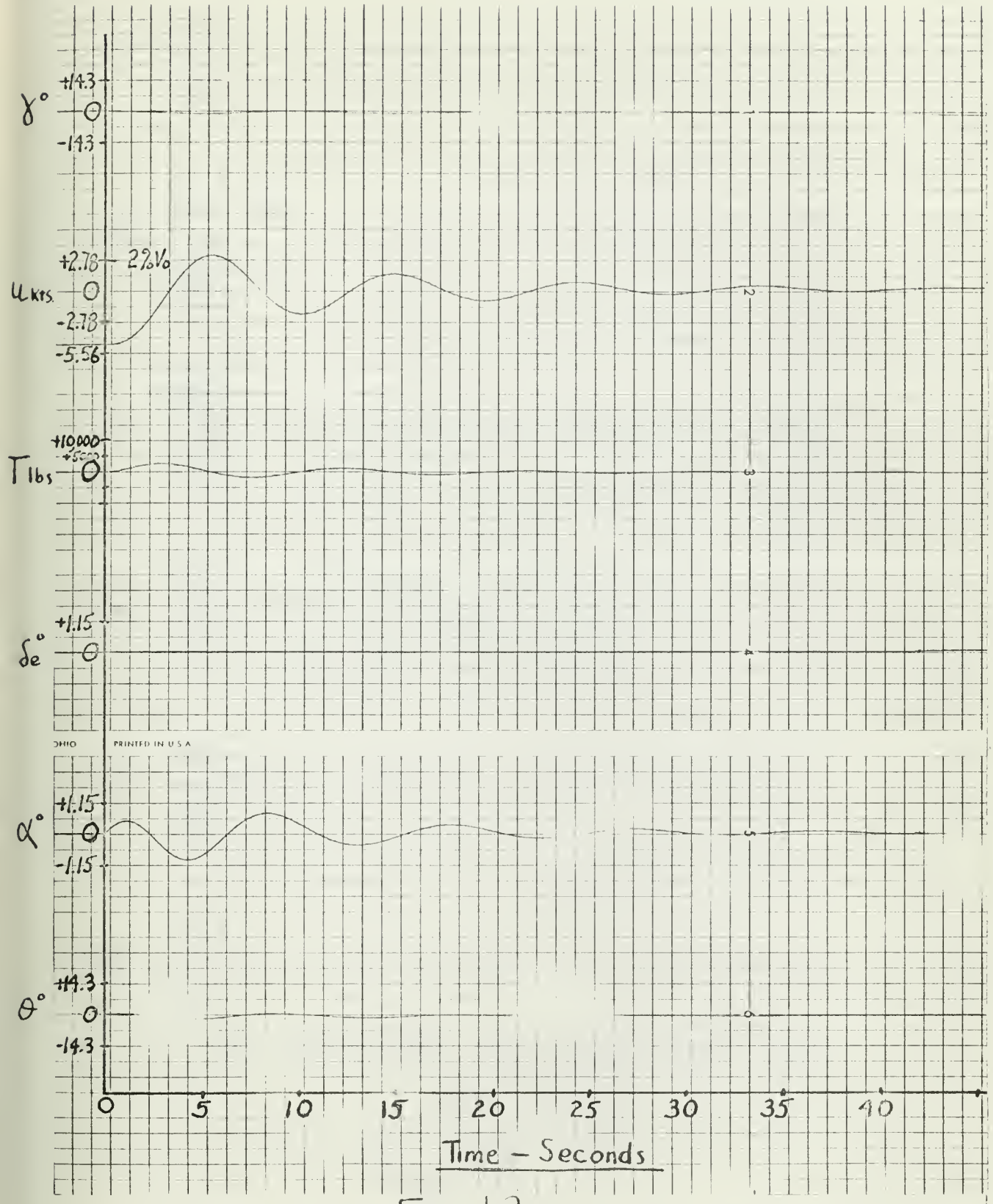

Fig. 13

Time History, 5 Knots Horizontal Gust Input, System 1-a

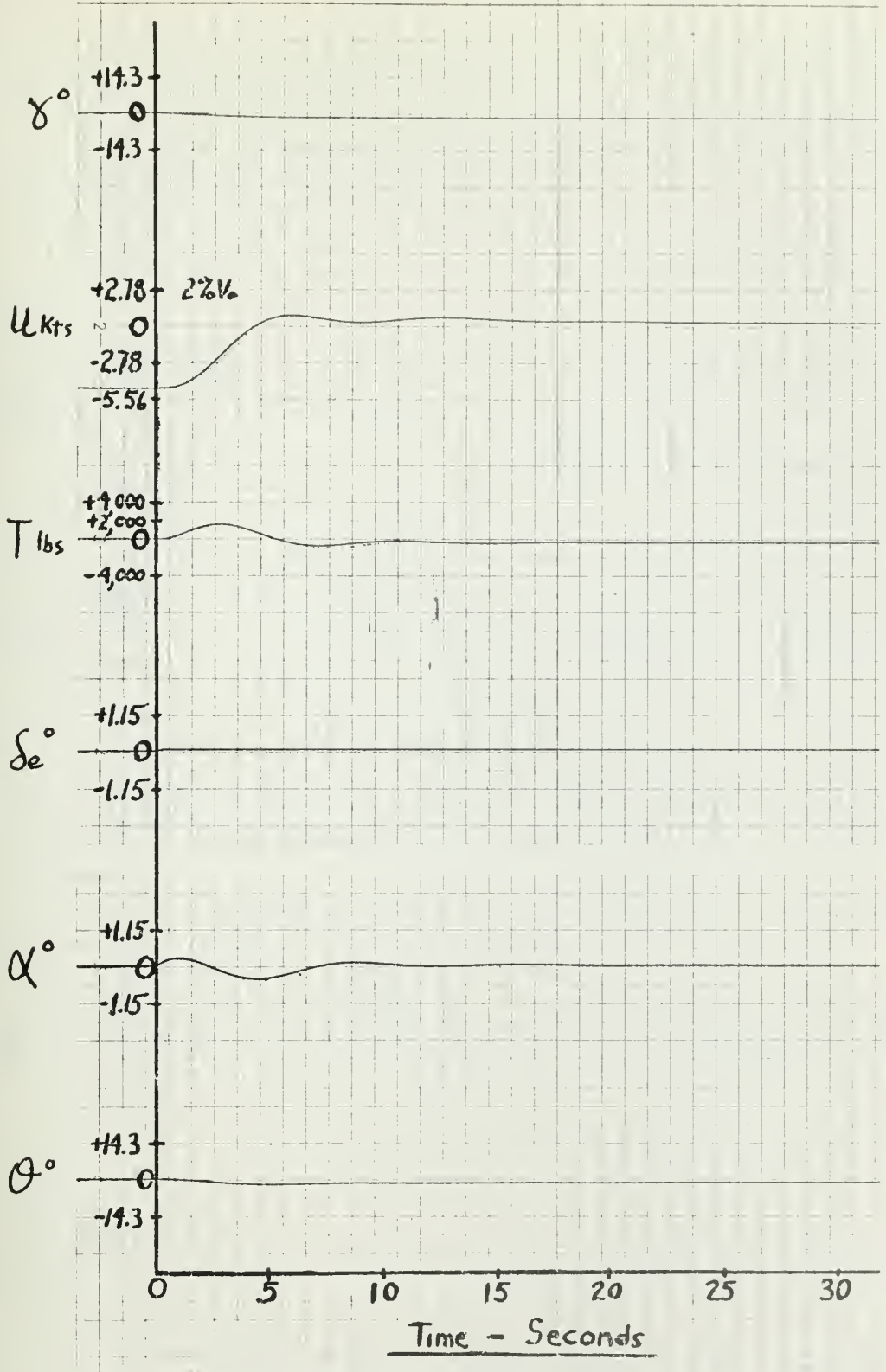

Fig. 14

Time History, 5 Knots Horizontal Gust Input, System 1-b

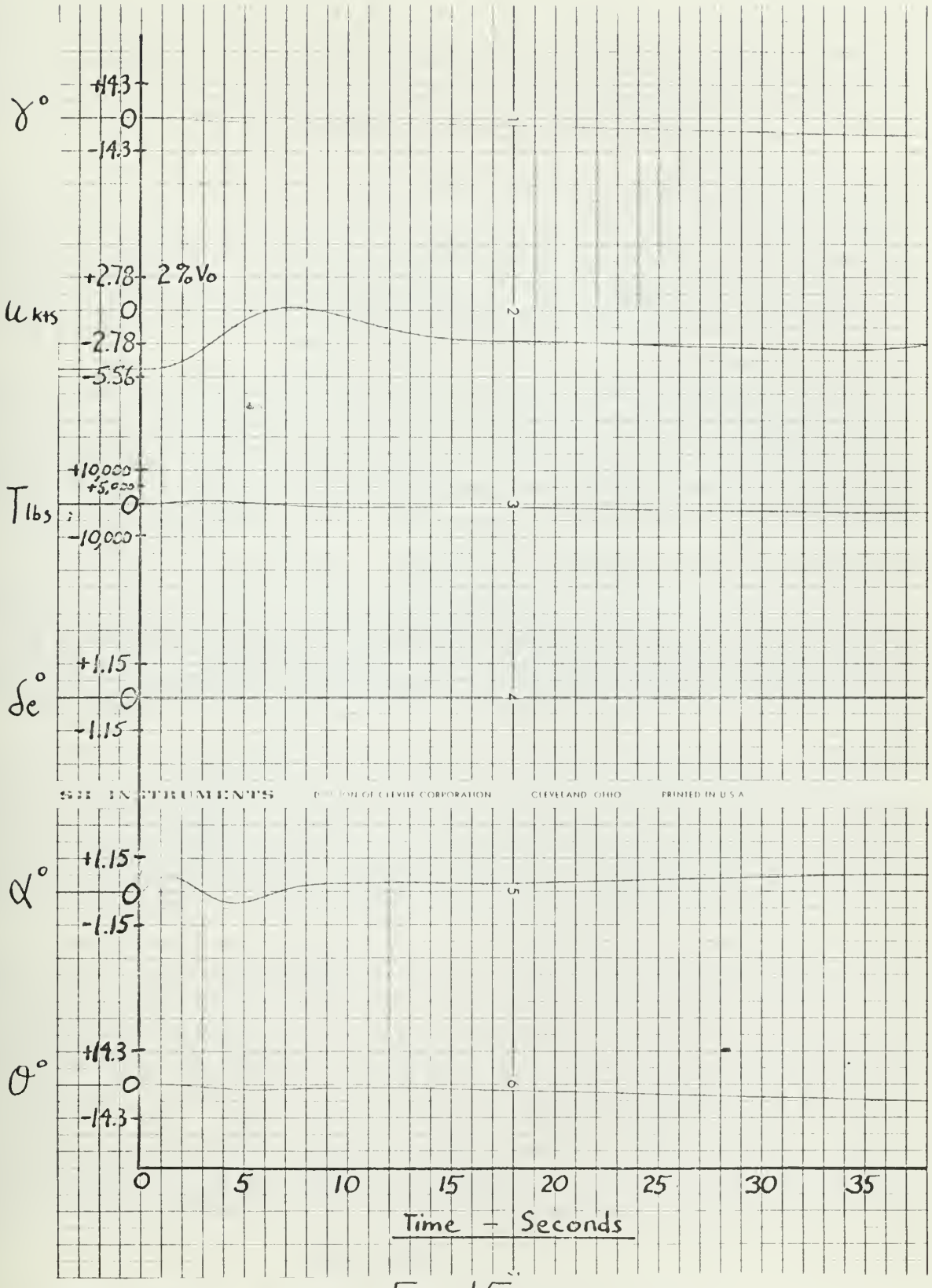

Fig. 15

Time History, 5 Knots Horizontal Gust Input, System 2

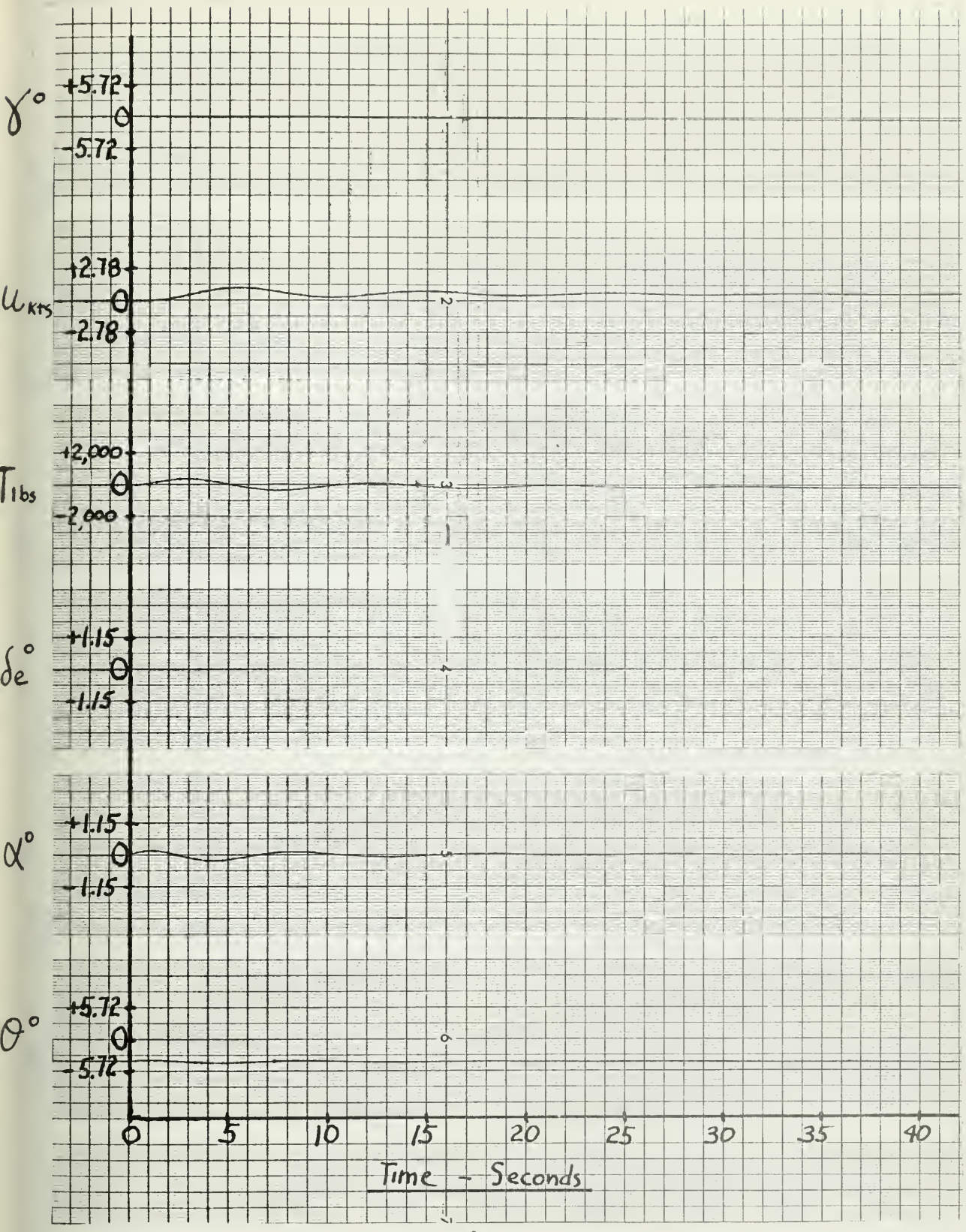

Fig. 16

Time History, 4° Step Input Pitch Angle, θ,
System 1-a

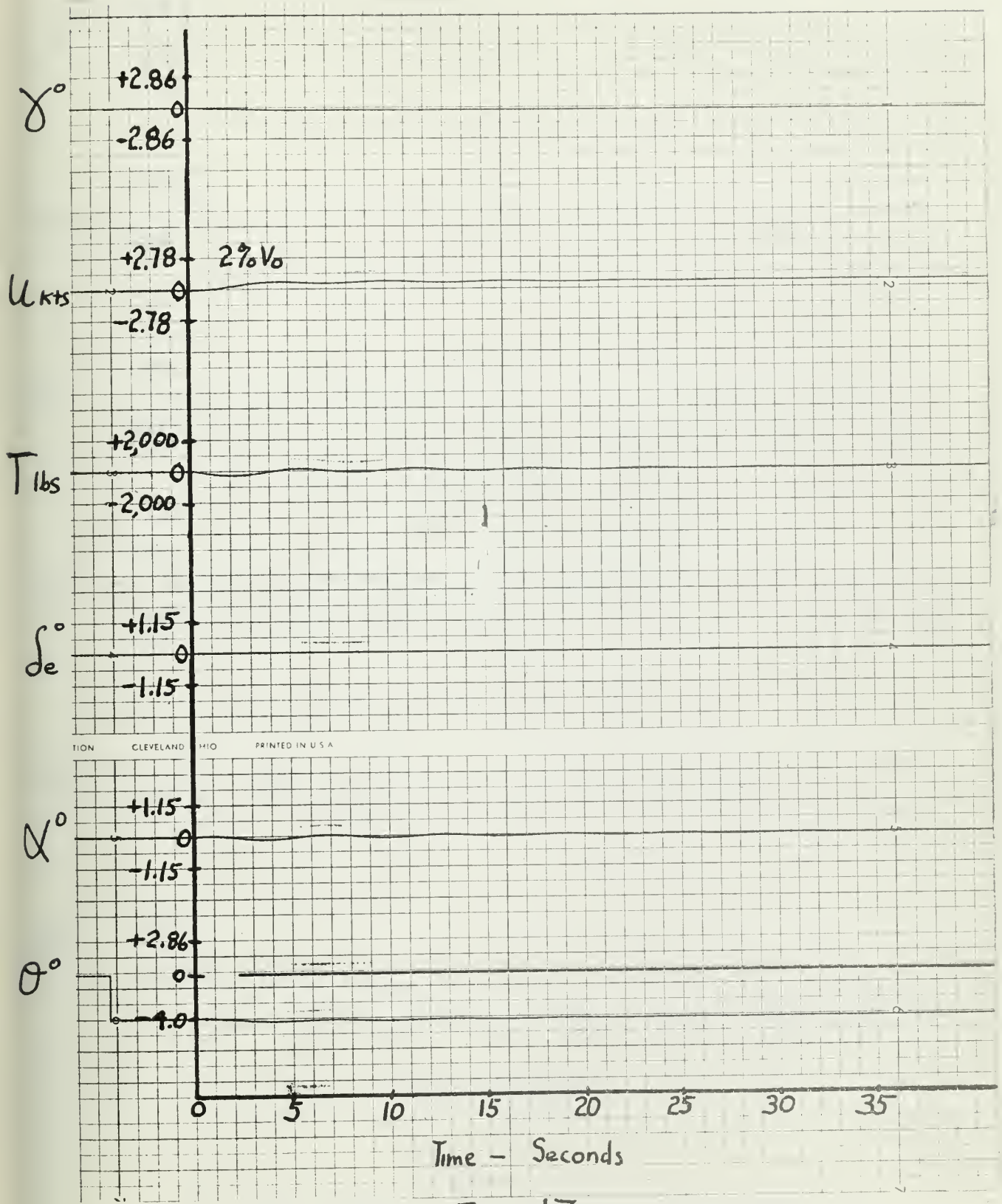

Fig. 17

Time History, 4° Step Input Pitch Angle, θ,
System 1-b

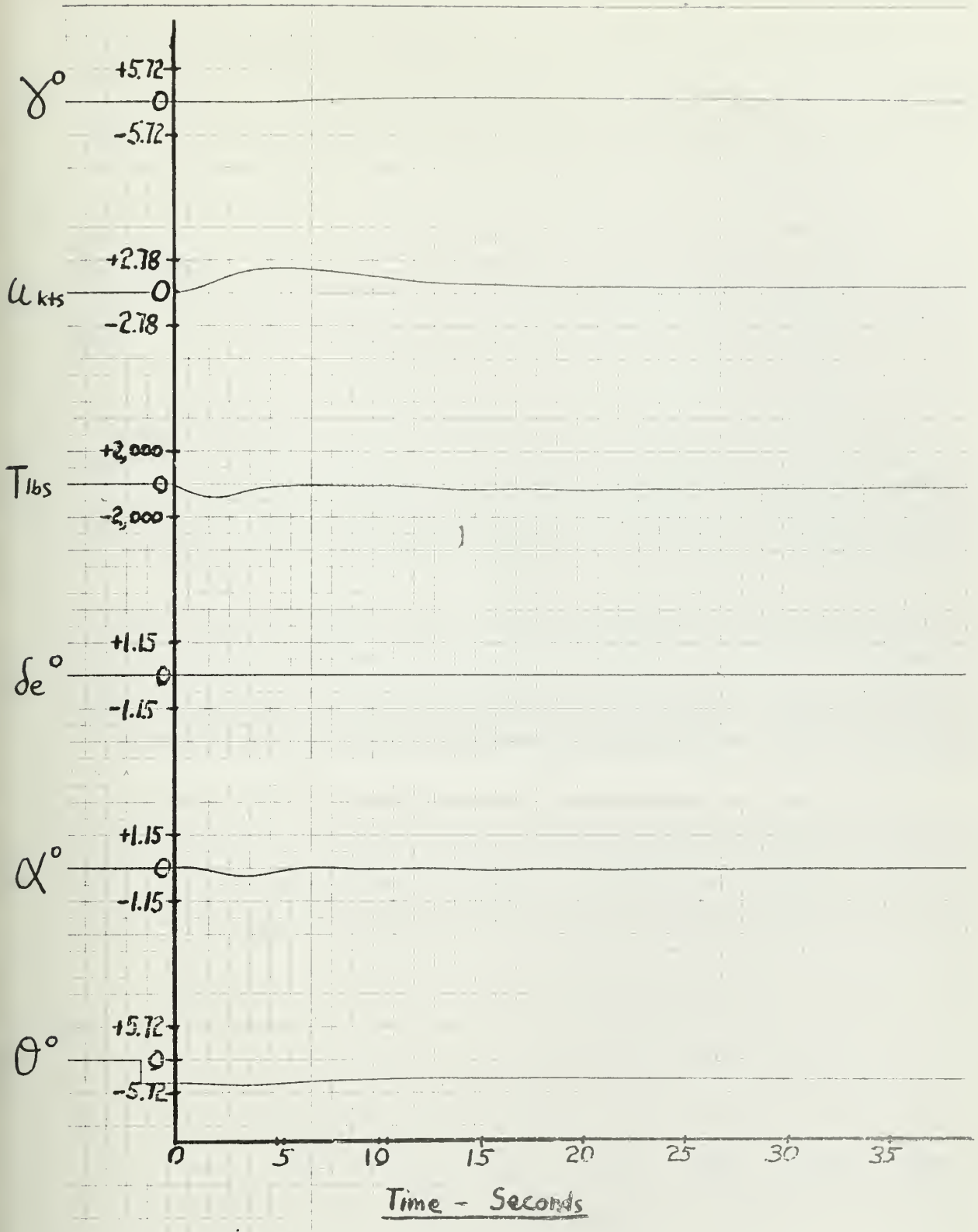

Fig. 18

Time History, 4° Step Input Pitch Angle, θ, System 2

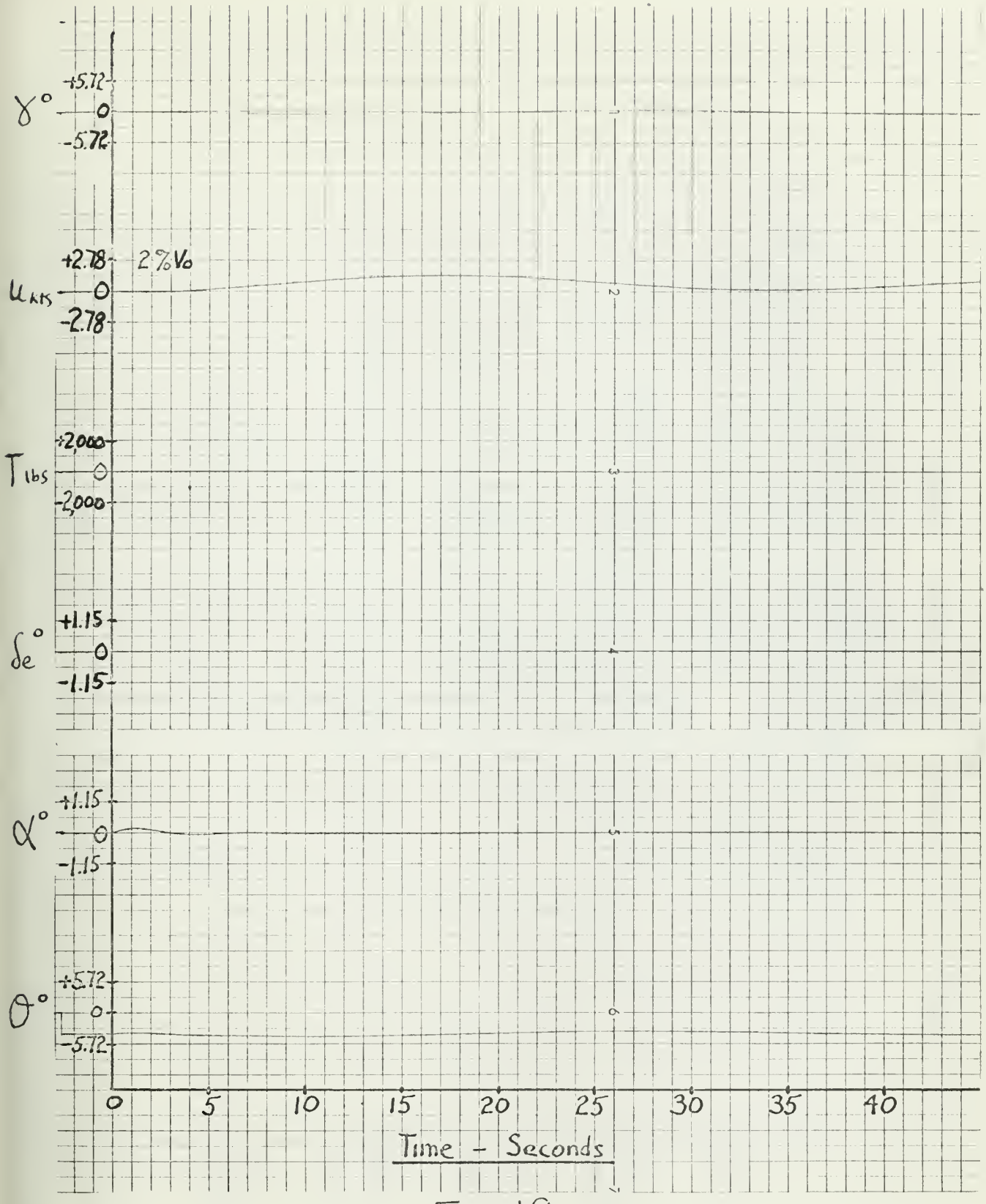

Fig. 19

Time History, 4° Step Input Pitch Angle, θ,

Basic Airframe

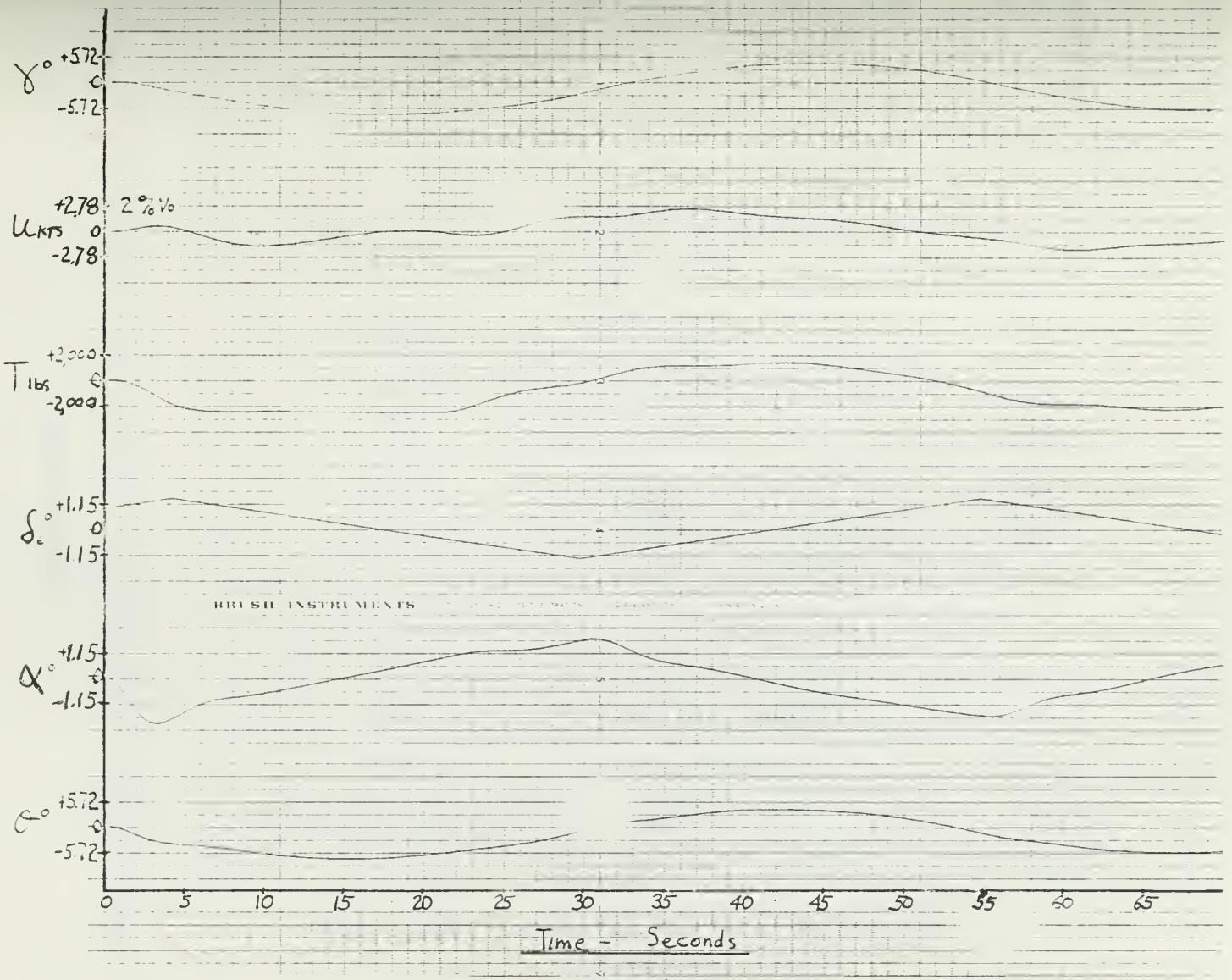

Fig. 20

Time History, .02 cps. Triangular 1.32° Elevator Deflection Input, System 1-a

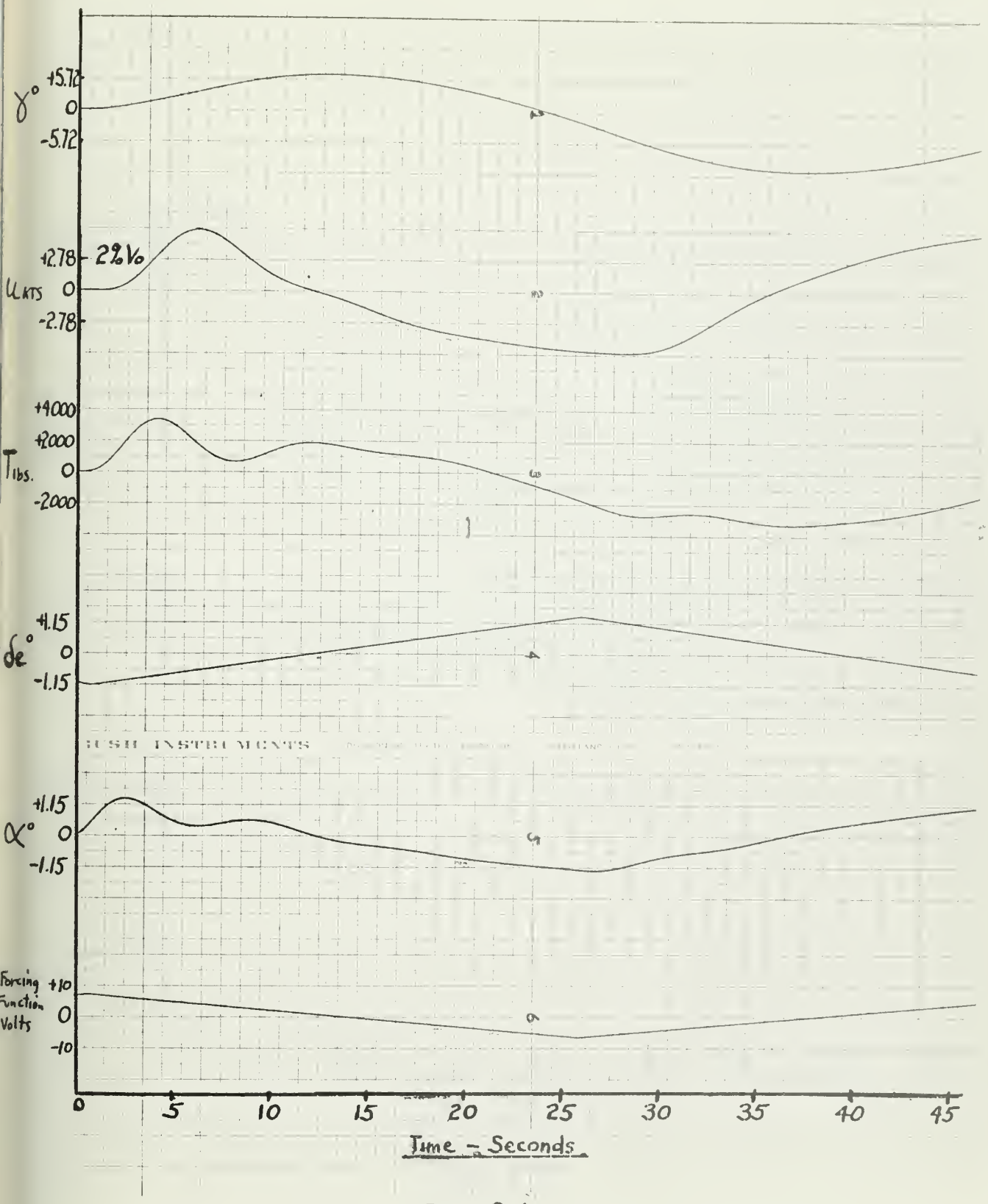

Fig. 21

Time History, .02 cps. Triangular 1.32° Elevator Deflection Input, System 1-b.

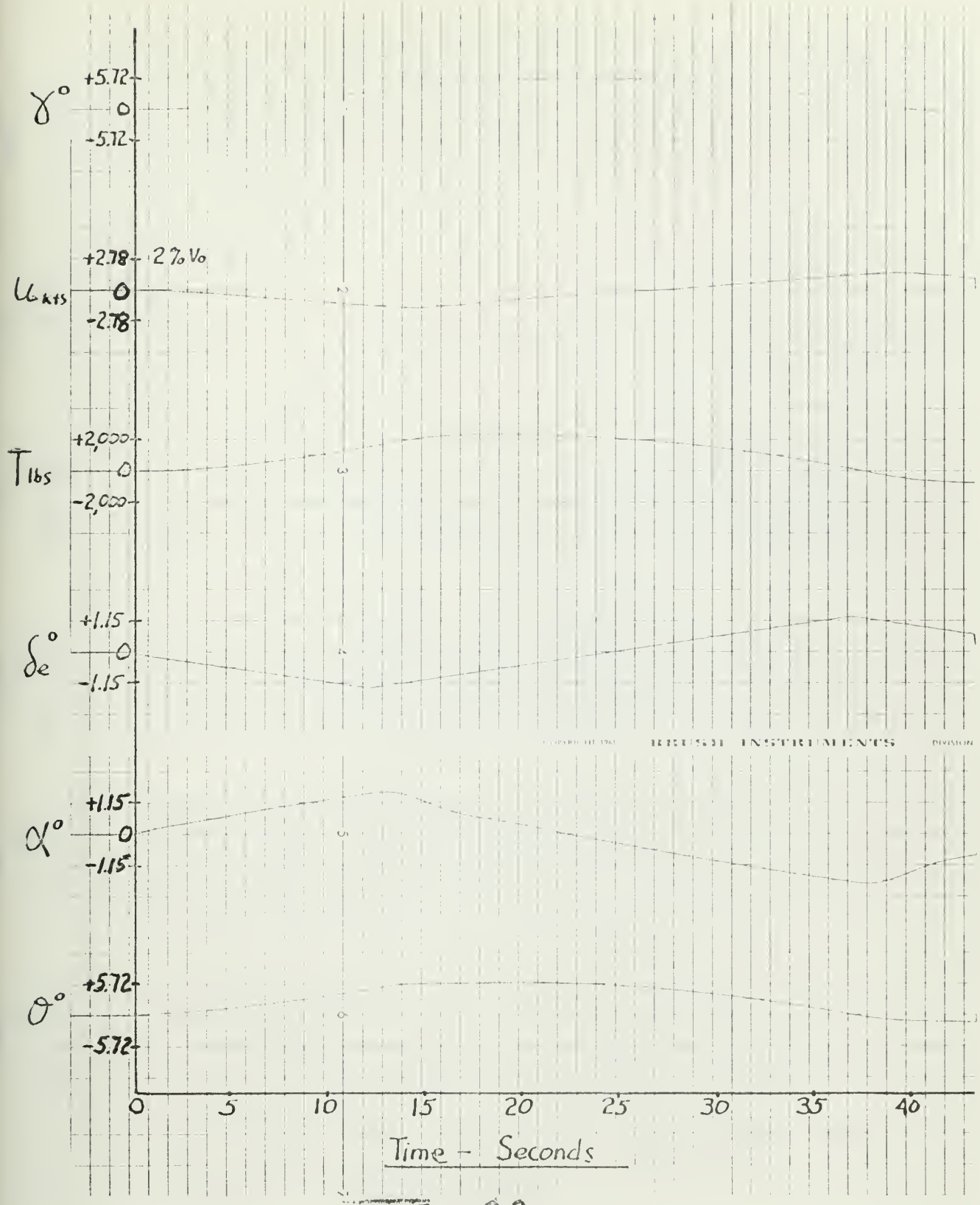

Fig. 22

Time History, .02 cps. Triangular 1.32°
Elevator Deflection Input, System 2

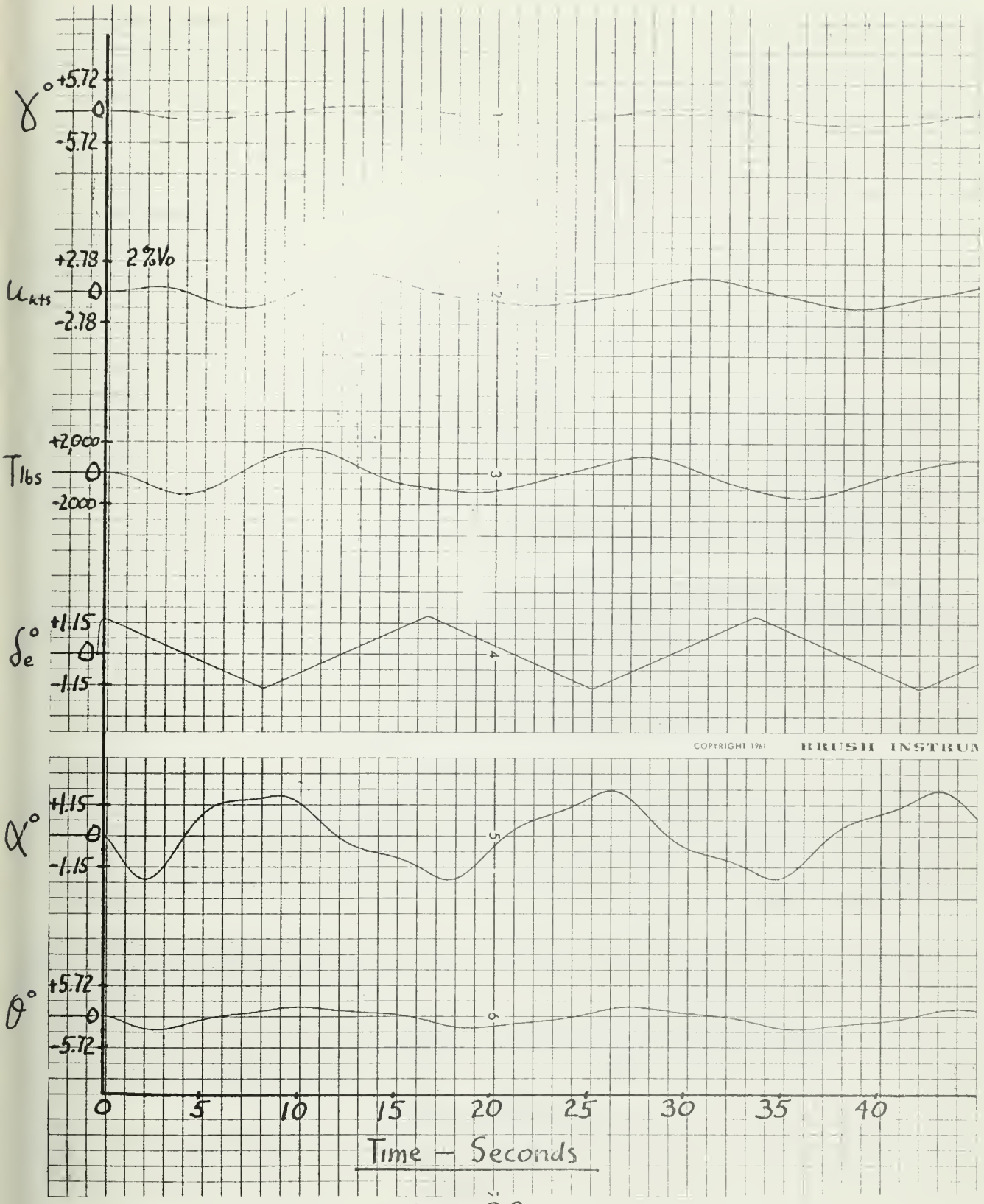

Fig. 23

Time History, .06 cps Triangular 1.32° Elevator Deflection Input, System 1-a

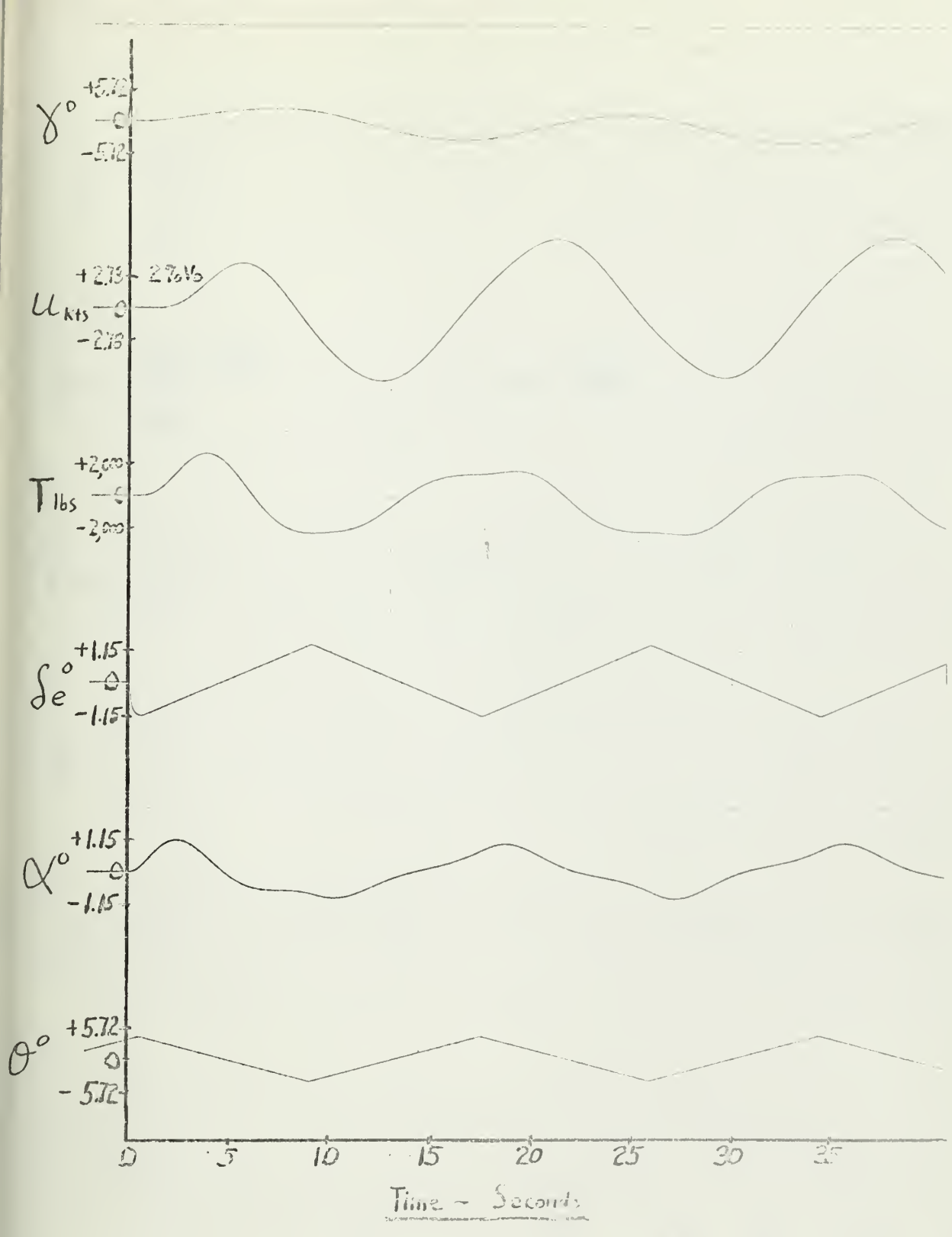

Fig. 24

Time History, .06 cps. Triangular 1.52° Elevator Deflection Input, Section 4-b

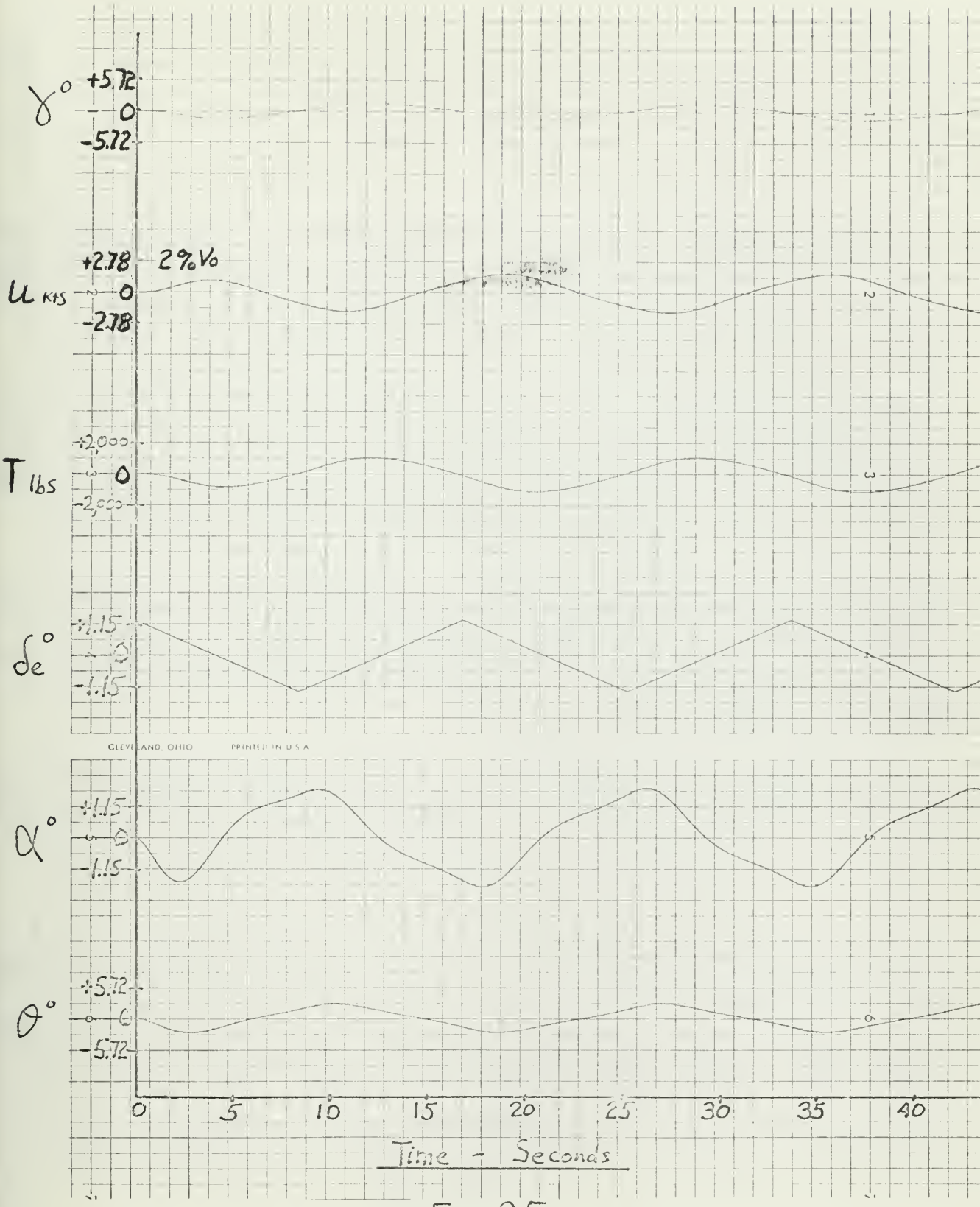

Fig. 25

Time History, .06 cps. Triangular 1.32° Elevator Deflection, Input, System 2

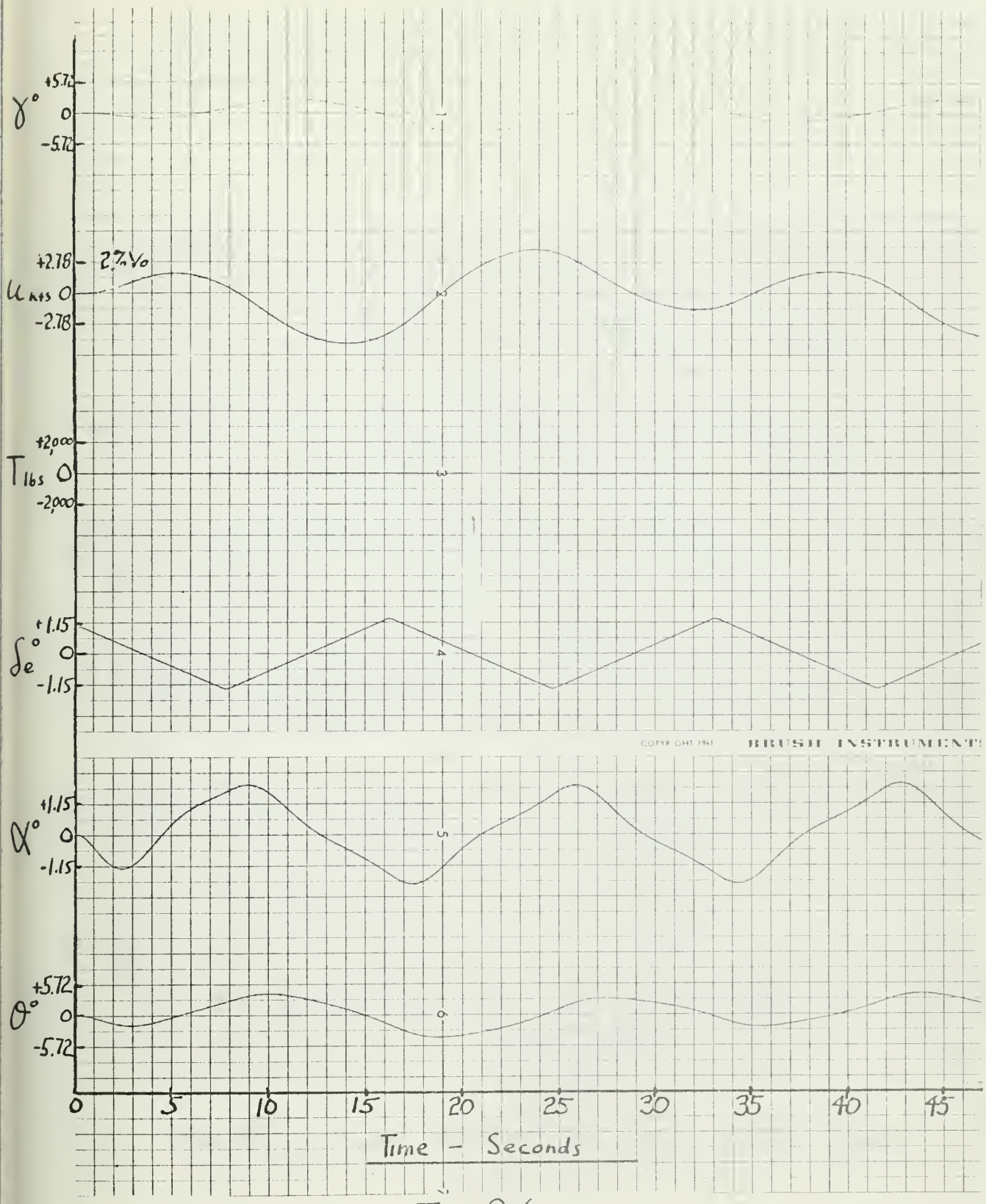

Fig. 26

Time History, .06 cps. Triangular 1.32° Elevator Deflection Input, Basic Airframe

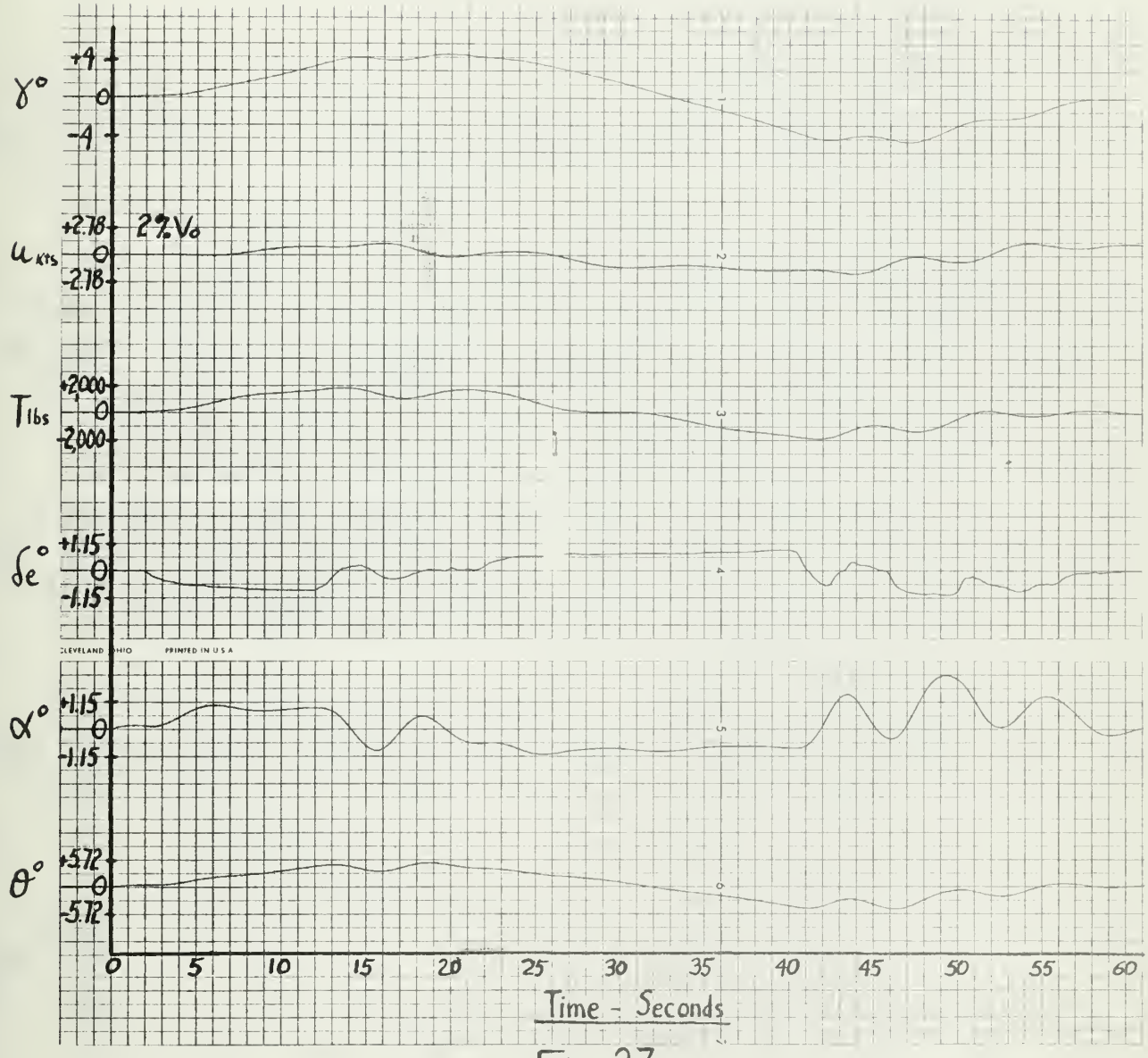

Fig. 27

Time History, Human Pilot Controlled Flight on Glide Slope, System 1-a

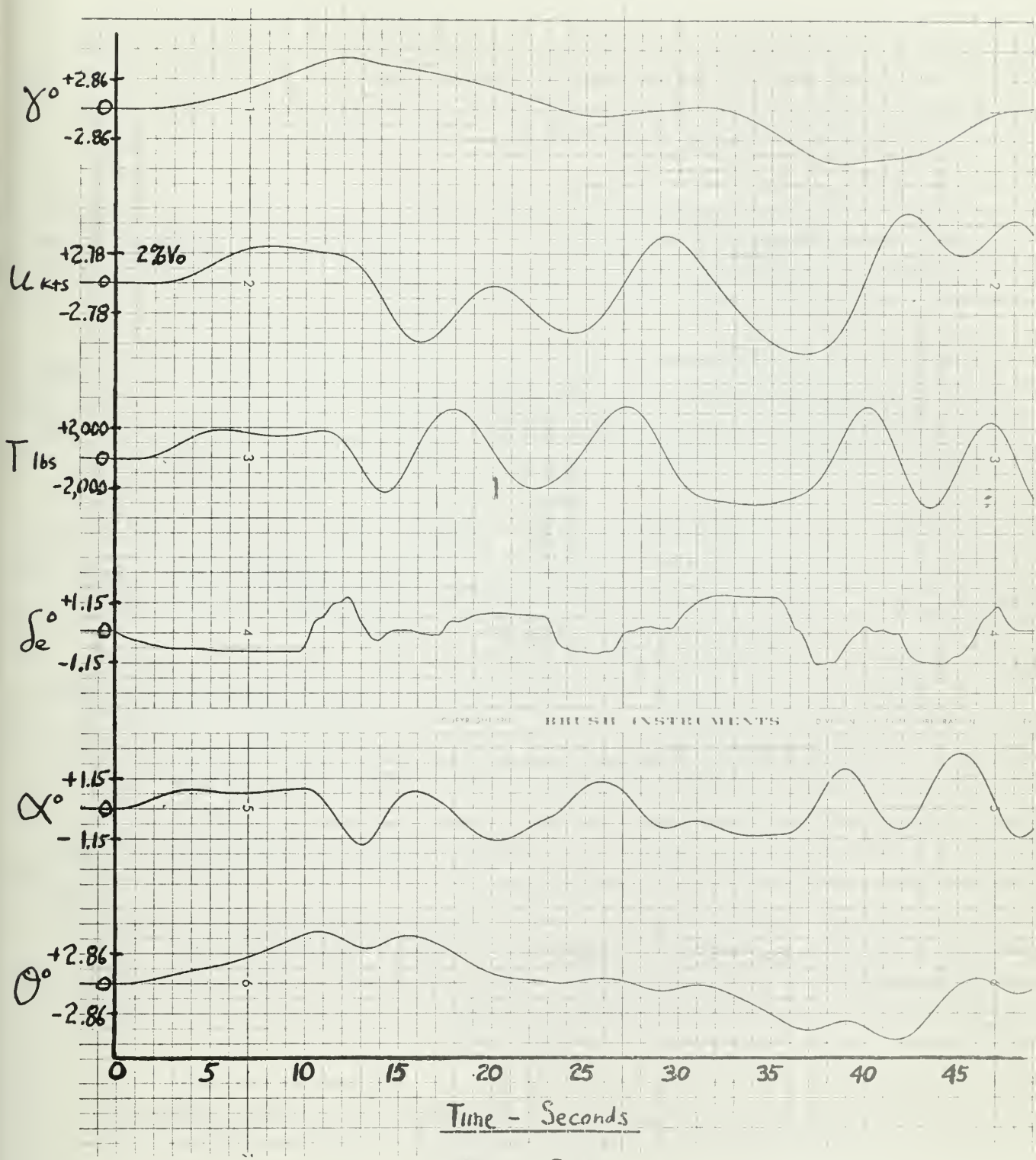

Fig. 28

Time History, Human Pilot Controlled Flight on Glide Slope, System 1-b

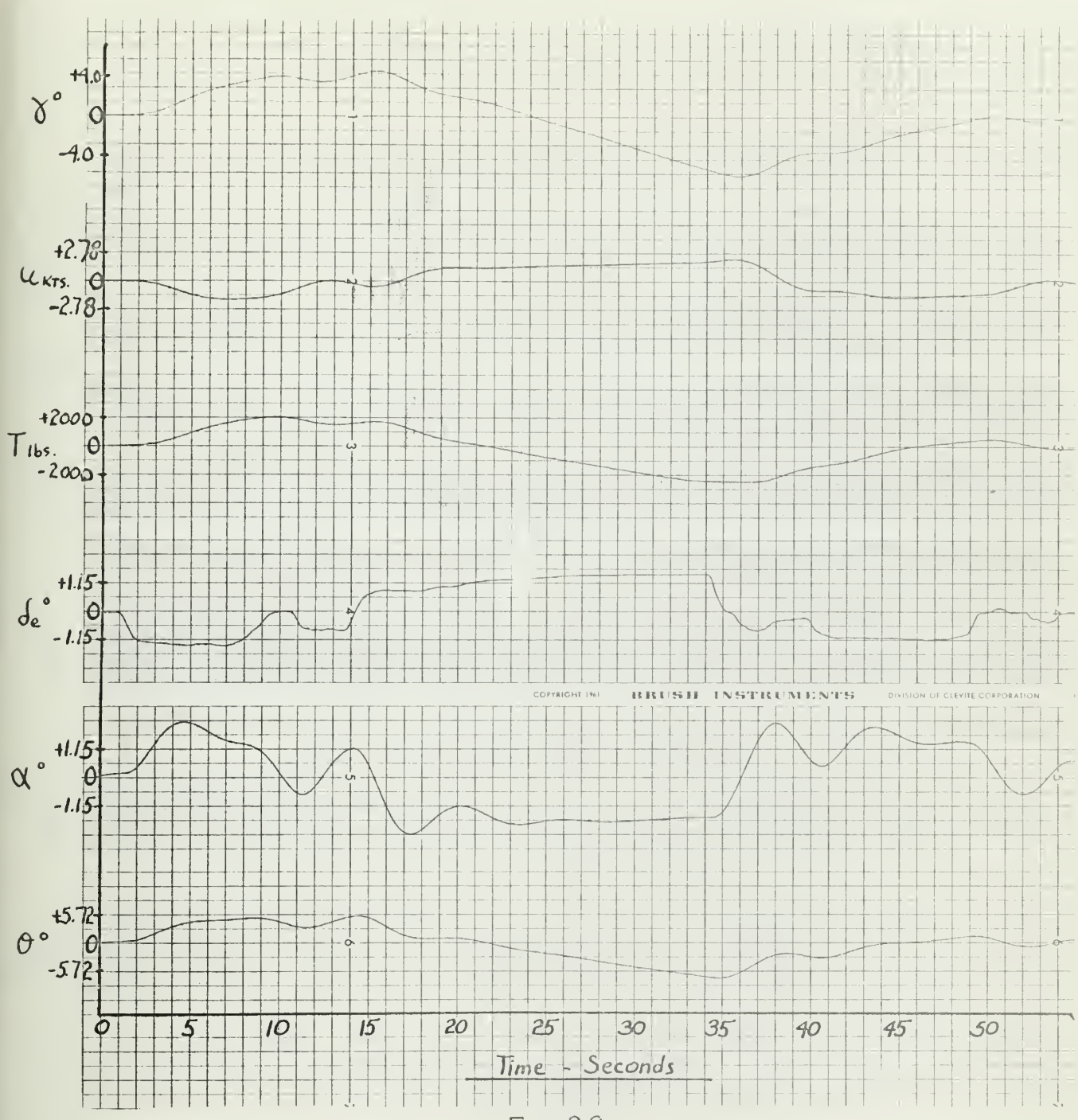

Fig. 29

Time History, Human Pilot Controlled Flight on Glide Slope, System 2.

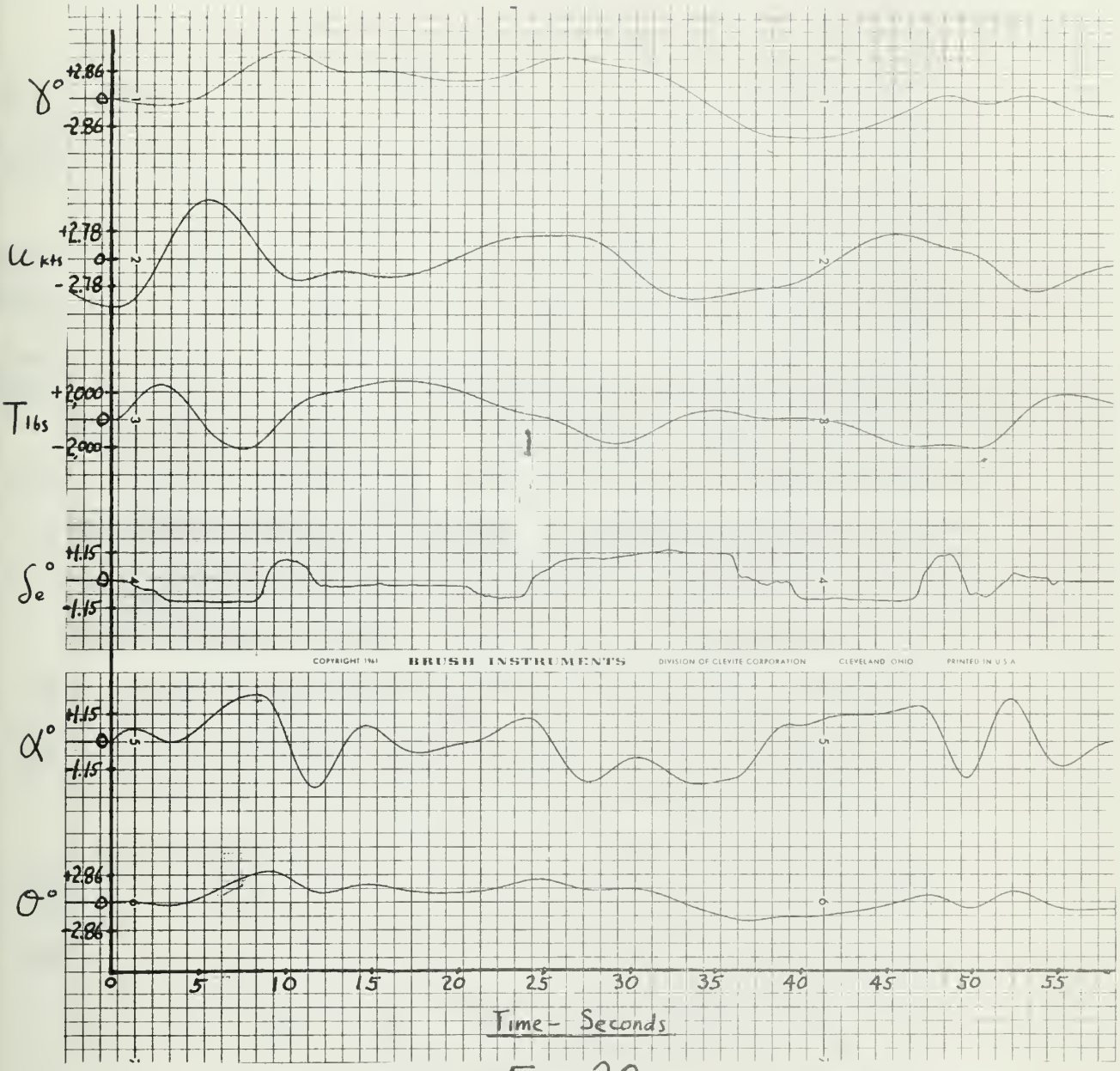

Fig. 30

Time History, Human Pilot Controlled Flight on Glide Slope, Sinusoidal Input of 5 Knots Horizontal Gust, System 1-a

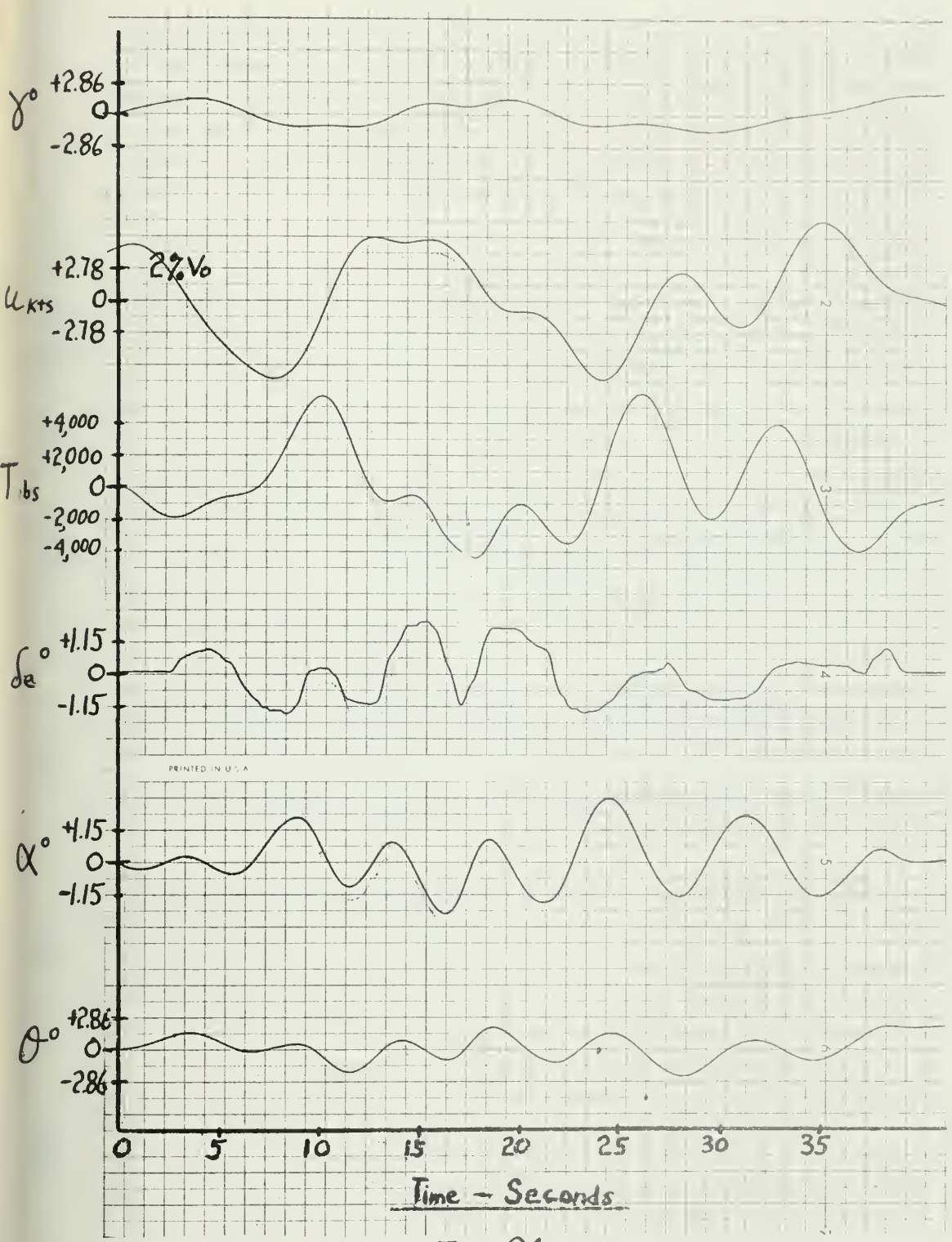

Fig. 31

Time History, Human Pilot Controlled Flight on Glide Slope, Sinusoidal Input of 5 Knots Horizontal Gust, System 1-b

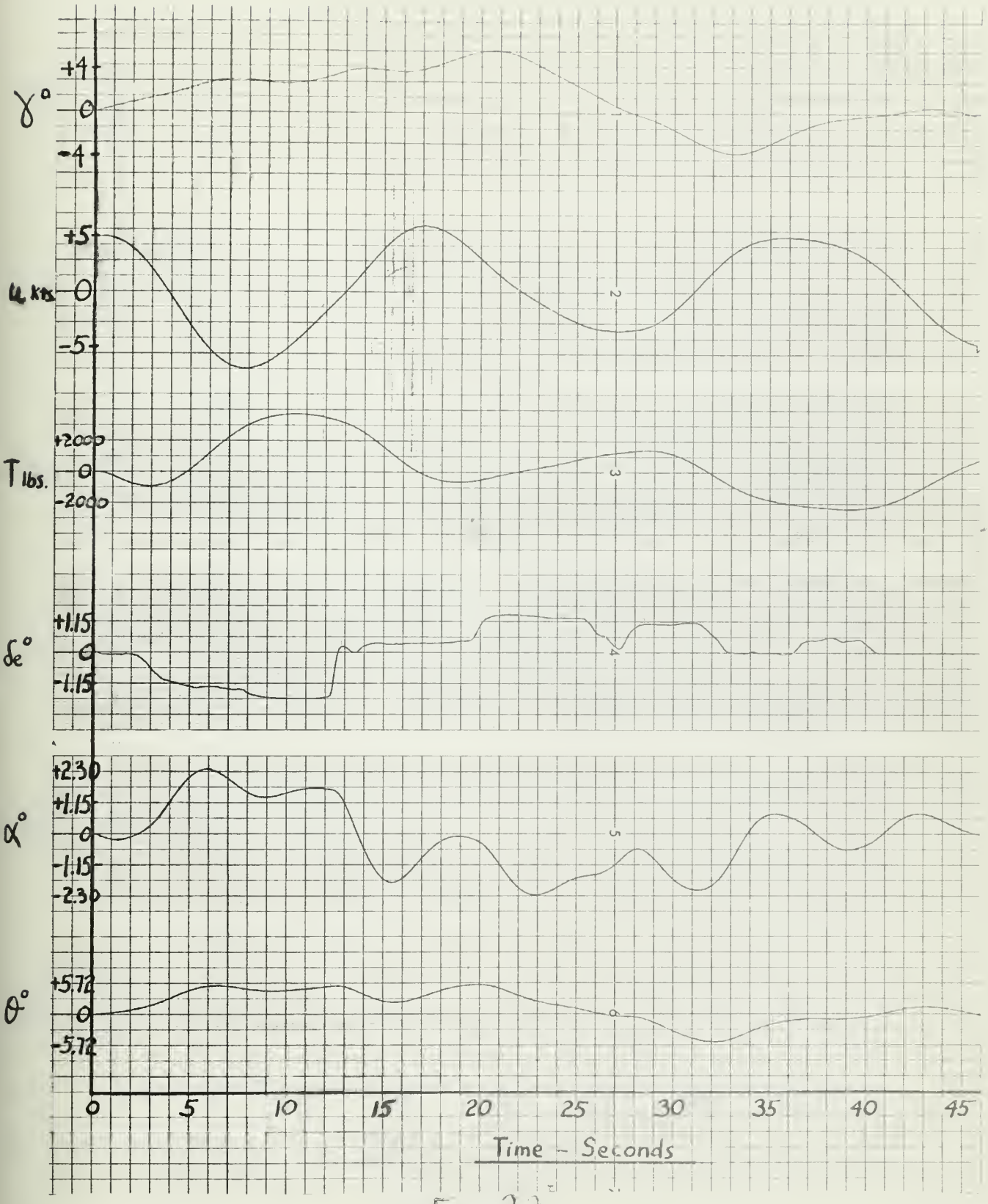

Fig. 32

Time History, Human Pilot Controlled Flight on Glide Slope, Sinusoidal Input of 5 Knots Horizontal Gust, System 2.

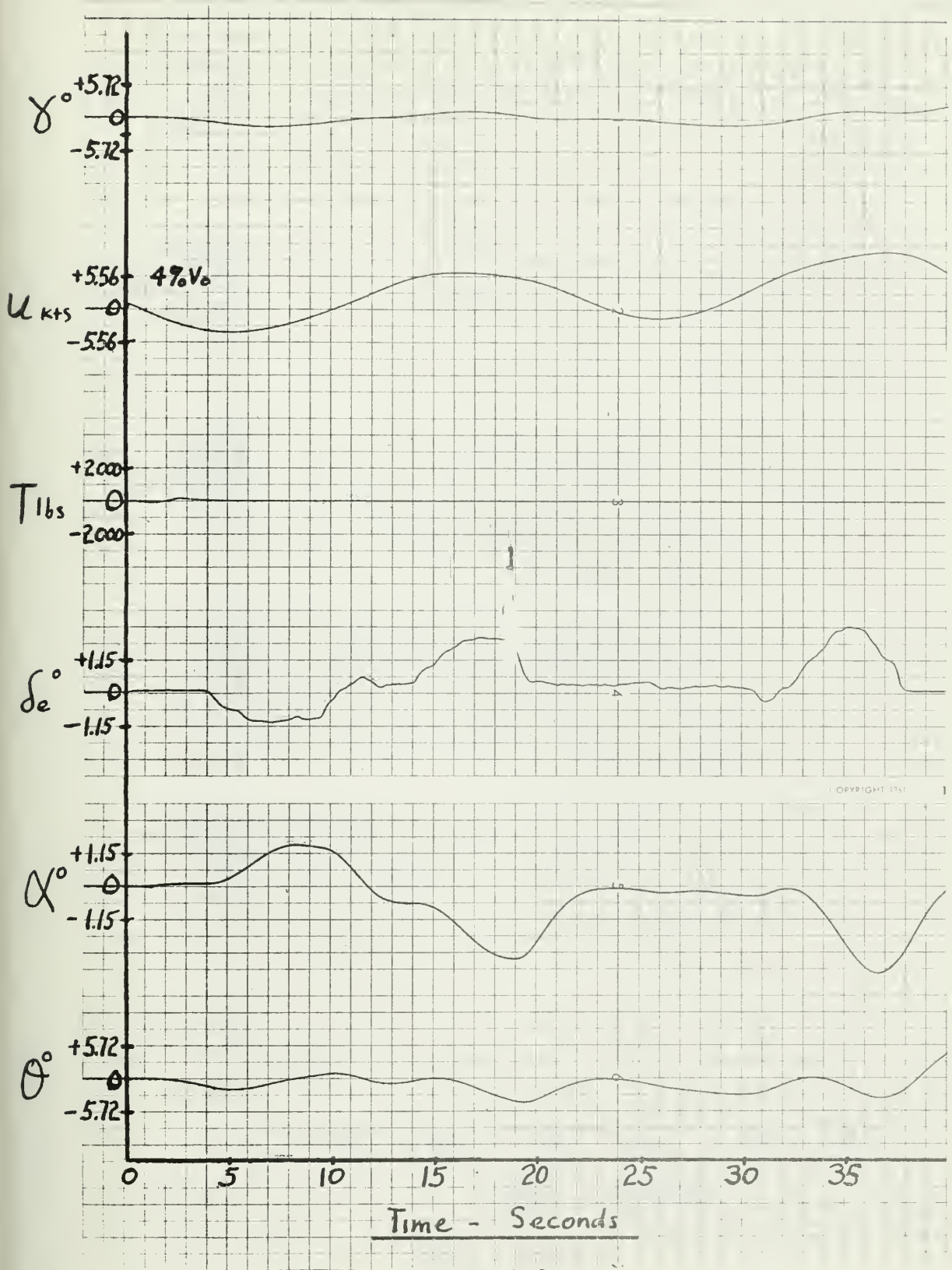

Fig. 33

Time History, Human Pilot Controlled Flight on Glide Slope, Sinusoidal Input of 5 Knots Horizontal Gust, Without Auto-Throttle

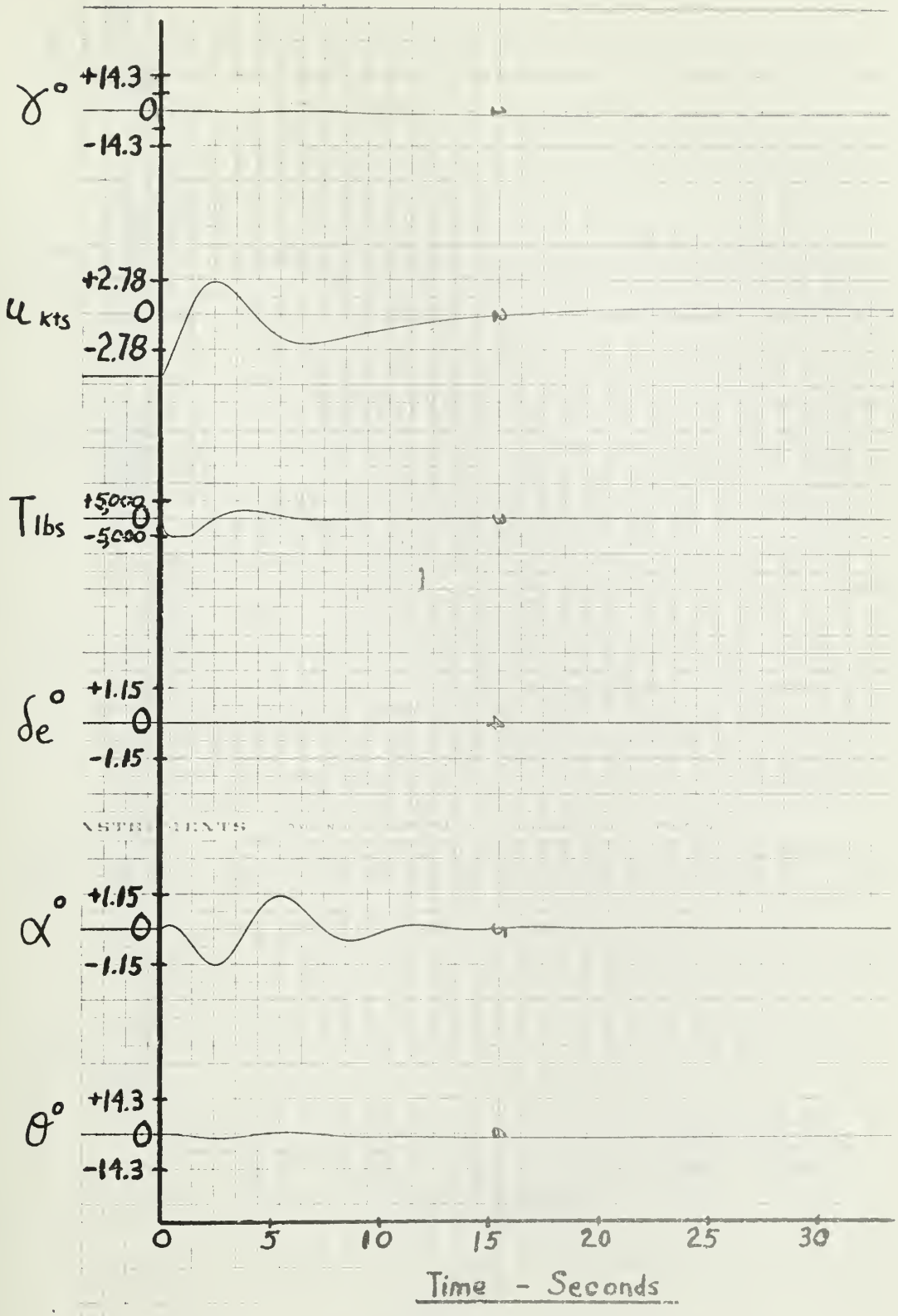

Fig. 34

Time History, 5* Knots Horizontal Gust Input,
Anti-Thrust System

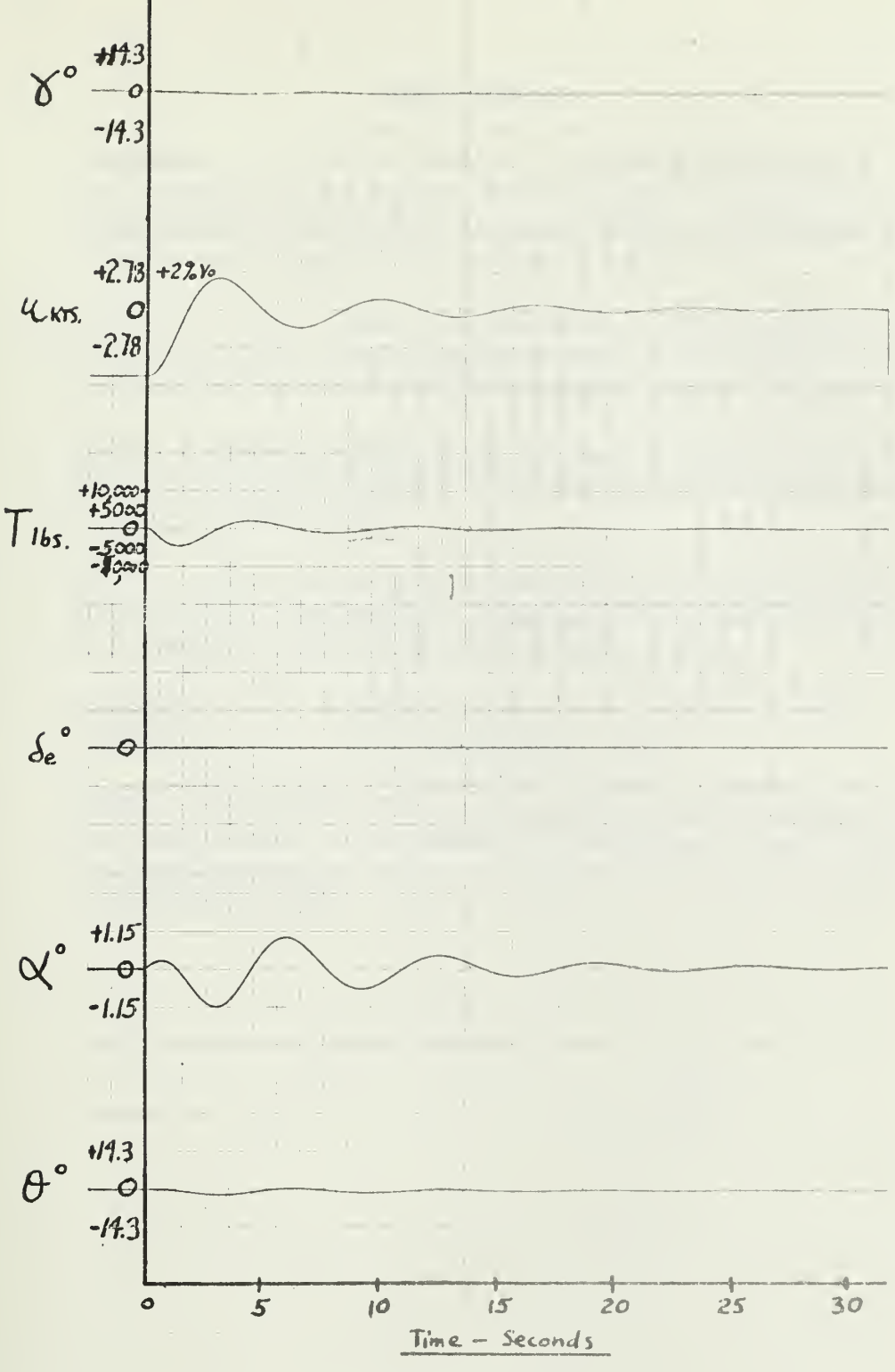

Fig. 35

Time History, 5 Knots Step Horizontal Gust Input, Anti-Thrust System with Changed Gain Constants

BIBLIOGRAPHY

1. Drinkwater, Fred J. III, George E. Cooper and Maurice D. White, An Evaluation of the Factors Which Influence the Selection of Approach Speeds, Advisory Group for Aeronautical Research and Development, Report 230, October, 1958.

2. Lean, D., and R. Eaton, The Influence of Drag Characteristics on the Choice of Landing Approach Speeds, Advisory Group for Aeronautical Research and Development, Report 122, May, 1957.

3. Anon., Dynamic Stability of an Airplane in Straight Flight with Plane of Symmetry Vertical, Royal Aeronautical Society, Aircraft 00.00.02, July, 1947.

4. Anon., Model F8U-2N Airplane Landing Configuration Data, Chance Vought Corporation, Division of Ling-Temco-Vought Inc., Report 2-53300/2L2048, September, 1962.

5. Richards, D. B., Approach Power Control System - F8U, Specialties, Inc., ltr of 4 September, 1962.

6. Anon., Comparison of Two Automatic Throttle Controllers for the F8U-2NE Aircraft, U. S. Naval Air Development Center, Engineering Development Laboratory Report No. NADC-ED-L6292, 30 November, 1962.

APPENDIX I

Derivation of Transfer Functions

The dimensional derivatives shown in Table I were used to calculate the analytic transfer functions. Calculated values of these derivatives using F8 data, are shown in Table II.

The longitudinal Equations of Motion written in Matrix Laplace Form are (neglecting negligible terms);

$$\begin{pmatrix} s-X_u & -X_w & +g \\ -Z_u & s-Z_w & -sU_o \\ -M_u & -(sM_{\dot{w}}+M_w) & s^2-M_q s \end{pmatrix} \begin{pmatrix} u(s) \\ w(s) \\ \theta(s) \end{pmatrix} = \begin{pmatrix} 0 & X_{\Delta T} \\ Z_{\delta e} & 0 \\ M_{\delta e} & M_{\Delta T} \end{pmatrix} \begin{pmatrix} \delta e \\ \\ \Delta T \end{pmatrix}$$

The Transfer function $\left(\frac{u}{\delta e}\right)$ Airframe then can be written as (in determinant form):

$$\frac{\begin{vmatrix} 0 & -X_w & +g \\ Z_{\delta e} & s-X_w & -sU_o \\ M_{\delta e} & -(sM_{\dot{w}}+M_w) & s^2-M_q s \end{vmatrix}}{D_1} = \frac{N_u}{D_1}$$

Where D_1 = determinant of homogeneous equations

Expanded $D_1 = As^4 + Bs^3 + Cs^2 + Ds + E$

Where A = 1

$$B = -(M_q + X_u + Z_w + U_o M_{\dot{w}})$$

$$C = M_q Z_w - U_o M_w + X_u(M_q + Z_w + U_o M_{\dot{w}}) - X_w Z_u$$

$$D = -X_u(M_q Z_w - U_o M_w) - M_u U_o X_w + M_q X_w Z_u + g(M_{\dot{w}} Z_u + M_u)$$

$$E = g(M_w Z_u - M_u Z_w)$$

Expanded $N_u = B_u s^2 + C_u s + D_u$

Where $B_u = Z_{\delta e} X_w$

$C_u = -Z_{\delta e}(g M_{\dot{w}} + M_q X_w) + M_{\delta e}(U_o X_w - g)$

$D_u = g(M_{\delta e} Z_w - M_w Z_{\delta e})$

Substituting values for these derivatives

$$\left(\frac{u}{\delta e}\right)_{Airframe} = \frac{.1971[s^2 + 450s + 85.2]}{s^4 + .865s^3 + 11.529s^2 + .696s + .416} = \frac{N_u}{D_1}$$

By a similar procedure,

$$\left(\frac{\theta}{\delta e}\right)_{Airframe} = \frac{-2.50[s^2 + .2155s + .00568]}{D_1}$$

(Positive elevator deflection is down)

The determinant for calculating $\left(\frac{u}{\Delta T}\right)_{Airframe}$ can be written as

$$\frac{\begin{vmatrix} X_{\Delta T} & -X_w & +g \\ 0 & s - Z_w & -sU_o \\ M_{\Delta T} & -(sM_{\dot{w}} + M_w) & s^2 - M_q s \end{vmatrix}}{D_1}$$

Expanded:

$$\left(\frac{u}{\Delta T}\right)_{Airframe} = \frac{A_T s^3 + B_T s^2 + C_T s + D_T}{D_1}$$

Where

$A_T = X_{\Delta T}$

$B_T = -X_{\Delta T}[Z_w + M_q] + U_o M_{\dot{w}}$

$C_T = X_{\Delta T}[Z_w M_q - U_o M_w] + M_{\Delta T}[U_o X_w - g]$

$D_T = M_{\Delta T} g Z_w$

After substituting in values:

$$\left(\frac{u}{\Delta T}\right)_{Airframe} = \frac{.00145[s^3 + .8049s^2 + 11.59s + .0430]}{D_1}$$

APPENDIX - I

TABLE I-A

LONGITUDINAL DIMENSIONAL STABILITY DERIVATIVE PARAMETERS

(STABILITY AXIS SYSTEM)

QUANTITY	IN TERMS OF BASIC STABILITY DERIVATIVES			IN TERMS OF NON-DIMENSIONAL STABILITY DERIVATIVE PARAMETERS
	DIMENSIONAL		NON-DIMENSIONAL	
	DEFINITIONS	UNIT		
X_u	$-\frac{1}{m}\frac{\partial X}{\partial u}$	$\frac{1}{sec}$	$-\frac{\rho SU}{m}\left(-C_D - C_{D_u}\right)$	$-\frac{1}{\tau} x_u$
X_w	$-\frac{1}{m}\frac{\partial X}{\partial w}$	$\frac{1}{sec}$	$-\frac{\rho SU}{2m}\left(C_L - C_{D_\alpha}\right)$	$-\frac{1}{\tau} x_w$
X_{δ_E}	$-\frac{1}{m}\frac{\partial X}{\partial \delta_E}$	$\frac{ft}{sec^2 rad}$	$-\frac{\rho SU^2}{2m}\left(-C_{D_{\delta_E}}\right)$	$-\frac{U}{\tau} x_{\delta_E}$
Z_u	$-\frac{1}{m}\frac{\partial Z}{\partial u}$	$\frac{1}{sec}$	$-\frac{\rho SU}{m}\left(-C_L - C_{L_u}\right)$	$-\frac{1}{\tau} z_u$
Z_w	$-\frac{1}{m}\frac{\partial Z}{\partial w}$	$\frac{1}{sec}$	$-\frac{\rho SU}{2m}\left(-C_{L_\alpha} - C_D\right)$	$-\frac{1}{\tau} z_w$
$Z_{\dot{w}}$	$-\frac{1}{m}\frac{\partial Z}{\partial \dot{w}}$	$\frac{1}{1}$	$-\frac{\rho Sc}{4m}\left(-C_{L_{\dot{\alpha}}}\right)$	$-\frac{c}{\tau U} z_{\dot{w}}$
Z_q	$-\frac{1}{m}\frac{\partial Z}{\partial q}$	$\frac{ft}{sec\text{-}rad}$	$-\frac{\rho SUc}{4m}\left(-C_{L_q}\right)$	$-\frac{c}{\tau} z_q$
Z_{δ_E}	$-\frac{1}{m}\frac{\partial Z}{\partial \delta_E}$	$\frac{1}{sec^2 rad}$	$-\frac{\rho SU^2}{2m}\left(-C_{L_{\delta_E}}\right)$	$-\frac{U}{\tau} z_{\delta_E}$
M_u	$-\frac{1}{I_y}\frac{\partial M}{\partial u}$	$\frac{1}{sec\text{-}ft}$	$-\frac{\rho SUc}{I_y}\left(C_m + C_{m_u}\right)$	$-\frac{2}{\tau c} m_u$
M_w	$-\frac{1}{I_y}\frac{\partial M}{\partial w}$	$\frac{1}{sec\text{-}ft}$	$-\frac{\rho SUc}{2I_y} C_{m_\alpha}$	$-\frac{1}{\tau c} m_w$
$M_{\dot{w}}$	$-\frac{1}{I_y}\frac{\partial M}{\partial \dot{w}}$	$\frac{1}{ft}$	$-\frac{\rho Sc^2}{4I_y} C_{m_{\dot{\alpha}}}$	$-\frac{1}{\tau U} m_{\dot{w}}$
M_q	$-\frac{1}{I_y}\frac{\partial M}{\partial q}$	$\frac{1}{sec\ rad}$	$-\frac{\rho SUc^2}{4I_y} C_{m_q}$	$-\frac{1}{\tau} m_q$
M_{δ_E}	$-\frac{1}{I_y}\frac{\partial M}{\partial \delta_E}$	$\frac{1}{sec^2 rad}$	$-\frac{\rho SU^2 c}{2I_y} C_{m_{\delta_E}}$	$-\frac{U}{\tau c} m_{\delta_E}$

APPENDIX - I

TABLE I-B

LONGITUDINAL NON-DIMENSIONAL STABILITY DERIVATIVES

(STABILITY AXIS SYSTEM)

BASIC NON-DIMENSIONAL STABILITY DERIVATIVES			NON-DIMENSIONAL STABILITY DERIVATIVE PARAMETERS
TOTAL AIRFRAME		THEORETICAL HORIZONTAL TAIL CONTRIBUTION	
DEFINITIONS	UNIT		
$C_D = \frac{DRAG}{qS}$	$\frac{1}{1}$		
$C_{D_u} = \frac{U}{2}\frac{\partial C_D}{\partial U}$	$\frac{1}{1}$		$x_u = (-C_D - C_{D_u})$
$C_{D_\alpha} = \frac{\partial C_D}{\partial \alpha}$	$\frac{1}{rad}$		$x_\alpha = \frac{1}{2}(C_L - C_{D_\alpha})$
$C_{D_{\delta_E}} = \frac{\partial C_D}{\partial \delta_E}$	$\frac{1}{rad}$		$x_{\delta_E} = -\frac{1}{2} C_{D_{\delta_E}}$
$C_L = \frac{Lift}{qS}$	$\frac{1}{1}$		
$C_{L_u} = \frac{U}{2}\frac{\partial C_L}{\partial U}$	$\frac{1}{1}$		$z_u = (-C_L - C_{L_u})$
$C_{L_\alpha} = \frac{\partial C_L}{\partial \alpha}$	$\frac{1}{rad}$	$\left[C_{L_\alpha}\right]_H = C_{L_{\alpha_H}} \frac{q_H}{q}\frac{S_H}{S}\left(1 - \frac{\partial \epsilon}{\partial \alpha}\right)$	$z_\alpha = \frac{1}{2}(-C_{L_\alpha} - C_D)$
$C_{L_{\dot\alpha}} = \frac{\partial C_L}{\partial\left(\frac{\dot\alpha c}{2U}\right)}$	$\frac{1}{rad}$	$\left[C_{L_{\dot\alpha}}\right]_H = 2C_{L_{\alpha_H}} \frac{q_H}{q}\frac{S_H}{S}\frac{l_H}{c}\frac{\partial \epsilon}{\partial \alpha}$	$z_{\dot\alpha} = -\frac{1}{4} C_{L_{\dot\alpha}}$
$C_{L_q} = \frac{\partial C_L}{\partial\left(\frac{qc}{2U}\right)}$	$\frac{1}{rad}$	$\left[C_{L_q}\right]_H = 2C_{L_{\alpha_H}} \frac{q_H}{q}\frac{S_H}{S}\frac{l_H}{c}$	$z_q = -\frac{1}{4} C_{L_q}$
$C_{L_{\delta_E}} = \frac{\partial C_L}{\partial \delta_E}$	$\frac{1}{rad}$	$C_{L_{\delta_E}} = C_{L_{\alpha_H}} \frac{q_H}{q}\frac{S_H}{S}\frac{\partial \alpha_H}{\partial \delta_E}$	$z_{\delta_E} = -\frac{1}{2} C_{L_{\delta_E}}$
$C_m = \frac{M}{qSc}$	$\frac{1}{1}$		
$C_{m_u} = \frac{U}{2}\frac{\partial C_m}{\partial U}$	$\frac{1}{1}$		$m_u = \frac{1}{2}\left(\frac{c}{k_y}\right)^2 (C_m + C_{m_u})$
$C_{m_\alpha} = \frac{\partial C_m}{\partial \alpha}$	$\frac{1}{rad}$	$\left[C_{m_\alpha}\right]_H = -\frac{l_H}{c}\left[C_{L_\alpha}\right]_H$	$m_\alpha = \frac{1}{2}\left(\frac{c}{k_y}\right)^2 C_{m_\alpha}$
$C_{m_{\dot\alpha}} = \frac{\partial C_m}{\partial\left(\frac{\dot\alpha c}{2U}\right)}$	$\frac{1}{rad}$	$\left[C_{m_{\dot\alpha}}\right]_H = \frac{-l_H}{c}\left[C_{L_{\dot\alpha}}\right]_H$	$m_{\dot\alpha} = \frac{1}{4}\left(\frac{c}{k_y}\right)^2 C_{m_{\dot\alpha}}$
$C_{m_q} = \frac{\partial C_m}{\partial\left(\frac{qc}{2U}\right)}$	$\frac{1}{rad}$	$\left[C_{m_q}\right]_H = -\frac{l_H}{c}\left[C_{L_q}\right]_H$	$m_q = \frac{1}{4}\left(\frac{c}{k_y}\right)^2 C_{m_q}$
$C_{m_{\delta_E}} = \frac{\partial C_m}{\partial \delta_E}$	$\frac{1}{rad}$	$C_{m_{\delta_E}} = -\frac{l_E}{c} C_{L_{\delta_E}}$	$m_{\delta_E} = \frac{1}{2}\left(\frac{c}{k_y}\right)^2 C_{m_{\delta_E}}$

Appendix I Table II

Dimensional Stability Derivatives

$M_q = \frac{\rho U S c^2 C_{mq}}{4 I_{yy}} = \frac{2.08\,(11.78)^2(-4.5)}{4\,(96,000)} = -.338 \frac{1}{\text{sec Rad}}$

$M_{\dot{w}} = \frac{\rho S c^2}{4 I_{yy}} C_{m\dot{\alpha}} = \frac{(2.378\cdot 10^3)(375)(11.78)^2(-.55)}{(4)\,(96,000)} = -.0001766 \frac{1}{ft}$

$M_w = \frac{\rho U S c}{2 I_{yy}} C_{m\alpha} = \frac{(208)(11.78)(-.380)}{(2)\,(96,000)} = -.0485 \frac{1}{\text{sec-ft}}$

$M_u = \frac{\rho U S c}{I_{yy}} (C_{mu} + C_m) = \frac{(208)(11.78)(.0074)}{96,000} = .000189 \frac{1}{\text{sec-ft}}$

$Z_w = \frac{\rho U S}{2m} (-C_{L_\alpha} - C_D) = \frac{(208)}{2(683)} (-2.598 - .197) = -.426 \frac{1}{\text{sec}}$

$Z_u = \frac{\rho U S}{m} (-C_{Lu} - C_L) = \frac{(208)}{683} (-.870) = -.265 \frac{1}{\text{sec}}$

$X_u = \frac{\rho U S}{m} (-C_{Du} - C_D) = \frac{208}{683} (-.197) = -.060 \frac{1}{\text{sec}}$

$X_w = \frac{\rho U S}{2m} (C_L - C_{D\alpha}) = \frac{208}{2(683)} (.870 - .963) = -.01415 \frac{1}{\text{sec}}$

$C_m = -C_T \frac{z_T}{c} = \frac{(.195)(.437)}{11.78} = .00723$

$Z_{\delta e} = \frac{\rho U^2 S}{2m} C_{L\delta e} = \frac{(65.105)(375)(.3897)}{683} = -13.94 \frac{1}{\text{sec}^2 \text{Rad}}$

$M_{\delta e} = \frac{\rho U^2 S c}{2 I_{yy}} C_{m\delta e} = \frac{(65.1)(375)(11.78)(-.835)}{(96,000)} = -2.50 \frac{1}{\text{sec}^2 \text{Rad}}$

$X_{\Delta T} = \frac{\cos(\xi + \gamma_o)}{m} = .00145 \frac{ft}{\text{sec}^2 lb}$

$M_{\Delta T} = \frac{-z_j}{I_{yy}} = -4.55 \times 10^{-6} \frac{1}{\text{sec}^2 lb}$

APPENDIX II

DYNAMIC STABILITY FORTRAN PROGRAM

Longitudinal - Program LONGSTAB

This program, once entered with required airplane parameters, computes the longitudinal stick fixed and/or stick free (when pertinent) stability derivatives, and the corresponding stability equation coefficients. It then solves these equations for roots, periods, and times to damp to 1/2 amplitude for both the phugoid and short period modes. In addition the value of Routh's discriminant is determined. The sequence of computations can be repeated for as many different flight regimes as desired.

There are a total of five data cards required for the stick-fixed only solutions, with an additional two cards required for a stick-free solution. Thus for a combination stick-fixed and free solution, there will be a total of seven data cards required for each flight regime desired.

The initial data card controls the types of solutions desired (stick-fixed, free, or both), and the number of consecutive runs to be made. A list of program symbols with their meanings appear in Table I to this Appendix.

The second card contains an alpha-numeric run identification or an arbitrary title.

The third card is the first of the general input data cards. This card should have entered on it:

S_t (tail area), S_w (wing area), $C_{L\alpha t}$, η tail, S_B (body area), l_B (body length), ρ, g (acceleration).

The parameters are entered eight to a card, each being allowed 10 columns. There are 80 columns on each card. Each parameter may be entered anywhere in its assigned ten columns, but must have a decimal point included in it. This same format is followed for each of the succeeding cards.

The fourth card should have the following aircraft parameters entered on it:

W (aircraft weight, lbs.); $\frac{\partial \varepsilon}{\partial \alpha}$; θ_o in degrees; h, (distance from c.g. to thrust line, ft.); C_t (coefficient of thrust); $C_{m\alpha}$; I_{YY} (slug ft^2.); V (forward velocity ft./sec.).

The fifth card should have the following:

C_D; $C_{L\alpha}$; ETTA ; $C_{L\ wing}$; c (wing chord); l_t (c.g. to a.c. tail, ft.); Xc.g. (x distance of c.g., ft.); XAC (x distance of wing a.c. in ft.).

Cards 2 through 5 are repeated for each different run, stick fixed. If it is desired to compute a stick free solution simultaneously, then two additional data cards (6 and 7) are required for each run.

Card 6 contains the following parameters:

C_T (tail chord, ft.); K_e^2 (radius of gyration, squared); μ_ε; B_1; B_2; B_2'; z_η ; $z_{\dot{\eta}}$.

Card 7 contains the following parameters:

m_η ; $m_{\dot{\eta}}$; m_e (mass elevator, slugs); S_e (area elevator, ft^2.).

Thus for one aircraft flight regime (say Sea Level, Mach 0.6), for both stick fixed and free, there would be required data cards 1 through 7. For each succeeding run, cards 2 through 7 would have to be repeated with the new parameters entered. Card one would have to be suitably prepared to reflect the total number of runs and mode of runs desired. See Fig. 1 this Appendix for sample data cards. Note the first card is of format 13 for the number of runs, and I1 for mode of operation. All other data cards are of 8F10.0 format (each card holds 8 fields of 10 columns, each, one data number to be entered per field, in floating point format; i.e., with a decimal point somewhere in the number.)

The program prints out the calculated stability derivatives as well as the computed solutions to equations.

TABLE I

PROGRAM SYMBOLS AND MEANINGS

Program LONGSTAB

Program mnenonic	Meaning
NOS	Number of runs to be made. I3 format. card 1
MODE	Decision stick fixed (1), or stick free (2). I1. card 1
ST	S_t, tail area. card 3.
SW	S_w, wing area. card 3.
CLALFAT	$C_{L\alpha_T}$, Tail lift curve slope. card 3.
ETATAIL	η_T, Tail efficiency, C_L/C_L. card 3.
SB	S_B, Body area card 3.
BL	l_B, Body length card 3.
RHO	ρ, Atmospheric density, card 3.
G	g, Acceleration due to gravity. card 3.
W	w, aircraft weight. card 4.
EPSALFA	$\frac{\partial \varepsilon}{\partial \alpha}$ card 4.
THETA1	θ_o, initial angle of pitch, degrees. card 4.
YH	h, distance from c.g. to thrust line. card 4.
CT	C_t, coefficient of thrust. card 4.
CMALFA	C_{m_α}, per radian. card 4.
YI	I_{yy}, moment of inertia. card 4.
V	V, forward velocity, ft./sec. card 4.
CSUBD	C_D, coefficient of drag. card 5.

CLALFA	C_{L_α}, winglift curve slope. card 5.
EPIA	ϵ_{TA}, card 5.
CSUBL	$C_{L\ wing}$, card 5.
C	c, wing chord. card 5.
TL	l_t, c.g. to a.c. tail. card 5.
XCG	$x_{c.g.}$, x distance of c.g. card 5.
XAC	$x_{a.c.}$, x distance of wing a.c. card 5.
CTAIL	C_t, Tail chord. card 6.
XKE	k_e^2, radius of gyration squared. card 6.
UE	μ_c, relative elevator density. card 6.
B1	B_1, $C_{h_{\alpha T}}$. card 6.
B2	B_2, $C_{h_{\delta e}}$. card 6.
B2PRIME	B_2, 1/2 $C_{h_{\dot{\delta} e}}$. card 6.
ZETA	ζ_η, card 6.
ZETADOT	$\zeta_{\dot{\eta}}$, card 6.
AMETA	m_η, card 7.
AMETADT	$m_{\dot{\eta}}$, card 7.
XME	m_e, mass elevator. card 7.
SE	S_e, area elevator. card 7.

Fig. 1 Sample Data Cards

LONGSTAB

0032
NOS MODE

Longstab Data 1 Control Card

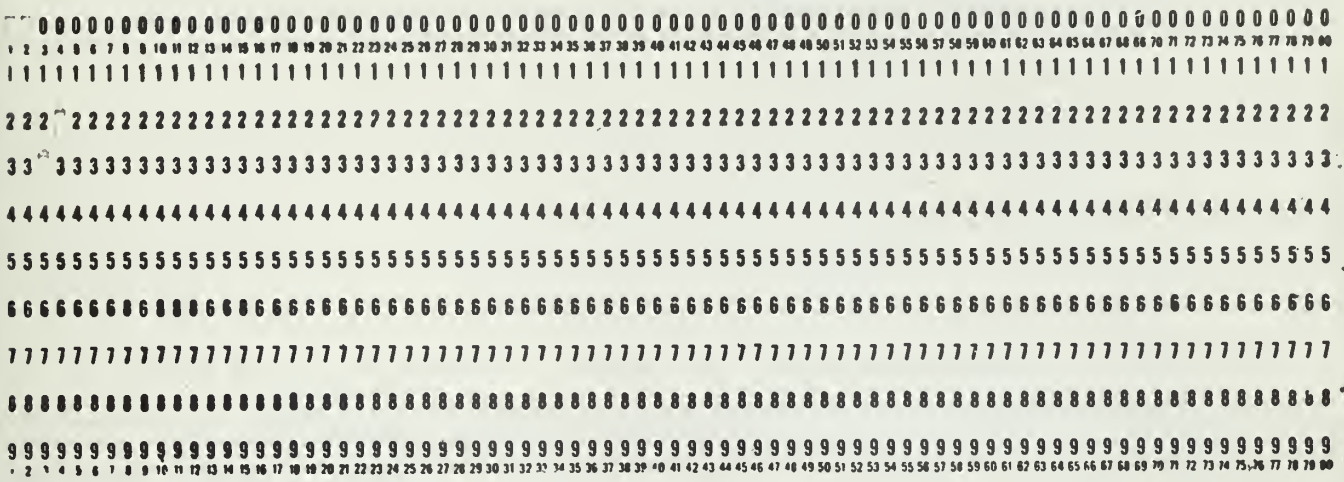

ALTITUDE SEA LEVEL MACH 0.6

LONGSTAB DATA 2

C FOR COMMENT | STATEMENT NUMBER | CONTINUATION | FORTRAN STATEMENT (KAPPA) | IDENTIFICATION

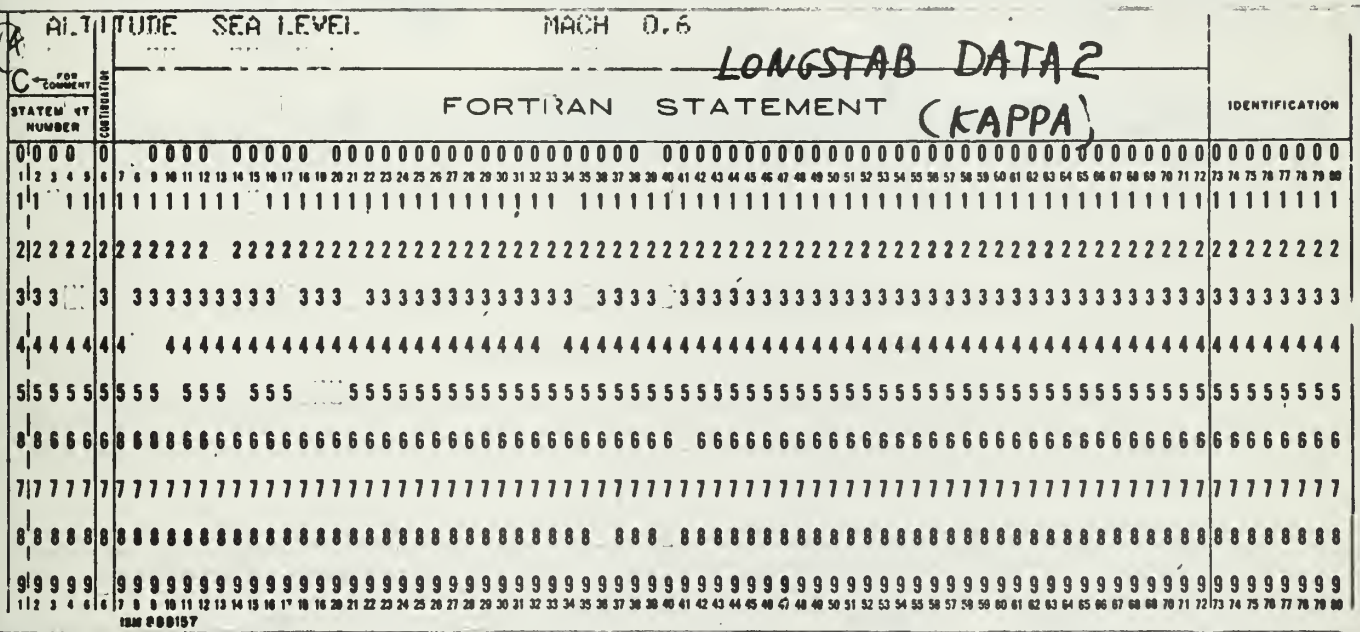

66.0 342.0 4.011 0.95 220.0 43.66 0.002378 32.17

ST

SW C_{L_T} η_T S_B l_B e g

C FOR COMMENT | STATEMENT NUMBER | CONTINUATION | FORTRAN STATEMENT LONGSTAB DATA 3 | IDENTIFICATION

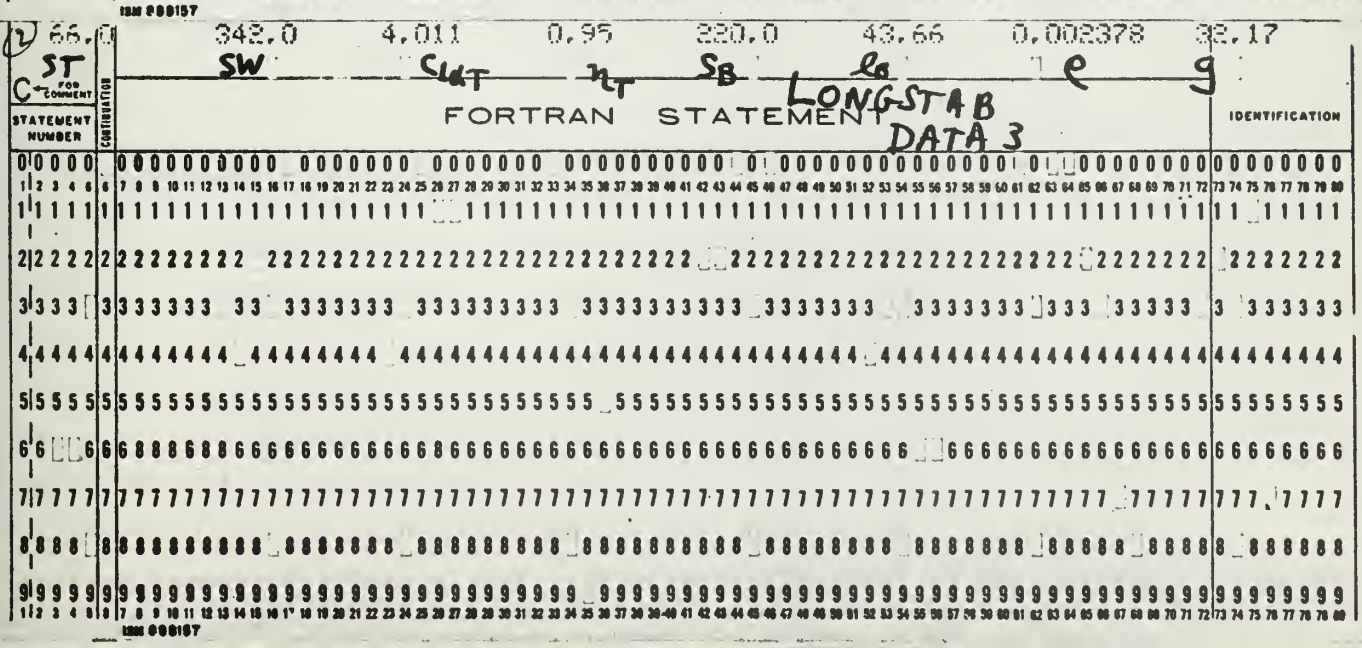

II - Fig. 1 continued

LONGSTAB DATA 4

①	12230.0	0.50	0.0	-.4514	.01828	-.67614	16000.0	670.14
	W	$\frac{\partial \varepsilon}{\partial \alpha}$	θ_0	h	C_T	C_{m_α}	I_{YY}	V

LONGSTAB DATA 5

①	0.01828	4.350	11.85	.0669	8.68	22.05	1.969	2.17
	C_D	$C_{L_\alpha w}$	PITA	C_{L_w}	C	ℓ_t	$X_{c.g.}$	$X_{a.c.}$

4.0	0.166666	85.1	-.200	-.565	-.6604	-.1585	-.0744
LC_t	k_e^2	μ_e	B_1	B_2	B_2'	Z_n	Z_i

LONGSTAB DATA 6

II - Fig. 2.

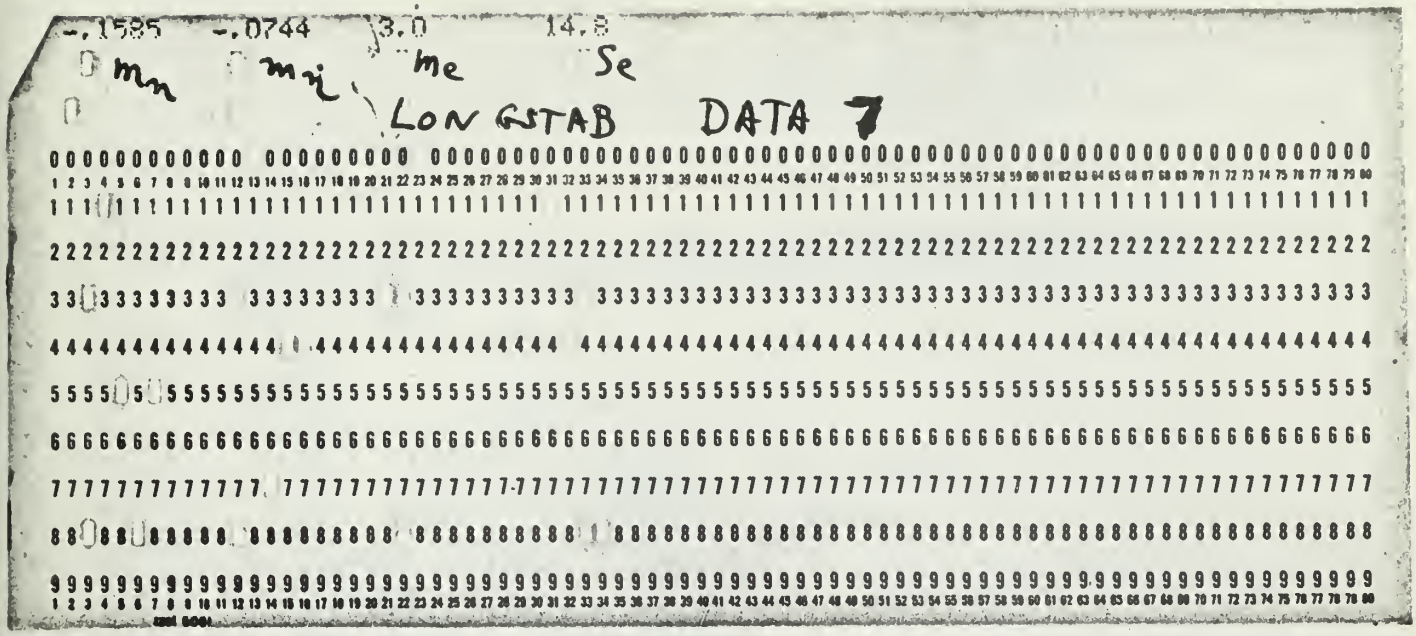

Fortran Program LONGSTAB

```
.JOB BELL*LONGSTAB      1.5 MINUTES
      PROGRAM LONGSTAB
C     PROGRAM FOR THE COMPUTATION OF THE ROOTS OF THE CHARACTERISTIC
C     DYNAMIC LONGITUDINAL STABILITY (STICK FIXED) EQUATIONS
      DIMENSION KAPPA(10),CPR(129),CPI(129),ROOTR(128),ROOTI(128)
      DIMENSION CRR(129),CRI(129),XR(4),XI(4),FXR(4),FXI(4),SR(3),SI(3)
      READ 66, NOS, MODE
   66 FORMAT (I3,I1    )
      DO 777 J =1, NOS
      ICOUNT = 0
    0CALL INPUT1 (CLALFA,EPIA,C,TL,XCG,XAC,ST,SW,CLALFAT,ETATAIL,SB,BL,
     1 RHO,G,W,EPSALFA,THETA1,YH,CT,CMALFA,YI,V,CSUBD,CSUBL,KAPPA      )
C          COMPUTATION OF STABILITY DERIVATIVES
      Q = .5 *RHO * V**2
      TCARAT = W /(G*RHO*V*SW)
      THETAC = THETA1 / 57.2957795
      XU = -CSUBD
      XW = .5*CSUBL*(1.0-(2.0*CLALFA/EPIA))
      ZW = -.5*(CLALFA + CSUBD )
      APRIME = .44 + 2.0*((XAC-XCG)/C)
      BPRIME = -.58 - CLALFA * APRIME * ((XAC-XCG)/C)
      WINGMQ = 0.25 *((C/TL)**2)*BPRIME
      TAILMQ = -.50* CLALFAT * (ST/SW) * ETATAIL
      BODYMQ = -0.01*   (SB/SW)*((BL/TL)**2       )
      TOTALMQ = WINGMQ + TAILMQ + BODYMQ
      YIB = YI/((W/G)*TL**2)
      WINGZQ = -.25*CLALFA*(C/TL)*(.44+(XAC-XCG)*2.0/C)
      TAILZQ= -.5*CLALFAT*(ST/SW)*ETATAIL
      U1 = W/(G*RHO*SW*TL)
      BARMWDT = -.5*CLALFAT*ETATAIL*(ST/SW)*EPSALFA
      TOTALZQ = WINGZQ + TAILZQ
      ZU = -CSUBL
      XTHETA = -.5*CSUBL
      ZTHETA = -.5*CSUBL*TANF(THETAC)
      AMU = -CT *YH/TL
      AMW = .5 * CMALFA * C/TL
       PRINT 5C5, ST, SW, CLALFAT, ETATAIL, SB, BL, RHO, G, W, EPSALFA, THETA1, YH,
     1  CT, CMALFA, YI
 5050FORMAT (1H1 /40H          INPUT PARAMETERS                          //
     111H TAIL AREA= F8.4,2X11H WING AREA= F9.4,2X,14H CL ALFA TAIL=
     2  F9.6,2X,10H ETA TAIL= F9.6,2X,11H BODY AREA= F9.2  /
     3  13H BODY LENGTH= F8.5,2X, 5H RHO= F10.7,2X, 5H GEE= F8.5,2X,
     4   8H WEIGHT= F12.4,1X,3HLBS 2X,18H D EPSILON/D ALFA= F9.6  /
     5  21H INITIAL PITCH ANGLE= F9.6,1X,7HDEGREES 2X,22H THRUST LINE DI
     6STANCE= F8.5,1X,4HFEET 2X,16H THRUST COEF CT= F8.6  /
     7   8H CMALFA= F9.6,2X,10H I SUB YY= F12.3,1X,15HSLUG FT SQUARED//)
      WRITE OUTPUT TAPE 5, 101
  101 FORMAT (/// 47H                    STABILITY  DERIVATIVES          //)
      WRITE OUTPUT TAPE 5, 105 ,V,TCARAT,Q
  105 FORMAT (19H FORWARD VELOCITY= F12.3,10H T CARAT=  F10.6, 4H Q=
     1      F 14.4     /          )
      WRITE OUTPUT TAPE 5, 106, CSUBL, CSUBD
  106  FORMAT ( 9H C SUBL=    F10.6, 9H C SUBD=    F10.6     /)
      WRITE OUTPUT TAPE 5,102,XU,XW,XQ,XTHETA,ZU,ZW,TOTALZQ
 1020FORMAT (5H XU= F7.4,6H  XW= F7.5,6H  XQ= F7.4,10H  XTHETA= F7.5,
     1 6H  ZU= F7.5, 6H  ZW= F7.4,12H  TOTAL ZQ= F7.4    /)
      WRITE OUTPUT TAPE 5,103,ZTHETA,AMU,AMW,BARMWDT,TOTALMQ,U1,YIB
 1030FORMAT ( 9H ZTHETA= F7.4, 6H  MU= F8.6, 6H  MW= F7.5,14H  MBAR W D
     1OT= F7.4, 6H  MQ= F7.4, 9H  MDONE= F7.3,13H I SUB BETA= F7.4   //)
     0CALL PREROOT (XU,XW,XQ,XTHETA,ZU,ZW,TOTALZQ,ZTHETA,AMU,AMW,BARMWDT
     1,TOTALMQ,U1,YIB,TCARAT,A1,B1,C1,D1,E1, CRI,CRR     )
      ROUTH = CRR(2)* CRR(3)* CRR(4)- CRR(1)* CRR(4)**2-CRR(2)**2*CRR(5)
      WRITE OUTPUT TAPE 5, 108, ROUTH
  108 FORMAT (////35H THE VALUE OF ROUTHS DESCRIMINANT =  F10.2        )
      IF (ROUTH) 11,11,12
   11 WRITE OUTPUT TAPE 5, 109
  109 FORMAT (28H  THE AIRCRAFT IS UNSTABLE      //  )
      GO TO 13
   12 WRITE OUTPUT TAPE 5, 110
  110 FORMAT (26H  THE AIRCRAFT IS STABLE        //  )
   13 CONTINUE
      N = 4
      CALL POLYMUL (CRR,CRI,N,KAPPA,TCARAT)
```

APPENDIX II, Fig. 2

```
C      DECISION  FOR LONG OR LATERAL, STICK FIXED(999),OR STICK FREE(201)
       GO TO (777,201,202,204),MODE
  201    CONTINUE
       WRITE  OUTPUT  TAPE 5,301
  3010FORMAT(//// 80H    STICK FREE LONGITUDINAL DYNAMIC STABILITY COEFF
      1ICIENTS                                          //// )
       WRITE OUTPUT TAPE 5, 302, KAPPA
  302  FORMAT ( 10A8 )
       OCALL  INPUT 2 (CTAIL,XKE,UE,B1,B2,B2PRIME,ZETA,ZETADOT,AMETA,
      1      AMETADT   )
       XKE = SQRTF(XKE)
        ZQ = TOTALZQ
       AMQ = TOTALMQ
       OCALL  PREROT2 (CTAIL,EPSALFA,XKE,YIB,U1,UE,TL,B1,B2,B2PRIME,ZW,
      1 ZTHETA,ZQ,ZETA,ZETADOT,AMW,AMQ,BARMWDT,AMETA,AMETADT, CRR,CRI    )
       N = 5
       CALL POLYMUL (CRR,CRI,N,KAPPA,TCARAT)
  777    CONTINUE
       END FILE 5
       STOP2
  202    STOP4
  203    STOP5
  204    STOP6
       END

       OSUBROUTINE INPUT1(CLALFA,EPIA,C,TL,XCG,XAC,ST,SW,CLALFAT,ETATAIL,
      1 SB,BL,RHO,G,W,EPSALFA,THETA1,YH,CT,CMALFA,YI,V,CSUBD,CSUBL,KAPPA)
       DIMENSION KAPPA(10),CPR(129),CPI(129),ROOTR(128),ROOTI(128)
       DIMENSION CRR(129),CRI(129),XR(4),XI(4),FXR(4),FXI(4),SR(3),SI(3)
       READ 65, KAPPA
  104  FORMAT ( 8F10.0 )
       READ 104,ST,SW,CLALFAT,ETATAIL,SB,BL,RHO,G
       READ 104, W,EPSALFA,THETA1,YH,CT,CMALFA,YI,V
       READ 104,CSUBD,CLALFA,EPIA,CSUBL,C,TL,XCG,XAC
   65  FORMAT ( 10A8)
       RETURN
       END
       SUBROUTINE  PREROOT (XU,XW,XQ,XTHETA,ZU,ZW,TOTALZQ,ZTHETA,AMU,AMW,
      1BARMWDT,TOTALMQ,U1,YIB,TCARAT,A1,B1,C1,D1,E1, CRI, CRR)
       DIMENSION KAPPA(10),CPR(129),CPI(129),ROOTR(128),ROOTI(128)
       DIMENSION CRR(129),CRI(129),XR(4),XI(4),FXR(4),FXI(4),SR(3),SI(3)
    1  A1 = 1.0
       ZQMU = (1.0 +(TOTALZQ / U1))
    2  B1 = -(XU + ZW)-(TOTALMQ/YIB)-(ZQMU * BARMWDT/YIB )
    3CC1 = (XU* ZW - XW* ZU ) + (TOTALMQ/YIB)*(XU+ ZW) +( XU*ZQMU - ZU *
      1(XQ/U1) - ZTHETA)* (BARMWDT/YIB) -(U1*AMW/YIB)*(ZQMU + XQ/U1)
    4OD1 = -(TOTALMQ/YIB)* (XU*ZW - XW * ZU) +(-XTHETA* ZU + ZTHETA *
      1 XU )*(BARMWDT/ YIB)+(U1*AMW/YIB)*( XU* ZQMU -ZU* XQ/U1 -ZTHETA)+
      2 (U1*AMU/YIB)*(-XTHETA -XW* ZQMU + ZW *XQ/U1 )
    5OE1 = (U1*AMW/YIB)*(-XTHETA*ZU +ZTHETA*XU)-(U1*AMU/YIB)*(-XTHETA*
      1ZW + ZTHETA* XW )
       WRITE OUTPUT TAPE 5,101, A1,B1,C1,D1,E1
  1010FORMAT (/3H A= 1X,F13.5,4H  B= 1X,F13.5, 4H  C= 1X,F13.5, 4H  D=
      1 1X,F13.5,4H  E= 1X,F13.5 //)
       CRR(1) = A1
       CRR(2) = B1
       CRR(3) = C1
       CRR(4) = D1
       CRR(5) = E1
       CRI(1) = 0.0
       CRI(2) = 0.0
       CRI(3) = 0.0
       CRI(4) = 0.0
       CRI(5) = 0.0
         RETURN
        END

       OSUBROUTINE INPUT2(CTAIL,XKE,UE,B1,B2,B2PRIME,ZETA,ZETADOT,AMETA,
      1      AMETADT   )
C      SUBROUTINE BRINGS IN STICK FREE FACTORS
       OREAD 1,CTAIL,XKE,UE,B1,B2,B2PRIME,ZETA,ZETADOT,AMETA,AMETADT,XME,
      1   SE
     1 FORMAT ( 8F10.0 /4F10.0)
```

```
      WRITE OUTPUT TAPE 5,2
    2CFORMAT(////10X70H                INPUT   PARAMETERS   STICK  FREE
     1                                    )
      END

      SUBROUTINE PREROT2 (CTAIL,EPSALFA,XKE,YIB,U1,UE,TL,B1,B2,B2PRIME,Z
     1W,ZTHETA,ZQ,ZETA,ZETADOT,AMW,AMQ,BARMWDT,AMETA,AMETADT,A,B          )
C     SUBROUTINE CALCULATES STABILITY STICK FREE QUINTIC COEFFICIENTS
      DIMENSION          A(129), B(129)
      UFACTOR = 2.0* UE /(U1**2)
      UFACT = UFACTOR
      FACTORK =(XKE / TL)**2
       XKFACT = FACTORK
      CTFACT  = CTAIL / TL
      ZFACT   = (1.0 +(ZQ/U1 ))
      EPSFACT  = 1.0- EPSALFA
      WRITE OUTPUT TAPE 5,2001, UFACT,XKFACT,CTFACT,ZFACT,EPSFACT
 2001OFORMAT (49H                      FACTOR CALCULATIONS                 //
     1  9H UFACTOR=  F14.7,  9H KFACTOR=  F14.7, 10H CTFACTOR=  F14.7,
     210H ZFACTOR=  F14.7,  16H EPSALFA FACTOR=  F14.7                   //)
C     A   COEFFICIENT  CALCULATION
      A(1)=UFACT *XKFACT * YIB
C     B   COEFFICIENT  CALCULATION
     0A(2)=UFACTOR* XKFACT*( BARMWDT *(ZETADOT*CTFACT/U1-ZFACT)-AMQ-Zw*
     1 YIB + AMETADT* CTFACT ) - B2PRIME * CTFACT * YIB / U1
C     C   COEFFICIENT  CALCULATION
     CA(3)=UFACT *XKFACT *(  ZW *AMQ + AMw*( ZETADOT *CTFACT- U1*(ZFACT)
     1 ) + BARMWDT *(ZETA - ZTHETA)+ U1 * AMETA - AMETADT * CTFACT *Zw )
     2 + B2PRIME * CTFACT / U1*( AMQ + ZW*YIB + ZFACT * BARMWDT ) - B2 *
     3 YIB -B1*( AMETADT *CTFACT/U1 + ZETADOT *CTFACT/U1 *( YIB*EPSFACT
     4  + BARMWDT /U1))
C     D   COEFFICIENT  CALCULATION
     CA(4) = UFACTOR * XKFACT  *(  U1*AMW*(ZETA-ZTHETA)- U1*AMETA*ZW )
     1 -B2PRIME * CTFACT /U1 *(  ZW *AMQ - U1*AMw*  ZFACT - ZTHETA *
     2 BARMWDT )+B2*(AMQ +Zw * YIB + BARMWDT * ZFACT)-B1*(AMETADT*CTFACT
     3 *(EPSFACT * ZFACT - ZW/U1)+ ZETADOT * CTFACT/U1*(AMW - AMQ *
     4 EPSFACT )+ ZETA *(BARMWDT/U1 + EPSFACT * YIB ) + AMETA )
C     E   COEFFICIENT  CALCULATION
     0A(5) = B2PRIME * CTFACT /U1 *U1 * AMW* ZTHETA + B2*( ZTHETA*BARMWD
     1T  - ZW * AMQ + U1 * AMW * ZFACT ) + B1*( ZETA *(EPSFACT * AMQ -
     2 AMW) + AMETA *( ZW -U1*EPSFACT * ZFACT )- AMETADT * CTFACT *
     3 EPSFACT * ZTHETA )
C     F   COEFFICIENT  CALCULATION
     0A(6) = U1* ZTHETA* (B2* AMW - AMETA * B1*EPSFACT )
      DO  1CC  J=1,129
  100 B(J) = C.0
      WRITE OUTPUT TAPE 5,3,CTAIL,XKE,UE,B1,B2
    3CFORMAT (/// 13H TAIL CHORD = F7.3,1X, 8HK SUB E= F9.5,1X,9HMU SUB
     1E= F9.5,1X,8HB SUB 1= F9.5,1X, 8HB SUB 2= F9.5      )
      WRITE OUTPUT TAPE 5,4,B2PRIME,ZETA,ZETADOT,AMETA, AMETADT
    4CFORMAT(/14H B SUB2 PRIME=  F9.5,1X, 11H Z SUB ETA=  F9.5,1X,
     115H Z SUB ETA DOT=  F9.5,1X,11H M SUB ETA=  F9.5,1X,16H M SUB ETA
     2 DOT=   F9.5                  ///)
      C1 = UFACT * XKFACT *( U1 * AMW * (ZETA -ZTHETA)- U1*AMETA* ZW)
      C2 = -B2PRIME /U1 * CTFACT*(ZW *AMQ-U1*AMW *ZFACT -ZTHETA*BARMWDT)
      D3 = B2*(AMQ +ZW*YIB + BARMWDT* ZFACT)
     0D4 = -B1*(AMETADT*CTFACT*(EPSFACT*ZFACT-ZW/U1)+ZETADOT/U1*CTFACT*(
     1 AMW - AMQ*EPSFACT) +ZETA*( BARMWDT/U1 +EPSFACT*YIB) +AMETA)
      D = D1+D2 +C3 + D4
      A(4) = D
    6OFORMAT (//   4H D1= F15.8, 4H D2= F15.8, 4H D3= F15.8,4H D4= F15.8
     1 ,  9H D TOTAL= F15.8,       //   )
      E1 =B2PRIME*CTFACT *(U1*AMW*ZTHETA)
      E2 =B2 *(                 BARMWDT -Zw*AMQ +U1 *AMW* ZFACT )
     0E3 =B1 *(ZETA*(EPSFACT*AMQ -AMw)+AMETA*(ZW-U1*EPSFACT*ZFACT)-
     1  AMETADT*CTFACT* EPSFACT * ZTHETA)
      E = E1 + E2 +E3
    7OFORMAT (// 4H E1= F15.8,4H E2= F15.8,4H E3= F15.8, 9H E TOTAL=
     1 F15.8,                    //)
     0C1 =UFACT *XKFACT *(Zw *AMQ+AMW*(ZETADOT*CTFACT-U1*ZFACT)+BARMWDT
     1    *(ZETA-ZTHETA)+U1*AMETA-AMETADT *CTFACT* ZW )
      C2 =B2PRIME/U1*CTFACT*(AMQ +ZW*YIB +ZFACT* BARMWDT)
     0C3 = -B2 *YIB -B1*(AMETADT/U1 *CTFACT+ ZETADOT/U1*CTFACT*(YIB *
```

```
     1  EPSFACT + BARMWDT/U1) )
        C = C1 + C2 + C3
        WRITE OUTPUT TAPE 5, 8, C1, C2, C3, C
        WRITE OUTPUT TAPE 5,6,D1,D2,D3,D4,D
        WRITE OUTPUT TAPE 5,7, E1,E2,E3,E
    80FORMAT (/// 4H C1= F15.8, 4H C2= F15.8, 4H C3= F15.8,5H C TOTAL=
     1  F15.8,       // )
        RETURN
        END
        SUBROUTINE POLYMUL (CRR,CRI,N,KAPPA,TCARAT)

        DIMENSION KAPPA(10),CPR(129),CPI(129),ROOTR(128),ROOTI(128)
        DIMENSION CRR(129),CRI(129),XR(4),XI(4),FXR(4),FXI(4),SR(3),SI(3)
        IMAX = 50
        DEL = C.1
        NUM = 5
        RATIO =5.0
        ALTER =1.COCOO1
        EP1 =.CCCOOOOOOOOCCCOOOOOO1
        EP2 =.COCOOOO1
        EP3 =.OCCCOC1
        EP4 =.CCCCOCO1
        SR(1)= -.5
        SI(1)= 0.0
        SR(2)= C.5
        SI(2)= C.0
        SR(3)= C.0
        SI(3)= 0.0
        MODE = 1
        NNN = N+1
  749 IF   (CRR(1))  750,751,750
  751 DO 753 L=1,NNN
        M = L +1
        CRR(L) = CRR(M)
  753   CONTINUE
  752 N = N-1
        GO TO 749
  750   CONTINUE
   65 FORMAT (1CA8)
        DO 5 I=1,1C
        KON=8F
        IF(KAPPA(I)-KON)2,5,2
    5   CONTINUE
        GO TC 999
    2   PRINT 65,KAPPA
   66   FORMAT(2X,2HN=I4,12X,5HIMAX=I3,10X,4HNUM=I3,11X,4HDEL=E8.2,
  661 6X,6HRATIO=E8.2,4X,6HALTER=F10.8/
  662 2X,4HEP1=E8.2,6X,4HEP2=E8.2,6X,4HEP3=E8.2,6X,4HEP4=E8.2/)
        MODE=MODE+1
   67   FORMAT(6H  SR1= E12.5,6H  SI1= E12.5,6H  SR2= E12.5,6H  SI2=
  671 E12.5,6H  SR3= E12.5,6H  SI3= E12.5)
        NP1=N+1
  710FORMAT (46HCTHE COEFFICIENTS OF THE GIVEN POLYNOMIAL ARE    ///
     1  11H REAL PART    )
  501 WRITE OUTPUT TAPE 5,71
  6810FORMAT(11CH       A           B           C           D           E
     1 F           G           H                                        //)
  687   CONTINUE
        WRITE OUTPUT TAPE 5, 680,(CRR(J),J=1,NP1)
  680 FORMAT (1H  8F15.7  / )
        WRITE OUTPUT TAPE 5, 682
  682 FORMAT (16H IMAGINARY PART  )
        WRITE OUTPUT TAPE 5, 680,(CRI(J),J=1,NP1)
  502   DO 6 I=1,NP1
        CPR(I)=CRR(I)
    6   CPI(I)=CRI(I)
        CALL COMAG(CRR(1),CRI(1),C1,KE)
        DO 3C5 K=1,N
        GO TC(9,609),MODE
   53   FORMAT(1HO2X4HRCOT5X7HITERANT6X2(10HREAL  PART1CX10HIMAG  PART10X)
     1,10HRCOT IS IN/2X6HNUMBER4X6HNUMBER7X2(9H CF  ROOT11X),2(9H CF  R(
     2Z)11X),11HA RADIUS OF)
    9   PRINT 53
```

```
6C9   I=1
      NP1=N+2-K
      NN=NP1-1
      IF(K+1-N)13,12,11
 11   CALL DIVD(-CRR(2),-CRI(2),CRR(1),CRI(1),XR(1),XI(1),KE)
      K1=1
      K2=1
      GO TO 16
 12   AR=CRR(1)
      AI=CRI(1)
      BR=CRR(2)
      BI=CRI(2)
      CR=CRR(3)
      CI=CRI(3)
      K1=1
      K2=1
      M4=2
      GOTO  123
 14   XR(1)=DBARR
      XI(1)=DBARI
      GO TO 16
 13   DO 15 J=1,3
      XR(J)=SR(J)
 15   XI(J)=SI(J)
      K1=1
      K2=3
 16   M1=1
      M2=1
      M3=1
      M4=1
700   DO 717 L=K1,K2
701   ZR=XR(L)
702   ZI=XI(L)
      CALL POLYNCM(NP1,ZR,ZI,CRR,CRI,RR,RI,KE)
710   FXR(L)=RR
711   FXI(L)=RI
      CALL COMAG(RR,RI,PMAG,KE)
713   RAD=ALTER*(PMAG/C1)**(1.0/FLOATF(NN))
714   GO TO (715,19,175),M3
715   GO TO(716,718),MODE
 55   FORMAT(    2(I6, 4X),  4E20.11,  5X,  E10.4  )
716   PRINT 55, K,I,ZR,ZI,RR,RI,RAD
718   POLYC=POLYN
      POLYN=PMAG
      IF(PMAG)717,300,717
717   I=I+1
      IF(K+1-N)17,300,300
 17   GO TO (18,200),M1
 18   VAL=DEL*POLYN
      DBARR=RAD
      DBARI=0.0
 19   K1=4
      K2=4
      M1=2
      M3=1
101   ABARR=XR(1)-XR(3)
102   ABARI=XI(1)-XI(3)
103   BBARR=XR(2)-XR(3)
104   BBARI=XI(2)-XI(3)
105   AMIBR=XR(1)-XR(2)
106   AMIBI=XI(1)-XI(2)
107   CALL MULT(ABARR,ABARI,BBARR,BBARI,TA,TB,KE1)
108   CALL MULT(TA,TB,AMIBR,AMIBI,DENR,DENI,KE2)
      CALL COMAG(DENR,DENI,TA,KE)
      CALL COMAG(XR(3),XI(3),T4,KE)
      IF(TA-EP1*T4)110,110,111
110   CALL DERIV(NP1,XR(3),XI(3),CRR,CRI,DR,DI,K50)
      CALL COMAG(RR,RI,TR,KE)
      CALL COMAG(DR,DI,TD,KE)
      IF(TR-EP4*TD)192,171,171
111   DELAR=FXR(1)-FXR(3)
112   DELAI=FXI(1)-FXI(3)
113   DELBR=FXR(2)-FXR(3)
```

```
      DELBI=FXI(2)-FXI(3)
      CALL MULT(BBARR,BBARI,DELAR,DELAI,TA,TB,KE5)
      CALL MULT(ABARR,ABARI,DELBR,DELBI,TC,TD,KE6)
      CALL DIVD(TA-TC,TB-TC,DENR,DENI,AR,AI,KE7)
      CALL MULT(ABARR,ABARI,TC,TD,T1,T2,KE8)
      CALL MULT(BBARR,BBARI,TA,TB,T3,T4,KE9)
      CALL DIVD(T1-T3,T2-T4,DENR,DENI,BR,BI,KE10)
      CR=FXR(3)
      CI=FXI(3)
      CALL MULT(BR,BI,BR,BI,T1,T2,KE11)
      CALL MULT(AR,AI,CR,CI,T3,T4,KE12)
      TA=T1-4.0*T3
      TB=T2-4.0*T4
      CALL CSQRT(TA,TB,TC,TD)
      T1=-BR+TC
      T2=-BI+TD
      T3=-BR-TC
      T4=-BI-TD
      CALL COMAG(T1,T2,TA,KE14)
      CALL COMAG(T3,T4,TB,KE15)
      IF(TA-TB)154,168,168
      TA=TB
      T1=T3
      T2=T4
  168 GO TO (157,159),M4
  157 IF(TA)161,161,158
  158 CALL COMAG(2.0*CR,2.0*CI,TB,KE16)
      IF(TB-RAD*TA)159,159,180
  159 CALL DIVD(2.0*CR,2.0*CI,T1,T2,DBARR,DBARI,KE17)
      GO TO (161,14),M4
  161 XR(4)=XR(3)+DBARR
  162 XI(4)=XI(3)+DBARI
      TR=ABSF(XR(4))
      TI=ABSF(XI(4))
      IF(TR)167,167,140
  140 IF(TI)167,167,169
  169 IF(TR-TI)164,167,163
  163 IF(TI-EP2*TR)165,167,167
  165 XI(4)=C.C
      GO TO(503,504),MODE
   56 FORMAT(40HCITERANT ALTERED TO BE PURE REAL NUMBER.)
  503 PRINT 56
  504 GO TO 167
  164 IF(TR-EP2*TI)166,167,167
  166 XR(4)=0.0
      GO TO(505,167),MODE
   57 FORMAT(45HCITERANT ALTERED TO BE PURE IMAGINARY NUMBER.)
  505 PRINT 57
  167 GO TO 700
  180 CALL DIVD(T1,T2,TA ,C.0,T1,T2,K20)
      CALL DIVD(CR,CI,TB ,C.0,CR,CI,K21)
      CALL MULT(CR,CI,RAD,C.0,CR,CI,K22)
      GO TO(506,507),MODE
   58 FORMAT(87H ITERANT IS OUTSIDE CIRCLE WHICH BOUNDS A ROOT.  INTERP
     1OLATE ITERANT TO EDGE OF CIRCLE.)
  506 PRINT 58
  507 GO TO 159
  171 CALL COMAG(ABARR,ABARI,T1,KR1)
          ENA(1)     STA(ITA)   ENA(3)     STA(ITB)
      IF(T1-EP3*T4)174,174,172
  172 CALL COMAG(BBARR,BBARI,T2,KR2)
          ENA(2)     STA(ITA)   ENA(3)     STA(ITB)
      IF(T2-EP3*T4)175,175,173
  173 CALL COMAG(AMIBR,AMIBI,T3,KR3)
          ENA(1)     STA(ITA)   ENA(2)     STA(ITB)
      IF(T3-EP3*T4)174,174,111
  174     ENA(1)     STA(K1)    STA(K2)    ENA(2)     STA(M3)    SLJ(178)
  175     ENA(2)     STA(K1)    STA(K2)    ENA(3)     STA(M3)
  178 XR(K1)=XR(K1)*(1.0+2.0*EP3)
      XI(K1)=XI(K1)*(1.0+2.0*EP3)
      GO TO(508,509),MODE
 60   FORMAT(11HCITERANTS X11,6H AND X11,41H ARE TOO CLOSE TOGETHER  ALT
     1ER ITERANT X I1,1H.)
```

```
 5C8   PRINT 6C,ITA,ITB,ITA
 5C9   GO TC 7C0
 179   POLYC=PMAG
       GO TC 19
 2C0   IF(POLYN-VAL)201,2C1,210
 2C1   VAL=CEL*POLYN
 2C2   LIM=I+NUM
 203   M2=2
       CALL DERIV(NP1,XR(4),XI(4),CRR,CRI,DR,DI,K6C)
       CALL COMAG(RR,RI,TR,KE)
       CALL COMAG(DR,DI,TC,KE)
       IF(TR-EP4*TC)192,21C,21C
 210   DLT=RATIO*POLYO/POLYN
 211   IF(1.0-DLT)22C,220,212
 212   CALL MULT(DBARR,DBARI,DLT,0.0,DBARR,DBARI,K3C)
 215   LIM=LIM+1
       GO TC (510,511),MODE
  72 FORMAT(120HOPOLYNOMIAL HAS INCREASED IN MAGNITUDE TOO MUCH WITH CU
  721RRENT STEP. THEREFORE REDUCE CURRENT STEP.                        )
 510   PRINT 72
 511   GO TC 161
 220   GO TC (221,231),M2
 221   IF(I-IMAX)250,250,222
 222 PRINT 62
       DO 684 J=1,NP1
 684 CRR(J) = 1C.C * CRR(J)
       ICOUNT = ICOUNT + 1
       IF ( ICOUNT - 3 ) 685,685,777
 685 WRITE OUTPUT TAPE 5,686
 6860FORMAT ( 55HOTHE REVISED COEFFICIENTS OF TEH GIVEN POLYNOMIAL ARE
     1      ///)
       K = 1
       GO TO 687
  62   FORMAT(69HOMAXIMUM NUMBER OF ITERATIONS REACHED WITHOUT REDUCING
  621P(Z) BY DELTA.)
 513   GO TC 777
 777     RETURN
 231   IF(I-LIM)250,250,300
 250   DO 251 L=1,3
       XR(L)=XR(L+1)
       XI(L)=XI(L+1)
       FXR(L)=FXR(L+1)
 251   FXI(L)=FXI(L+1)
       GO TC 1C1
 192   GO TC(514,300),MODE
  69   FORMAT(19HOFIRST DERIVATIVE ( E17.9,E20.9,55H) INDICATES THAT ITE
     1RANT IS SUFFICIENTLY CLOSE TO ROOT.)
 514   PRINT 69,DR,DI
 300   DO 3C2   J=2,NN
       CALL MULT(ZR,ZI,CRR(J-1),CRI(J-1),TR,TI,K4C)
       CRR(J)=TR+CRR(J)
 302   CRI(J)=TI+CRI(J)
  63   FORMAT(59HOTHE COEFFICIENTS OF THE REDUCED POLYNOMIAL ARE AS FOLL
  631CWS )
       ROOTR(K)=ZR
       ROOTI(K)=ZI
       GO TC(303,305),MODE
303   PRINT 63
  68   FORMAT(1H 6E18.9)
304   PRINT 68,(CRR(J),J=1,NN)
       PRINT 68, (CRI(J),J=1,NN)
 3C5   CONTINUE
       GO TC (515,516),MODE
 515   PRINT 75
 516   PRINT 8C
  80CFORMAT(1HC42X14HTABLE OF ROOTS//3X4HROOT8X  1CHREAL  PART10X10HIMA
     1G  PART 10X  6HPERIOD 10X 26HTIME TO DAMP TO HALF AMPL
     2             /2X6HNUMBER7X2(9H OF  ROOT11X) )
       DO 3C6 I=1,N
       CALL POLYNOM(N+1,ROOTR(I),ROOTI(I),CPR,CPI,RR,RI,KE)
       THALF = -.6931471 8C6/ROOTR(I)* TCARAT
       PERIOD = 6.2831853C72 /ABSF(ROOTI(I)) * TCARAT
 3C6 WRITE OUTPUT TAPE 5, 84, I, ROOTR(I),ROOTI(I),PERIOD,THALF
```

```
 84 FORMAT (I6,4X,F16.6,3X,F16.6,7X,F10.4,8H SECS    5X,F10.4,5H SECS)
 83  FORMAT(I6, 4X, 4E20.11)
     PRINT 75
 75  FORMAT(1H1)
     IMAX = 50
    NUM = 5
    DEL = C.1
    RATIO =5.C
    ALTER =1.COCOO1
    EP1 =.CCCCCCOOOOOCCCCCCCC1
    EP2 =.CCCOOOO1
    EP3 =.0000001
    EP4 =.OCCCCCC1
    SR(1)= -.5
    SI(1)= 0.0
    SR(2)= 0.5
    SI(2)= C.C
    SR(3)= 0.0
    SI(3)= 0.0
    MODE = 1
     GO TC 1
  1 RETURN
999  CONTINUE
     END
     SUBRCUTINE   DERIV(N,ZR,ZI,CR,CI,DR,DI,KER)
     DIMENSICN CR(129),CI(129)
        ENA(C)     STA(DR)    STA(DI)    STA(RR)    STA(RI)ENA(1)STA(KER).
     DO 2 J=1,N
     CALL MULT(ZR,ZI,RR,RI,TRR,TRI,K1)
     CALL MULT(ZR,ZI,DR,DI,TDR,TDI,K2)
        RSC(K1)    AJP1(L+2) RSC(K2)    AJP(1)     ENA(2) STA(KER)SLJ(3).
  1  DR=TDR+RR
     DI=TDI+RI
     RR=TRR+CR(J)
  2  RI=TRI+CI(J)
  3  CONTINUE
     END
     SUBRCUTINE   PCLYNOM(N,ZR,ZI,CR,CI,RR,RI,KER)
     DIMENSICN CR(129),CI(129)
        ENA(0)     STA(RR)    STA(RI)    ENA(1)     STA(KER)                .
     DO 2 J=1,N
     CALL MULT(ZR,ZI,RR,RI,TR,TI,K1)
        RSC(K1)    AJP(1)     ENA(2)     STA(KER)  SLJ(3)                  .
  1  RR=TR+CR(J)
  2  RI=TI+CI(J)
  3  CONTINUE
     END
     SUBRCUTINE CSQRT(XR,XI,YR,YI)
        CCN(SQ2=1.4142135624).
        LDA(XR)    LDQ(XI)    AJP2(L+1) LAC(XR)    QJP2(L+1) LQC(XI)
        STA(A)     STQ(B)     QJP1(1)   STQ(Q)     SLJ4(8) +STA(P)SLJ(5).
  1     AJP1(2)    LDA(B)     SLJ4(8)  +FDV(SQ2)   STA(P)
        SSK(XI)    SLJ(L+2)   LAC(P)   +STA(C)     SLJ(5)                  .
  2     THS(B)     SLJ(3)     STQ(S)    FDV(B)     STA(T)     STA(R)SLJ(4)
  3     STA(S)     LDA(B)     FDV(A)    STA(T)     LDA(1.C)   STA(R)SLJ(4)
  7  Y=SQRTF(X)
  8     SLJ(*)     STA(X)     SLJ(7)                                        .
  4     LDA(T)     FMU(T)     FAD(1.0)  SLJ4(8)   +FAD(R)     FDV(2.C)
        SLJ4(8)   +STA(T)     LDA(S)    SLJ4(8)   +FMU(T)     STA(P)
        LDA(XI)    FDV(2.C)   FDV(P)    STA(Q)                            .
  5     SSK(XR)    SLJ(6)     LDA(Q)    LQC(P)     AJP2(L+1) LAC(Q)
        SSK(XI)    LDQ(P)     STA(YR)   STQ(YI)    SLJ(L+3)                .
  6     LDA(P)     LDQ(Q)     STA(YR)   STQ(YI)                            .
     END
     SUBRCUTINE COMAG(XR,XI,Z,KER)
        LDA(XR)    LDQ(XI)    AJP2(L+1) LAC(XR)    QJP2(L+1) LQC(XI)
        STQ(T)    +THS(T)     LLS(48)   QJP(3)     STQ(T)    FDV(T)
        STA(H)     FMU(H)     FAD(1.0)  STA(H)                             .
     Y=SQRTF(H)
       -FMU(T)    +EXF7(141B)SLJ(L+2)  ENQ(1)     SLJ(3)     ENQ(2)        .
  3     STQ(KER)   STA(Z)                                                  .
     END
     SUBRCUTINE   DIVC(XR,XI,YR,YI,ZR,ZI,KER)
```

```
      CALL PRCD(XR,XI,YR,-YI,B1,B2,PR,PI,DR,DI)
         LCA(B2)     AJP1(1)     ENA(3)      SLJ(3)                          .
    2    ENA(2)      SLJ(3)                                                  .
    1  T=DR*DR+DI*DI
         LCA(B1)   -FDV(B2)   +EXF7(1418)SLJ(2)     STA(B1)
         LCA(PR)     FDV(T)   -FMU(B1)   +EXF7(1418)SLJ(2)     STA(ZR)
         LCA(PI)     FDV(T)   -FMU(B1)   +EXF7(1418)SLJ(2)    STA(ZI)ENA(1)
    3    STA(KER)                                                            .
      END
      SUBROUTINE    MULT(XR,XI,YR,YI,ZR,ZI,KER)
      CALL PRCD(XR,XI,YR,YI,B1,B2,PR,PI,D1,D2)
         LCA(B2)   -FMU(B1)   +EXF7(1418)SLJ(1)     STA(B1)                 .
         LCA(PR)   -FMU(B1)   +EXF7(1418)SLJ(1)     STA(ZR)                 .
         LCA(PI)   -FMU(B1)   +EXF7(1418)SLJ(1)     STA(ZI)
         ENA(1)     STA(KER)   SLJ(L+2)                                     .
    1    ENA(2)     STA(KER)
      END
      SUBROUTINE    PROD(XR,XI,YR,YI,B1,B2,PR,PI,DR,DI)
      CALL NORM(XR,XI,B1,AR,AI)
      CALL NORM(YR,YI,B2,DR,DI)
      PR=AR*DR-AI*DI
      PI=AI*DR+AR*DI
      END
      SUBROUTINE    NORM(A1,A2,B1,S1,S2)
   1A    SLJ(1)    +SEV7(70000B)          ZRO(C)    +ZRO(40000B)ZRO(C)      .
    1    LDA(1A+1) LDQ(A1)    QJP2(L+1) LQC(A1)     STL(E)     LDQ(A2)
         QJP2(L+1) LQC(A2)    LDL(1A+1)+THS(E)      SLJ(L+2)   LDA(E)
        +AJP1(L+2) STA(S1)    STA(B1)    SLJ(L+5) +ADD(1A+2)  STA(B1)
         LCA(A1)    FDV(B1)    STA(S1)    LDA(A2)    FDV(B1)   +STA(S2)     .
      END
      END

C031
  RUN 1  CG 26    V 224 FPS   F8U    1.29.63    BELL NUMBERS
93.4       375.0       2.393       1.0         288.5       52.8        .002378    32.
21000.0    .4772       8.1         -.437       0.195       -.2937      932CC.C    224.
.195       2.759       9.3845      .902        11.78       14.08       29.625     29.
F8U LONGITUDINAL RUN2 STICK FIXED  M=.209,V=234 CG24,V=1.13VSL
93.4       375.0       2.393       .95         232.C       52.8        .002378    32.
22000.0    .4772        5.6        -.437       .0511       -.380       960CC.C    234.
.19        2.59        9.3845      .90         11.78       14.08       29.375     29.
  RUN 3 C.G. 24, V=139 KTS,234 FPS 3/3/63 LEVEL FLITE
93.4       375.0       2.393       1.0         288.5       52.8        .002378    32.
22000.0    .4772       8.1         -.437       0.195       -.380       960CC.C    234.
.263       2.920       9.3845      .90         11.78       14.08       29.375     29.
```

APPENDIX III

SYSTEM MECHANIZATION FOR THE ANALOG COMPUTER

Fig. 1 to this Appendix displays the analog schematic for the equations of motion of the airframe. Fig. 2 includes the schematic for the System 1 auto-throttle, aircraft engine, and stick system dynamics simulations. Fig. 3 shows the System 2 auto-throttle schematic.

Table I lists the potentiometer settings for all systems. Table II lists the scale factors used in computing these settings. Table III describes the calculations used in arriving at these values.

Potentiometer Settings

Machine input variable	Pot Number	to Resistor	to Amplifier Number		Setting Syst. 1A	Setting Syst. 1B	Setting Syst. 2	
$-u$	1	1M	1		.056	.056	.056	
	2	1M	27		.408	.408		
$-\alpha$	3	1M	1		.013	.013	.013	
$-\theta$	4	1M	1		.349	.349	.349	
$+T$	5	1M	1		.640	.640	.640	
$+\alpha$	6	.1M	30		.678	.678	.678	
$+u$	7	.1M	30		.449	.449	.449	
$+\theta$	8	1M	30		.641	.641	.641	
$-D\theta$	9	.1M	30		.998	.998	.998	
$\eta, \delta e$	10	1M	30		.794	.794	.794	
$+D\theta$	11	1M	2		.215	.215	.215	
$+\alpha$	12	.1M	2		.169	.169	.169	
$+D\alpha$	13	1M	2		.061	.061	.061	
$-u$	14	1M	2		.014	.014	.014	
$\eta, \delta e$	15	.1M	2		.260	.260	.260	
$+T$	16	1M	2		.517	.517	.517	
$+D\theta$	17	1M	3		.312	.312	.312	
$+D\alpha$	18	1M	4		.778	.778	.778	
$-D\theta$	19	1M	26		.998	.998	.998	
	20				.500	.500	.500	
- Throttle Simulator	21	1M	5		.443	.443	.443	
$-\eta, \delta e$	22	1M	29		.200	.200	.200	
$+\Delta T$	23	1M	5		.874	.874	.874	
$+\alpha$	24	.025M	6		.680	.980		
	25	.1M	6		.500	.500		
	26	.1M	8		.618	.618	.182	
	27	.5M	12		.583	.583	.155	
	28	10K	12		.690	.115	.250	
	29	.5M	12		.856	.856	1.00	
	30	1M	9		.614	.614	.814	
$\eta, \delta e$	31	.5M	15		.653	.653	.653	
$+\alpha$	32	.1M	10		.700	.145	.	
	33	.1M	11		.301	.301		
$+D\alpha$	34	1M	26		1.000	1.000	1.000	
$+\alpha$	35	1M	26		.398	.398		
Stick Simulator	36	1M	20		$\approx .544$	$\approx .544$	$\approx .544$	

12ND NPS 95 (11-59) Appendix III Table I

Potentiometer Settings

Machine Input Variable	Pot Number	to Resistor	to Amplifier Number		Setting Syst. 1A	Setting Syst. 1B	Setting Syst. 2	
$-\delta pilot F$	37	.5M	29		.192	.192	.192	
$-S\delta_{TC_1}$	38	10K	6		.380	.380	.380	
$\delta T C_3$	39	.1M	27		.132	.132	.132	
Voltage limiter	40	Diode			.330	.330	.330	
$-S_{F3}$	41	.1M	13		.571	.571	.571	
$+F_1$	42	.1M	13		.303	.303	.303	
$-F_3$	43	.1M	13		.598	.598	.598	
$-F_3$	44	.1M	15		.625	.625	.625	
$+\alpha$	45	1M	23		.410	.410	.410	
-100V	46	1M	24		1.00	1.00	1.00	
$-D\theta$	47	1M	21		0.350	0.350	.350	
$+D\alpha$	48	1M	21		.440	.440	.440	

12ND NPS 95 (11-59)

Appendix III Table I (concluded)

TABLE II

SCALE FACTORS USED IN ANALOG SIMULATION

Scale Factor		Value
α_θ	=	.005 radians/volt = .286 degrees/volt
$\alpha_{D\theta}$	=	.005 radians/volt = .286 degrees/volt
α_α	=	.002 radians/volt = .115 degrees/volt
$\alpha_{D\alpha}$	=	.005 radians/volt = .286 degrees/volt
α_u	=	$.002V_o$ = .2% of V_o = .278 Kts/volt
$\alpha_{\delta e}$	=	.002 radians/volt = .115 degrees/volt
α_T	=	200 lbs/volt
α_{TC1}	=	40 lbs/radians - volt
α_{TC2}	=	50 lbs/kt - volt
α_{TC3}	=	120 lbs/radians -sec - volt
α_{DTC1}	=	210 lbs/radians - sec - volt
α_{DTC2}	=	30 lbs/radians - sec^2 - volt
α_{DTC3}	=	300 lbs/radians - sec^2 - volt
$\alpha_{\Delta V}$	=	2.5 kts/volt
α_{TCT}	=	100 lbs/volt for System 1, 50 lbs/volt for System 2
$\alpha_{TCpilot}$	=	50 lbs/volt
α_{F1}	=	2 lbs/volt
α_{F3}	=	.01 radians/volt
α_{DF3}	=	.1 lb/sec - volt
$\alpha_{Pilot\ F}$	=	.75 lbs/volt

α_{γ_s} = .286 degrees/volt

$\alpha_{\Delta n_z}$ = .02 g/volt

$\alpha_{\frac{H}{\sqrt{\sigma}}}$ = .01 ft/ft/sec - volt

Appendix III Table III

Potentiometer Setting Calculations

Potentiometer	Calculation	R value	($C_f = 1\mu f$ unless specified otherwise)
1.	$\frac{x_u}{\alpha_t} \frac{1}{R C_f} = -.058$	1M	
2.	$\frac{\alpha_{TC2}}{\alpha_{TCT}} R = .4$	1M	
3	$\frac{x_u \alpha_\alpha}{\alpha_u \alpha_t} R = -.01435$	1M	
4.	$\frac{x_\theta \alpha_\theta}{\alpha_u \alpha_t} R = -.3433$	1M	
5	$\frac{x_T \alpha_T}{\alpha_u \alpha_t} R = .6243$	1M	
6	$\frac{z_w \alpha_\alpha}{\alpha_{D\alpha}} \frac{R}{R_f} = -.556$	.1M	$R_f = .1M$
7.	$\frac{z_u \alpha_u}{\alpha_{D\alpha}} R = -.36$	.1M	
8.	$\frac{z_\theta \alpha_\theta}{\alpha_{D\alpha}} R = -.641$	1M	
9.	$\left(\frac{z_q}{\mu_1} + 1\right) \frac{\alpha_{D\theta}}{\alpha_{D\alpha}} R = .990$	.1M	
10.	$\frac{z_\eta \alpha_{\delta e}}{\alpha_{D\alpha}} R = .780$	1M	
11.	$\frac{m_q}{i_b} \frac{R C_f}{\alpha_t} = -.2139$	1M	
12.	$\frac{m_w}{i_b} \frac{\mu_1 \alpha_\alpha}{\alpha_{D\theta} \alpha_t} R = -.149$	.1M	
13.	$\frac{m_{\dot{w}}}{i_b} \frac{\alpha_{D\alpha}}{\alpha_{D\theta} \alpha_t} R = -.061$	1M	
14.	$\frac{m_u}{i_b} \frac{\mu_1}{\alpha_{D\theta}} \frac{\alpha_u}{\alpha_t} R = .0149$	1M	

Appendix III Table III continued

Potentiometer	Calculation	R value	
15.	$\frac{m_2 \mu_1}{i_b} \frac{\alpha_{se}}{\alpha_{D\theta} \alpha_t} = -.3279$	.1 M	
16.	$\frac{m_T}{i_b} \frac{\alpha_T \mu_1 R}{\alpha_{D\theta} \alpha_t} = -.517$	1 M	
17.	$\frac{\alpha_{D\theta}}{\alpha_\theta \alpha_t} R C_f = .3055$	1 M	
18.	$\frac{\alpha_{D\alpha}}{\alpha_\alpha \alpha_t} R C_f = .764$	1 M	
19.	$\frac{K_{\Delta V} \alpha_{D\theta}}{\alpha_{\Delta V}} \frac{R}{R_f} = .995$	1 M	$R_f = 1M$
20.	$\frac{\alpha_{TC2}}{\alpha_{TCT}} R = .500$	1 M	
21.	$\frac{1}{T} \frac{\alpha_{TCT}}{\alpha_T} R C_f = .4316$	1 M	
22.	$\frac{\alpha_{plot\ Force}}{\alpha_{F_1}} \frac{R}{R_f} = .200$	1 M	$R_f = 1M$
23.	$\frac{R_f C_f}{1.16} = .862$		$R_f = 1M$
24.	$\frac{K_\alpha \alpha_\alpha R}{J_1 J_2 \alpha_{DTC2}} = .6545$	.1 M	
25.	$\frac{1}{J_1 J_2} \frac{\alpha_{TC1}}{\alpha_{DTC1}} R = .400$	.1 M	
26.	$\frac{\alpha_{DTC1}}{\alpha_{TCT}} R = .500$	.1 M	
27.	$\frac{J_1 + 1}{J_1} R C_f = .55$	.5M	$C_f = .1 \mu f$
28.	$\frac{K_V}{J_1} \frac{\alpha_{\Delta V}}{\alpha_{DTC2}} R = .233$	10K	
29	$\frac{1}{J_1} \frac{\alpha_{TC2}}{\alpha_{DTC2}} R = .833$	.5M	

Appendix III Table III continued

Potentiometer	Calculation	R value	
30.	$\frac{\alpha_{DTC2}}{\alpha_{TC2}} R = .600$	1 M	
31	$\frac{1}{\tau} R C_f = .625$	.5M	$C_f = .1 \mu f$
32.	$\frac{K_\delta \alpha_\alpha R}{\tau_1 \alpha_{DTC3}} = .145$	.1M	
33.	$\frac{\alpha_{DTC3}}{\alpha_{TC3}} R = .301$	.1M	
34.	$\frac{K_1 \alpha_{\Delta\alpha}}{\alpha_{\Delta V}} \frac{R}{R_f} = .996$	1 M	$R_f = 1M$
35.	$K_2 \frac{\alpha_\alpha}{\alpha_{\delta V}} R = .388$	1 M	
36.	Stick Trimmer = .508		
37.	$\frac{\alpha_{pilot\,Force}}{\alpha_{F1}} R = .1875$	.5M	
38.	$\frac{\tau_1 + \tau_2}{\tau_1 \tau_2} R = .120$	10K	
39.	$\frac{\alpha_{TC3}}{\alpha_{TCT}} R = .120$	.1M	
40.	Thrust limiter = .330		
41.	$\frac{b}{m} R = .490$	1M	
42.	$\frac{K_1}{m} \frac{\alpha_{F1}}{\alpha_{DF3}} R C_f = .270$	.1M	$C_f = .1 \mu f$
43.	$\frac{k}{m} \frac{\alpha_{F3}}{\alpha_{DF3}} R = .515$	.1M	
44.	$\frac{1}{\tau} \frac{\alpha_{F3}}{\alpha_{\delta e}} R = 625$	.1M	

Appendix III Table III concluded

Potentiometer	Calculation	R value
45.	$\frac{\alpha_\alpha}{\alpha_\gamma} R = .400$	1 M
47.	$K_{nz} \frac{\alpha_{D\theta}}{\alpha_{nz}} R = .907$	1 M
48	$K_{nz} \perp \hat{\epsilon} \frac{\alpha_{D\alpha}}{\alpha_{nz}} R = .440$	1 M

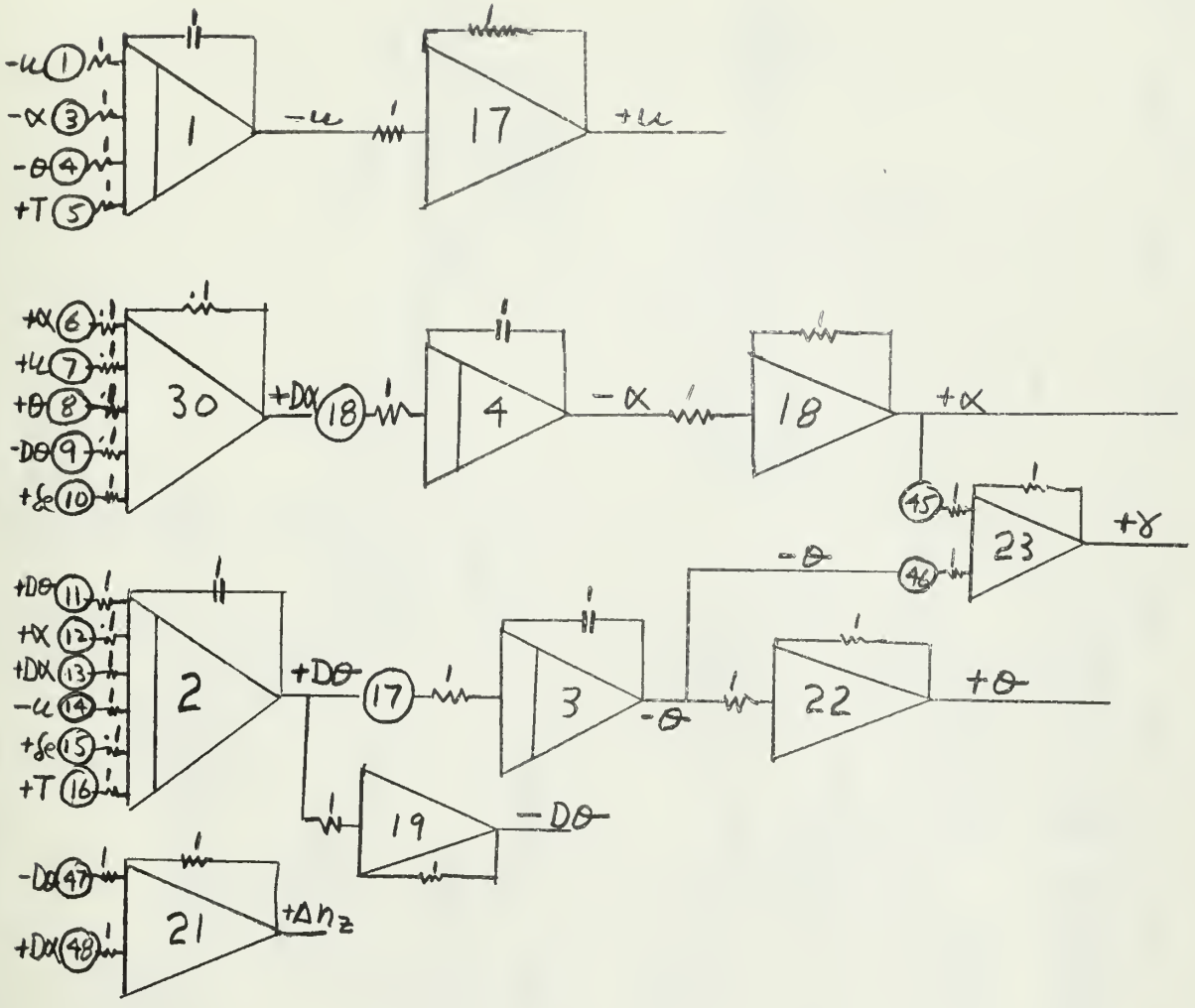

Equations :

1. $\left[\frac{d}{\bar{t}dT} - X_u\right]\frac{u}{U_0} - X_w\alpha - \left[X_\theta - \frac{X_{\dot{\alpha}}}{\mu_1}\frac{d}{\bar{t}dT}\right]\theta = X_T\Delta T$

2. $-Z_u\frac{u}{U_0} + \left[\frac{d}{\bar{t}dT} - Z_w\right]\alpha - \left[\left(1+\frac{Z_{\dot{\alpha}}}{\mu_1}\right)\frac{d}{\bar{t}dT} + Z_\theta\right]\theta = (Z_{n_2} + Z_{n_1})n$

3. $\left[\frac{-\mu_1 m_u}{i_b}\right]\frac{u}{U_0} + \left[-\frac{\bar{m}_w}{i_b}\frac{d}{\bar{t}dT} - \frac{\mu_1 m_w}{i_b}\right]\alpha + \left[\left(\frac{d}{\bar{t}dT} - \frac{m_{\dot{\alpha}}}{i_b}\right)\frac{d}{\bar{t}dT}\right]\theta = \left[\frac{\mu_1 m_{n_2}}{i_b}\right]n + \left[\frac{\mu_1 m_T}{i_b}\right]\Delta T$

Appendix III Fig. 1

Analog Schematic, Airframe Equations of Motion

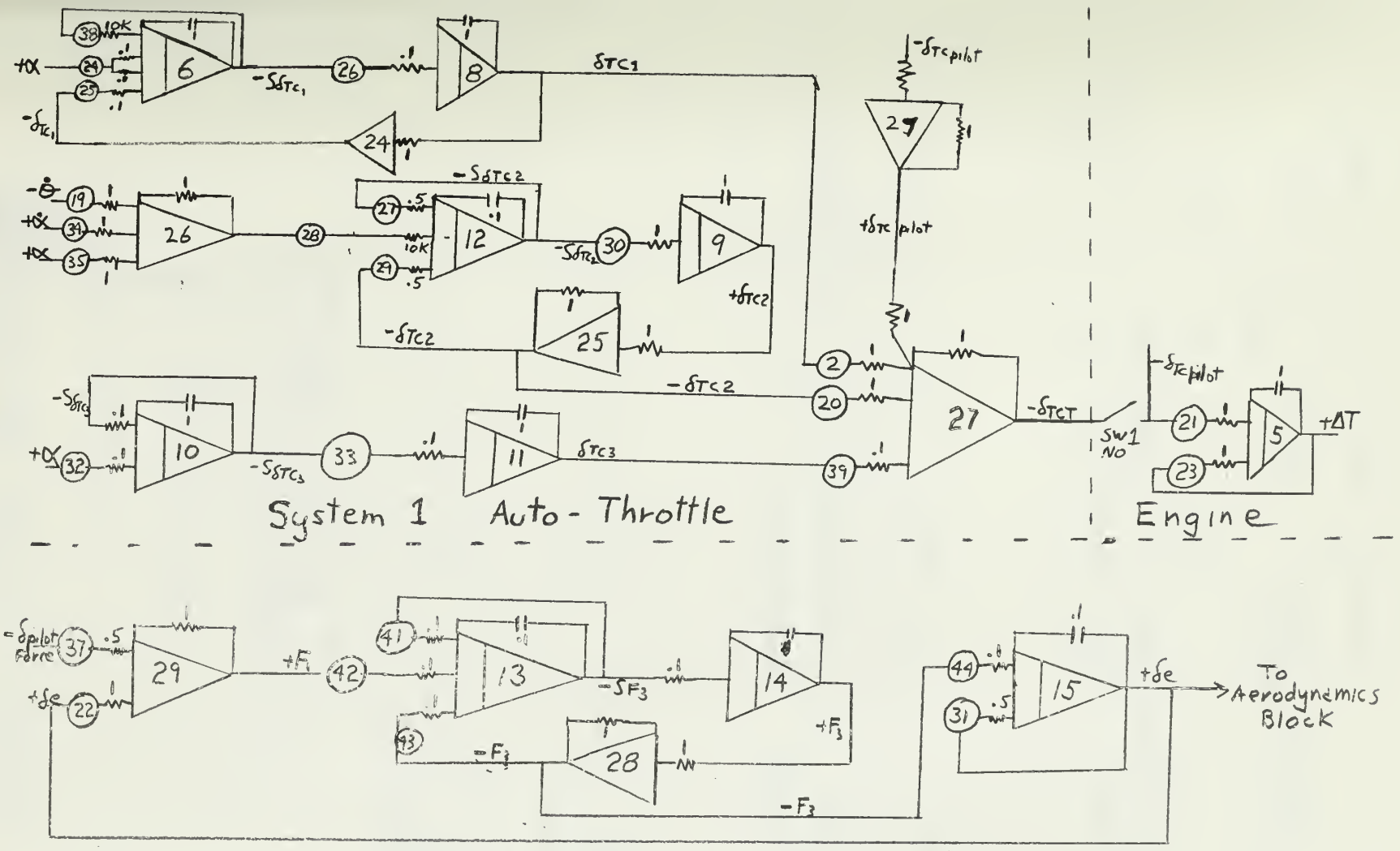

Appendix III Fig. 2

Analog Schematic, System 1 Auto-Throttle, Aircraft Engine, Stick System Dynamics

System 1 Auto-Throttle Equations:

$$\Delta T = \frac{1}{1+.1s}\left[\frac{K_\alpha \Delta\alpha}{1+.5s} - \frac{K_{\alpha v}\Delta V}{1+s} + \frac{K_\gamma \Delta\alpha}{s}\right]$$

where $\Delta V = \left(\Delta n_z - \frac{\Delta\alpha}{\alpha_o}\right)$

Δn_z = change of normal acceleration, g's

α_o = reference angle of attack

Longitudinal Control System Dynamics, Linearized

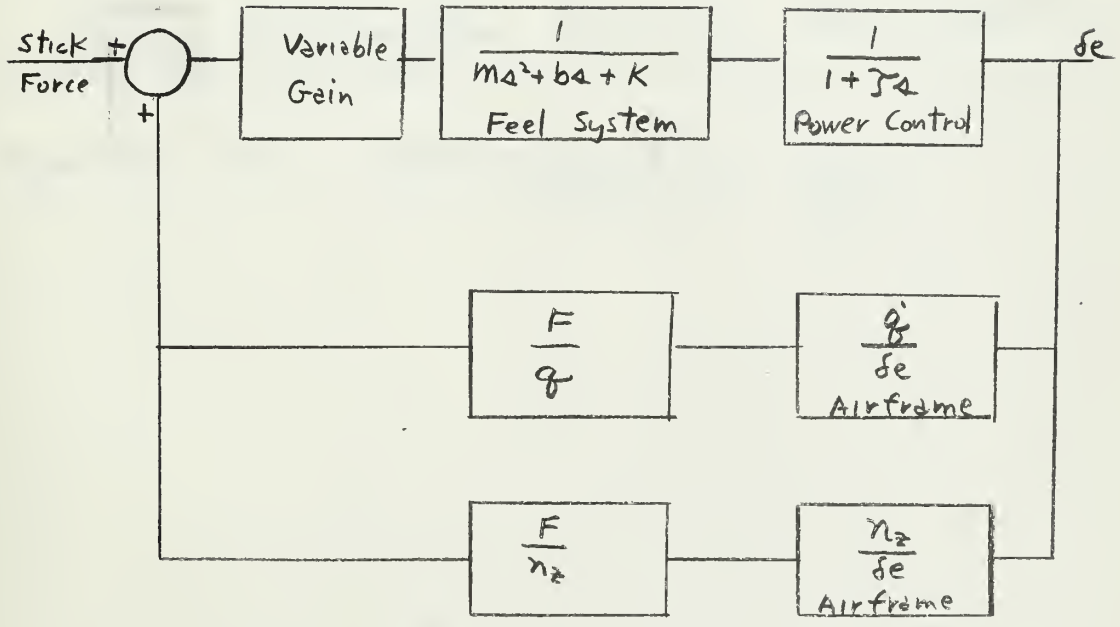

Variable Gain = 3° δe / inch Stick
m = .0388 lb. sec² / inch
b = 1.9 lb. / inch stick / sec
K = 20 lb. / inch stick
τ = 1/12.5 sec
$\frac{F}{\dot{q}}$ = 9.27 lbs / rad / sec²
$\frac{F}{n_z}$ = 2.56 lbs / g

Appendix III Fig. 2 continued

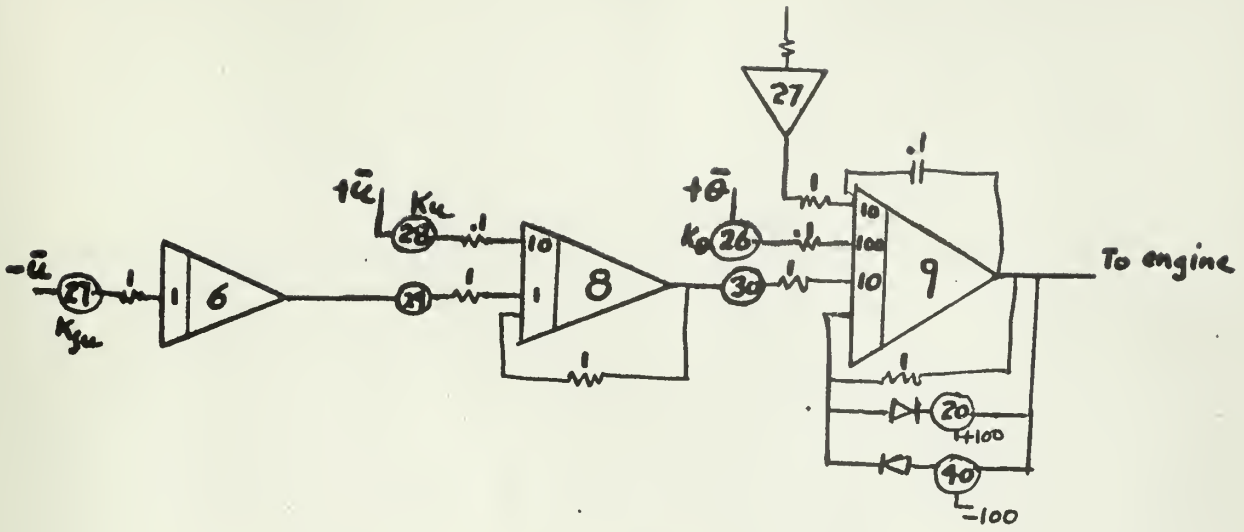

Analog Mechanization System 2 Auto-Throttle

Equation: $\Delta T = K_\theta \Delta\theta - \frac{u}{(1+.1s)}\left[K_u + \frac{K_{\int u}}{s}\right]$

Appendix III Fig. 3